Targeting the Hypnozoites: Towards an in vitro System for Malaria Drug Discovery

INAUGURALDISSERTATION

zur

Erlangung der Würde eines Doktors der Philosophie

vorgelegt der

Philosophisch-Naturwissenschaftlichen Fakultät

der Universität Basel

von

Mélanie Pellisson

aus Huningue (Frankreich)

Basel, 2020

Genehmigt von der Philosophisch-Naturwissenschaftlichen Fakultät

auf Antrag von

Prof. Dr. Pascal Mäser, Dr. Matthias Rottmann, and Prof. Dr. Volker Heussler

Basel, November 19, 2019

Prof. Dr. Martin Spiess

The Dean of the Faculty

Table of contents

Summary

Malaria still has a global incidence of about 219 million cases per year and the World Health Organization estimates that nearly half of the world's population is at risk of the disease in 2017. The majority of the available antimalarials on the market exclusively target the asexual and proliferative stages of malaria parasites. However, in order to eliminate malaria, we will need drugs that prevent parasite transmission and eliminate the dormant liver stages found after infection with *Plasmodium vivax (P. vivax)* and *Plasmodium ovale*. These quiescent forms called hypnozoites can survive for months in the liver and reactivate into mature liver schizonts causing relapses in patients. Up to date, primaquine and tafenoquine are the only available and efficient drugs against hypnozoites, but their use is limited due to severe side effects in glucose-6-phosphate dehydrogenase-deficient patients.

In order to elucidate the mechanisms underlying liver stage dormancy and to accelerate drug discovery for *P. vivax* malaria, we developed an in vitro infection model using stem cell-derived hepatocytes that allows studies of the hypnozoites. Considering the difficulties related to *P. vivax* in vitro work, the simian parasite *Plasmodium cynomolgi (P. cynomolgi)*, which also produces hypnozoites, was chosen as a surrogate model. Hepatocyte-like cells were generated using induced pluripotent stem cells (iPS) derived from *Macaca fascicularis* (i.e. cynomolgus monkey) somatic cells. IPS cells were established by reprogramming of fibroblasts using the four Yamanaka transcription factors Oct3/4, Sox2, Klf4 and, c-Myc. The pluripotency of these non-human primate cells was evaluated by immunofluorescence staining, flow cytometry, and their differentiation potential into the three germ layers (endoderm, ectoderm, and mesoderm). The produced iPS cells were differentiated into hepatic cells via inducible overexpression of key transcription factors for liver embryogenesis. The resulting simian hepatocyte-like cells displayed specific marker expression and functions similar to their human counterparts. However, the cells started to detach and die after 8 days of culture. This problem was overcome by screening about 4,000 compounds for their potential to prolong the lifespan of iPS-derived hepatocytes. A combination of three small molecules was identified and allowed maintenance of the cells up to 17 days. This improved culture conditions enabled infection of iPS-derived hepatocytes with *P. cynomolgi* sporozoites and observation of liver stage parasites for 12 days post-infection (dpi). Immunofluorescence analysis of *P. cynomolgi* Hsp70 and UIS4 revealed the presence of uninucleated parasites at 2 dpi. As in primary simian hepatocytes we distinguished, both dividing and non-dividing forms at 4 dpi and their respective development were followed until 12 dpi. At this time, both persistent hypnozoites and asynchronously

developed schizonts were identified. With our collaborators at the Biomedical Primate Research Center (BPRC), we also infected iPS-derived hepatocytes with a transgenic *P. cynomolgi* parasite line, confirming that expression of LISP2 protein over time enables live imaging of liver stage parasites and, more importantly, discrimination between hypnozoites and liver schizonts. The efficiency of this transgenic parasite line in iPS-derived hepatocytes further demonstrated that the iPS-based model supports the development of liver schizonts and hypnozoite persistence.

In summary, we report the development of a new iPS-based model that allows hypnozoite formation and persistence until 12 dpi. Using the iPS technology for malaria drug discovery presents great advantages, as iPS cells can be amplified from the same donor for screening purposes. They can be derived from any donor, which offers the possibility to study host-parasite interactions and glucose-6-phosphate dehydrogenase polymorphism. Moreover, the combination of the iPS technology with new molecular tools such as transgenic parasite lines can be used to screen for compounds with activity against hypnozoites. In conclusion, this iPS-based in vitro system overcomes the limitations of *P. vivax* and primary hepatocytes and provides a promising and versatile system to investigate the dormant liver stage of malaria.

Acknowledgments

This Ph.D. thesis would not have been possible without the precious support of many people. First, I would like to thank the members of the Walter Fischli Foundation for their financial support, their great interest in this project and their amiability. I particularly enjoyed the pleasant and fruitful discussions during our annual meetings at Novartis.

I am extremely grateful to my supervisors, Pascal Mäser, Matthias Müller, and Matthias Rottmann for giving me the opportunity to conduct this fascinating project even though I had no background on malaria and no experience in iPS cell culture. This was a challenge and I enjoyed it very much! You gave me valuable guidance through each stage of this thesis, your doors were always opened and I was delighted to work with you all during these four years.

I want to thank Volker Heussler for reviewing my thesis, for his genuine interest in this project and the insightful discussions during our annual meetings. You were always encouraging, curious about my progress and helpful for specific questions on the liver stage parasite.
In addition, I am thankful to Damien Portevin and Hans-Peter Beck for reviewing my Ph.D. research proposal and pointing out the challenges of this project. I will always remember the comment of Hans-Peter Beck: “This is a high risk, high gain project!”

I would also like to acknowledge the BPRC and the NITD for their wonderful collaboration, their contribution and their expertise, which allowed me to achieve key milestones of this project. I am particularly grateful to Anne-Marie Zeeman and her team who sent me sporozoites regularly to conduct my experiments. I want to thank them all for their warm welcome during my visit in The Netherlands. I had a great time in Delft, riding my Dutch bike every day to go to the BPRC. I discovered a different facet of malaria research, I learned new techniques and I deeply exchanged scientifically with experts – Thank you very much for this opportunity!
Then, I would like to thank our collaborators at NITD. First, Pablo Bifani and Andi Yip who kindly accepted to perform a proof-of-concept experiment in Singapore. I also had a great support from the scientists in Emeryville who believed in our project and were always willing to help us. A special thank goes to Lucy Kirchhofer-Allan who was highly cooperative and invested a lot of time in the establishment of the iPS technology in their laboratory.

I am grateful to my colleagues from the iPS group at Novartis. You supported me greatly and were always willing to help me when I needed. I am thankful to Thierry Doll who taught me a lot about the generation of iPS cells and hepatocytes. Isabelle Fruh, Bettina Leonhard, Carole Manneville and Annick Werner were extremely helpful in troubleshooting and giving ideas to

improve the system. Besides science, I very much enjoyed spending time with all of you. I had a good time during our yearly Christmas lunches at Dodici and coffee breaks with Isabelle and Thierry. You often convinced me to take a break when I did not want to and this was always a good idea! Thank you also to the bachelor and master students Nadine Heimhofer, Nicole Pina and Linda Mauch for their kindness and their friendliness. A special thank goes to my buddy Laura Colombo who shared so many exciting and frustrating moments with me. Most importantly, you provided happy distraction to rest my mind outside of my research.
I would also like to acknowledge our colleagues in Cambridge for the good moments spent with them in the United States. I enjoyed attending the ISSCR congress with you in 2017 and I had a great time in September this year during my short visit. Thank you all very much for your time and warm welcome!

I would like to acknowledge additional colleagues from Novartis who contributed to the success of this project. I am thankful to Guglielmo Roma's group for the generation of the RNA-seq data and especially to Sven Schuierer who analyzed the sequencing data and helped me in understanding the analysis. Thank you to Isabelle Claerr for her technical assistance with high content imaging. I thank Olaf Galuba for his support in conducting the survival screen, Dominic Trojer for his continuous help in microscopy, Benoit Fischer and Marianne Uteng for providing RNA samples from primary hepatocytes and William Gareth conducted the metabolic study on primaquine. I also want to thank Dominic Hoepfner, Ulrich Hassiepen, Ulf Neumann, and Juerg Hunziker for their interest in our assay and for their suggestions of compounds to be tested.

Then, I would like to thank the members of the MolBio meeting for their helpful inputs and for the nice discussions during the coffee breaks on Fridays. More generally, I thank the members of the PCU unit for their friendliness. Even though I did not spent so much time at SwissTPH, each meeting, each discussion in the corridor and each coffee break with you were good moments that I will remember! Not to mention the skitags, which were great days spent together with a lot of fun! Finally, I thank all my other colleagues and friends from the helminth, the malaria regulation units and, of course, Fabien Haas and Thierry Brun for their conviviality.

I am deeply grateful to my parents, my sister and my entire family for always believing in me and for giving me the freedom, strength and support to pursue my career path. Finally yet importantly, a huge thank you goes to Nicolas who is always there for me, supporting, helping, and cheering up in all circumstances. Thank you for your patience, your compassion and for bringing so much joy to my life.

Abbreviations

2D	Two-dimensional
3D	Three-dimensional
A1AT	α1-antitrypsin
AAALAC	Association for Assessment and Accreditation of Laboratory Animal Care
ABC	ATP-binding cassette
ABCB1	ATP-binding cassette subfamily B member 1
ABCB11	ATP-binding cassette subfamily B member 11
ABCC2	ATP-binding cassette subfamily C member 2
ABCG2	ATP-binding cassette super-family G member 2
aCGH	Array Comparative Genomic Hybridization
AFP	α-fetoprotein
ALB	Albumin
ALK2	Activin receptor-like kinase-2
ANOVA	Analysis of variance
AP2-G	ApiAP2 transcription factor essential for sexual commitment
AP2-Q	ApiAP2 transcription factor potentially involved in quiescence
ApiAP2	Apicomplexan apetala2
ATF5	Activating transcription factor 5
Bax	B-cell lymphoma 2-like protein 4
Bcl2	B-cell lymphoma 2
bFGF	Basic fibroblast growth factor
BMP	Bone morphogenetic protein
BMP4	Bone morphogenetic protein 4
BPRC	Biomedical Primate Research Centre
BSA	Bovine serum albumin
c/EBPα	CCAAT/ enhancer-binding protein alpha
CAG	Chicken β-actin promoter
cAMP	Cyclic adenosine monophosphate
Cas9	CRISPR-associated protein 9
CD81	Cluster of differentiation 81
CDM	Chemically defined medium
CEN	Centromere
Ch	Chicken

CO_2	Carbon dioxide
Con A	Concanavalin A
CRISPR	Clustered regularly interspaced short palindromic repeats
crRNA	CRISPR RNA
Cyn	Cynomolgus monkey
CynHLCs	Cynomolgus monkey iPS-derived hepatocyte-like cells
CynIPS cells	Cynomolgus monkey induced pluripotent stem cells
CYP or CYP450	Cytochrome P450
CYP1A2	Cytochrome P450 family 1 subfamily A member 2
CYP2A6	Cytochrome P450 family 2 subfamily A member 6
CYP2B6	Cytochrome P450 family 2 subfamily B member 6
CYP2C19	Cytochrome P450 family 2 subfamily C member 19
CYP2C9	Cytochrome P450 family 2 subfamily C member 9
CYP2D6	Cytochrome P450 family 2 subfamily D member 6
CYP3A4	Cytochrome P450 family 3 subfamily A member 4
D	Day
DE	Definitive endoderm
Dex	Dexamethasone
DHODH	Dihydroorotate dehydrogenase
Dk	Donkey
DMEM	Dulbecco's modified Eagle's medium
DMSO	Dimethylsulfoxide
DNA	Deoxyribonucleic acid
DNase	Deoxyribonuclease
Dox	Doxycycline
Dpi	Days post infection
EB	Embryoid body
EEFs	Exoerythrocytic forms
EGFP	Enhanced green fluorescent protein
ELISA	Enzyme-linked immunosorbent assay
EPCAM	Epithelial cell adhesion molecule
EphA2	Ephrin type-A receptor 2
ERK	Extracellular signal–regulated kinases
ES cell	Embryonic stem cell
FACS	Fluorescence-activated cell sorting

FBS	Fetal bovine serum
FCS	Fetal calf serum
FITC	Fluorescein isothiocyanate
FOXA2	Forkhead box protein A2
FOXA3	Forkhead box protein A3
FXR	Bile acid receptor farnesoid X-receptor
G418	Geneticin
G6PD	Glucose-6-phosphate dehydrogenase
GFP	Green fluorescent protein
Gt	Goat
GTP	Guanosine-5'-triphosphate
h	Human
hESC	Human embryonic stem cell
HGF	Hepatocyte growth factor
HLCs	Hepatocyte-like cells
HNF1A	Hepatocyte nuclear factor 1 homeobox A
HNF4A	Hepatocyte nuclear factor 4 alpha
Hsp70	70 kilodalton heat shock proteins
HSV	Herpes simplex virus
HSVtk	Minimal promoter fragment from HSV thymidine kinase promoter
I^{ary} hep	Primary hepatocyte
ID	Identifier
IGF-1R	Insulin-like growth factor 1 receptor
IgG	Immunoglobulin G
IMDM	Iscove's modified Dulbecco's medium
IPS	Induced pluripotent stem
ITS	Insulin-Transferrin-Selenium
IUPAC	International Union of Pure and Applied Chemistry
JNK2	C-Jun N-terminal kinase 2
JNK-p38	C-Jun N-terminal kinase-p38
Klf4	Kruppel like factor 4
KRT18	Cytokeratin 18
KRT19	Cytokeratin 19
LISP2	Liver specific protein 2
MAPK	Mitogen-activated protein kinase

Max	Maximum
MEFs	Mouse embryonic fibroblasts
MEK	Mitogen-activated protein kinase kinase
MEM	Minimum essential medium
Min	Minimum
MKK4	Mitogen-activated protein kinase kinase 4
MMP-7	Matrix metalloproteinase-7
MoA	Mode of action
mRNA	Messenger ribonucleic acid
MSP-1	Merozoite surface protein-1
Nb	Number
NEAA	Non-essential amino acids
NeoR	Neomycin resistance gene
NeuN	Neuronal nuclei
NF200	200 kDa neurofilament
NIH	National Institutes of Health
NITD	Novartis Institute for Tropical Diseases
Ns	Not significant
OCT4 or Oct3/4	Octamer-binding transcription factor 3/4
OncM	Oncostatin M
P	Passage number
P.	*Plasmodium*
PAS	Periodic acid schiff
PB	PiggyBac DNA transposon
PBS	Phosphate buffered saline
PCS	PreClinical Safety
PE	Phycoerythrin
PerCP	Peridinin chlorophyll protein complex
PI4K	Phosphatidylinositol 4-kinase
PQ	Primaquine
PROX1	Prospero homeobox protein 1
PVM	Parasitophorous vacuole membrane
R&D	Research and Development
Raf	Rapidly accelerated fibrosarcoma
Rb	Rabbit

RNA	Ribonucleic acid
RNA-seq	RNA sequencing analysis
rtTA	Transactivator protein gene
SAPK2	Stress-activated protein kinase 2
Sox2	Sex determining region Y-box 2
SRB1/SCARB1	Scavenger receptor, class B type 1
SSEA-1	Stage-specific embryonic antigen-1
SSEA-3	Stage-specific embryonic antigen-3
SSEA-4	Stage-specific embryonic antigen-4
Stdev	Standard deviation
SwissTPH	Swiss Tropical and Public Health Institute
T2A	Self-cleavage peptides from *Thosea asigna* virus
TACSTD2	Tumor-associated calcium signal transducer 2
TET	Tetracycline-controlled transcriptional activation
TGF-β	Transforming growth factor beta
Tpm	Transcripts per million
TQ	Tafenoquine
tracrRNA	*trans* crRNA
TRE	TET responsive element
tRNA	Transfer ribonucleic acid
TTR	Transthyretin
UDCA	Ursodeoxycholic acid
UIS4	Upregulated in infective sporozoites gene 4
ULA	Ultra-low attachment
WHO	World Health Organization
Wnt	Portmanteau created from the name Wingless and the name Int-1

Chapter I
Introduction

Introduction

1. From malaria control to elimination?

Malaria is a severe infectious disease caused by *Plasmodium* parasites that are transmitted to humans through the bites of infected female *Anopheles* mosquitoes. Six *Plasmodium* species can cause the disease (*P. falciparum*, *P. vivax*, *P. malariae*, *P. ovale curtisi, P. ovale wallikeri* (Ansari et al., 2016) and *P. knowlesi (Antinori et al., 2013)*) but *P. falciparum* and *P. vivax* are the most predominant and severe forms for the worldwide population. Malaria had an estimated global incidence in 2017 of 219,000,000 and a death toll of 435,000 (WHO, 2018). Thus, in spite of the recent successes in the fight against the disease (Rabinovich et al., 2017), malaria remains to be a main killer in the tropics. Maintaining that *"The only sustainable approach to addressing malaria is eradication of the parasite"*, Bill and Melinda Gates have strongly pushed to put malaria elimination back on the global health agenda (www.gatesfoundation.org/What-We-Do/Global-Health/Malaria). Elimination and even eradication are theoretically possible because the animal reservoir of the human-pathogenic *Plasmodium* species is negligible for human transmission. Yet enormous challenges persist, particularly in Africa, which accounts for over 90% of today's malaria cases in 2017. Reported increases, all greater than half a million cases, in 2017 compared to 2016 in Nigeria, Madagascar and the Democratic Republic of the Congo are alarming findings that preclude a challenging elimination process (WHO, 2018). Major threats are the evolution of drug-resistant *Plasmodium* parasites (Ashley et al., 2014) and insecticide-resistant *Anopheles* mosquitoes (Sokhna et al., 2013). However, the ultimate hindrance to *P. vivax* malaria elimination are the hypnozoites. These are dormant stages that can survive for months or even years in the liver of asymptomatic patients and reactivate to resume development into mature hepatic schizonts and ultimately into the disease causing blood stages, thus jeopardizing any attempts to eradicate the parasite (Dembele et al., 2014).

2. Malaria life cycle

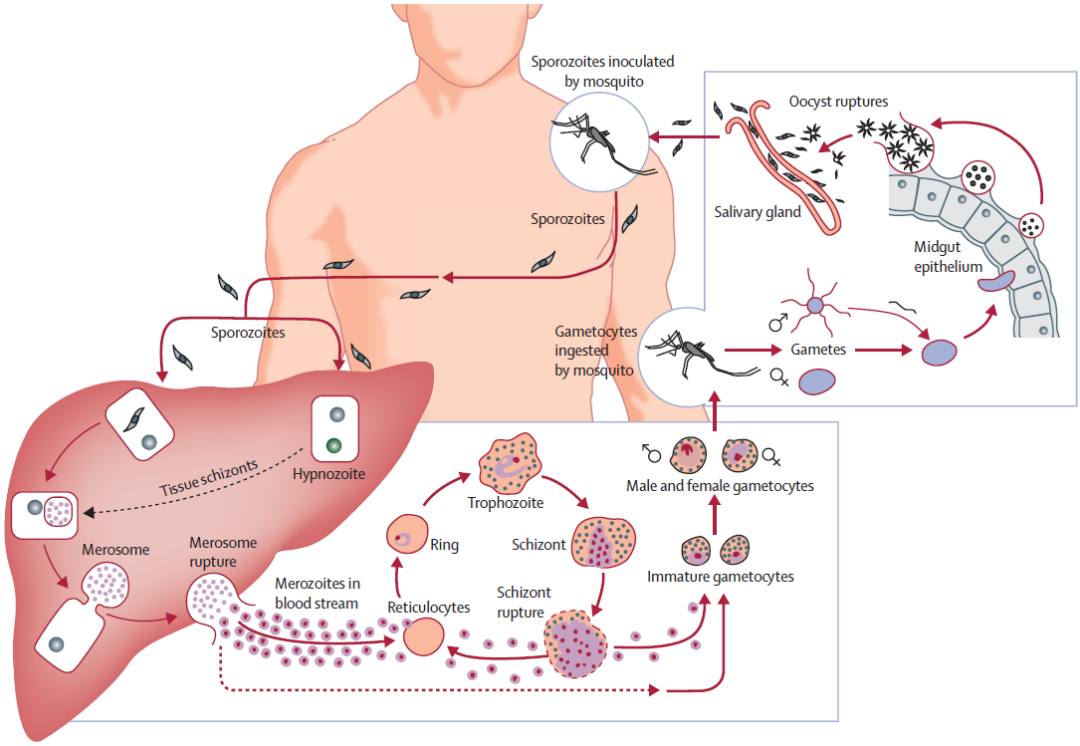

Fig. 1. Life cycle of the human malaria parasite *P. vivax (Mueller et al., 2009)*

The malaria life cycle in the vertebrate host (Fig. 1) starts when an infected female mosquito feeds on a human host. During this blood meal, the sporozoites contained in the mosquito's saliva penetrate into the bloodstream and travel rapidly to the liver where they invade hepatocytes. In all species of *Plasmodium*, these sporozoites establish pre-erythrocytic hepatic parasites that mature and multiply in the form of schizonts. These multinucleated structures contain thousands of merozoites, which are released into the bloodstream when the schizonts rupture. Sporozoites from some *Plasmodium* species (*P. vivax, P. ovale, P. simiovale, P. cynomolgi,* and *P. fieldi*) can also establish hypnozoites once they have penetrated a hepatocyte. Upon reactivation, these hypnozoites resume schizogony and cause relapses in patients. The major clinical symptoms and the pathology of the disease appear when merozoites have exited from the hepatocytes and infect erythrocytes in the bloodstream. At this stage, the parasite consumes the erythrocyte's hemoglobin and becomes a trophozoite. The latter matures into a schizont and undergoes asexual amplification again. The process of infection, multiplication, bursting and reinfection of naïve red blood cells continues until the immune system manages to control the infection or until a treatment is administrated to the patient. Some of the blood-stage parasites do not develop into schizonts but are committed to differentiate into male or female gametocytes. Gametocytogenesis depends on the activation of a stage specific transcription

factor named AP2-G (Kafsack et al., 2014, Sinha et al., 2014). It was recently discovered that limited host-lipid lysophosphatidylcholine availability in *P. falciparum* might be the environmental trigger that induces AP2-G activation and subsequently parasite sexual differentiation towards gametocytes (Brancucci et al., 2017). Ingestion of these gametocytes by a female mosquito during a blood meal activates the formation of gametes in the mosquito midgut lumen. Male gametogenesis in the form of exflagellation might be induced by different environmental factors including the presence of a mosquito-derived molecule xanthurenic acid, a drop in temperature, and an increase of pH (Billker et al., 1998, Billker et al., 1997). The male gamete fertilizes the female gamete leading to the formation of a zygote. The latter rapidly develops into a motile ookinete that penetrates the midgut wall of the female mosquito and matures into an oocyst. Like schizonts, oocysts progressively grow, divide, and rupture releasing haploid forms called sporozoites, which travel to the salivary glands and complete their maturation to invade mammalian cells (Matuschewski, 2006). The cycle is re-initiated when the vector mosquito takes a blood meal on another human host.

3. *P. vivax*, the neglected and underrated form of malaria

While the most prevalent and dangerous form of malaria is malaria tropica caused by *P. falciparum*, tertian malaria caused by *P. vivax* contributes significantly to worldwide malaria morbidity. Adapted to develop also in cooler climates, *P. vivax* is responsible for the majority of today's malaria cases outside tropical Africa (Mendis et al., 2001). It was also the causative agent of endemic malaria in Europe from ancient Greece until post-World War II. Africa has a very low prevalence of *P. vivax* (Fig. 2) due to the high proportion of Duffy-negative people (*P. vivax* merozoites use the host cell's Duffy blood group antigens for infection). In agreement with the hypothesis that *P. vivax* is of African origin (Liu et al., 2014, Loy et al., 2017), this illustrates the selective power of pathogens on human evolution. However, recent reports of *P. vivax* mutants that can infect Duffy-negative people may signalize the re-invasion of *P. vivax* to tropical Africa (Gunalan et al., 2018, Twohig et al., 2019, Zimmerman, 2017). For these reported cases, it is still unknown if *P. vivax* adapted to Duffy-negative people or if the previous cases were incorrectly diagnosed as *P. falciparum* malaria. Indeed, the molecular tools enabling the detection of low levels of *P. vivax* infection were not available until recently. Moreover, the high prevalence of Duffy negative people and the focus of malaria control programmes on *P. falciparum* may have contributed to the underestimation of *P. vivax* spreading in Africa (Gunalan et al., 2018). In spite of these alarming developments, the research activities on *P. vivax* are currently very limited.

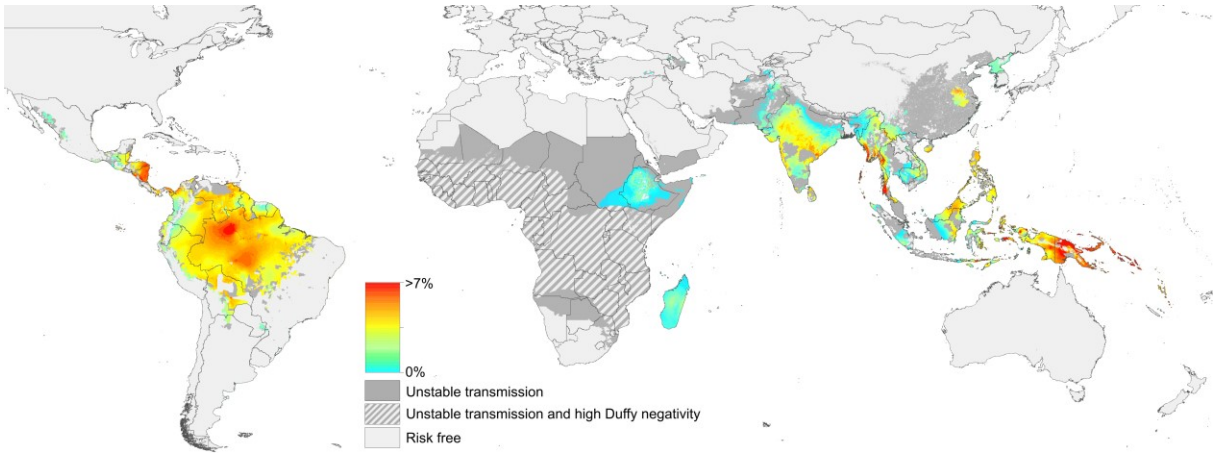

Fig. 2. Global incidence of *P. vivax* malaria as of 2010 (Gething et al., 2012). Note that in 2011, over 30 autochthonous *P. vivax* cases were reported from Greece, one of which with fatal outcome (Gougoutsi et al., 2014).

P. vivax is an elusive parasite that is hardly amenable to experimental investigation. Unlike *P. falciparum*, it only infects immature erythrocytes (i.e. reticulocytes), which only represent 1% of total red blood cells from adult human peripheral blood. Thus, *P. vivax* cannot be propagated in vitro despite the diverse and numerous improvements in cultivation media, parasite and reticulocyte sources (Trager and Jensen, 1976, Udomsangpetch et al., 2008, Noulin et al., 2013, Bermudez et al., 2018). Indeed, in vitro drug efficacy tests and investigations on hypnozoite biology are presently performed on fresh *P. vivax* isolates from patients, which is impracticable for drug R&D (Tachibana et al., 2012). To overcome these difficulties, scientists have been using *P. cynomolgi* as a surrogate model for *P. vivax.* This non-human-pathogenic malaria parasite is closely related to *P. vivax* and possesses a hypnozoite stage causing relapses in the infected non-human primates (Bray et al., 1985). A recent protocol enabling long-term in vitro culture of *P. cynomolgi* erythrocytic stages marked an important step towards the development of a system to study tertian malaria (Chua et al., 2019b). Using this protocol in combination with a liver model suitable for investigating hypnozoite biology would offer a powerful platform to find a radical cure of *P. vivax* malaria.

4. The hypnozoite reservoir: The hidden obstacle to malaria elimination

Up to date, hypnozoite biology remains poorly understood which hampers the development of novel drugs that kill this dormant liver stage of the parasite. Hypnozoites were discovered by Krotoski in 1982 in rhesus monkeys (*Macaca mulatta*) infected with *P. cynomolgi* sporozoites (Krotoski et al., 1982). Since then, they have been observed several times in relapsing *Plasmodium* parasites, thus progressively defining this enigmatic hypnozoite as a uninucleated and non-dividing form which persists in the liver of patients longer than the usual liver-stage

maturation period (Dembele et al., 2014). Since the discovery of primaquine (PQ) in the 1950's (Elderfield et al., 1955), no efficient and safe drug with anti-hypnozoite activity was approved and it is only recently that tafenoquine (TQ), another 8-aminoquinoline with improved pharmacokinetic properties, was approved by the Food and Drug Administration and Australian Therapeutic Goods Administration for the radical cure of *P. vivax* malaria (Lacerda et al., 2019). However, these drugs have non-negligible disadvantages for the treatment of malaria patients. First, they cannot be administered to glucose-6-phosphate dehydrogenase (G6PD) deficient patients as they could induce severe hemolysis (Howes et al., 2013). Second, PQ and TQ need to be metabolized by cytochrome P450 2D6 (CYP2D6) to be active against *Plasmodium*. However, this enzyme is highly polymorphic and thus, influences the effect of 8-aminoquinoline treatment (Baird et al., 2018, Ingelman-Sundberg, 2004, Pybus et al., 2013). Consequently, malaria patients should undergo both G6PD and CYP2D6 genotyping before receiving PQ or TQ. To develop better drugs against hypnozoites, a better understanding of this quiescent parasite's biology is urgently needed.

5. Available tools to study hypnozoites and ultimately kill this dormant parasite

5.1. Hypnozoite transcriptome

In order to access the hypnozoite transcriptome, new tools such as transgenic *P. cynomolgi* parasites stably expressing the green fluorescent protein (GFP) have been developed recently (Voorberg-van der Wel et al., 2013). These labeled parasites can be sorted by fluorescence-activated cell sorting (FACS) for subsequent RNA-seq analysis. This revealed an overall shutdown of the transcriptional activity in the dormant stage compared to the developing liver schizonts. However, no specific gene that would facilitate the distinction between hypnozoites and schizonts was identified (Bertschi et al., 2018). Laser dissection microscopy is another cutting-edge technology, which was applied in infected primary monkey hepatocytes to capture individual hypnozoites and schizonts to conduct transcriptomic studies. Using this technique, a member of the plant-derived Apicomplexan Apetala2 (ApiAP2) family of transcription factors, named AP2-Q, was identified as a potential regulator of dormancy (Cubi et al., 2017). This suggests that dormancy and subsequent reactivation are driven epigenetically. Dembele et al. have also raised this hypothesis as TM2-115, an inhibitor of histone mehyltransferase, induced hypnozoite reactivation in primary hepatocytes infected with *P. cynomolgi* sporozoites (Dembele et al., 2014). The hypnozoite transcriptome of *P. vivax* was also recently assessed using a micro-patterned co-culture of human primary hepatocytes with fibroblasts (March et al., 2015, Gural et al., 2018). Cells were infected with *P. vivax* sporozoites and RNA-seq

analysis was performed on mixed parasite liver stages and on cultures that had been treated with the phosphatidylinositol 4-kinase (PI4K) inhibitor to kill the liver schizonts and enrich for hypnozoites. Again, there was a low transcriptional activity in hypnozoites, which is in accordance with *P. cynomolgi* data and a suppression of functions related to maturation, merozoite invasion, and egress based on gene ontology enrichment analysis of the differentially expressed genes. AP2-Q was not differentially expressed, in either hypnozoites or mixed parasite liver stages, but another AP2-encoding transcript, PVP01_0916300, was significantly more abundant in the hypnozoite-enriched samples (Gural et al., 2018). Taken together, the different transcriptomic data suggest that the identification of potential hypnozoite-specific markers is challenging due to the technical difficulties linked to the small biomass, the limited number of genes expressed in the quiescent stage, and the variability of the results across the different existing systems.

5.2. Strategies for hypnozoite elimination

Screening campaigns usually aim to find lethal compounds. However, when Dembele et al. discovered that inhibitors of histone methyltransferases could accelerate hypnozoite activation, they suggested a new approach to attack the quiescent parasites (Dembele et al., 2014). Molecules that induce hypnozoite activation and subsequently resume schizogony would make these parasites susceptible to drugs that kill proliferative liver stages (e.g. atovaquone). In this strategy, a radical cure treatment would consist of a combination of a first drug that reactivates hypnozoites and a second drug that kills the newly formed schizonts. In addition, the molecules must not induce side effects in patients, particularly in G6PD deficient carriers. A successful screening campaign for such drugs would ideally require a hypnozoite-specific marker, a good source of sporozoites of high infectivity, and a good source of uniform hepatocytes.

5.3. In vitro models to study hypnozoites

The gold standard to study hypnozoites and perform drug screening is to use human or simian primary hepatocytes infected with *P. vivax* or *P. cynomolgi* sporozoites, respectively (Zeeman et al., 2014, Roth et al., 2018). Although this approach results in the full development of parasite liver stages, including developing schizonts and persistent hypnozoites, it presents some disadvantages. Freshly isolated and cryopreserved primary hepatocytes are in limited supply, are costly, present a high donor-to-donor variability, and have a relatively low infection rate (March et al., 2013, Dembele et al., 2014). Recently, efforts have been made to improve these systems. A cost efficient, miniaturized model for drug screening of compounds against *P. falciparum* and *P. vivax* was developed using cryopreserved primary human hepatocytes.

Reducing the format to 384-well plate and optimizing sporozoite isolation as well as hepatocyte cultivation allowed maintenance of physiological hepatic properties for 30 days and observation of liver stage parasites in high numbers (0.5-2% infected hepatocytes for *P. vivax*) (Roth et al., 2018). Another approach consists of co-cultivating primary hepatocytes with a human hepatoma cell line named HepaRG. The latter proliferates in vitro only until confluence is reached and thus, fills the gaps resulting from the traversal of sporozoites within the hepatic population (Dembele et al., 2014). Overlaying the culture with Matrigel after sporozoite inoculation maintains hepatic functions and provides a long-term in vitro system to study relapsing parasites (Dembele et al., 2014). In addition, primary hepatocyte maintenance can be supported by a chemical approach. Xiang et al. showed that five chemicals, selected based on transcriptomic data comparing freshly isolated and 24-hour cultured primary hepatocytes, sustained hepatic characteristics and ultimately supported long-term hepatitis B virus infection in vitro (Xiang et al., 2019). This method might be applicable to other infectious disease including malaria. Maintaining liver functions can also be achieved via a 3D approach. For instance, 3D spheroid-cultured primary hepatocytes were successfully infected with either *P. vivax* or *P. cynomolgi* sporozoites. Cultivating primary hepatocytes in 3D improved hepatocyte susceptibility to infection and maintenance of specific liver functions including cell polarity (Chua et al., 2019a). Finally, human liver chimeric mouse models have been developed to provide a *P. vivax* in vivo model using engrafted human primary hepatocytes with retained viability and metabolic activity (Mikolajczak et al., 2015).

Using hepatoma cell lines is a more affordable alternative to primary cells or humanized mice. HC-04 and HepG2 cells are permissive to *P. vivax* sporozoites and adaptable to many microplate formats (Hollingdale et al., 1985, Pewkliang et al., 2018, Sattabongkot et al., 2006). However, infection rates are low, their long-term use is difficult due to their fast growth and they have a reduced CYP450 activity, which hampers testing of prodrugs like 8-aminoquinolines. Finally, human hepatocytes derived from induced pluripotent stem (iPS) cells were also suggested as an option to study *P. vivax* malaria infection. Ng et al. generated human iPS-derived hepatocyte-like cells and reported successful infection with *P. berghei*, *P. yoelii*, *P. falciparum*, and *P. vivax* sporozoites (Ng et al., 2015). In contrast to hepatoma cell lines, iPS-derived cells have a controlled cell growth, are scalable, can be genetically manipulated to study host-parasite interactions and can be derived from any donor, which allows assessment of donor-specific drug responses.

6. IPS technology: A new tool for antiplasmodial drug discovery

A pluripotent cell has the capacity to self-renew and to differentiate into all cell types of the human body (Fig. 3). The best example of this type of cells is the embryonic stem cell (ES cell), which derives from the inner cell mass of a blastocyst. However, the source of primate ES cells is limited due to ethical issues.

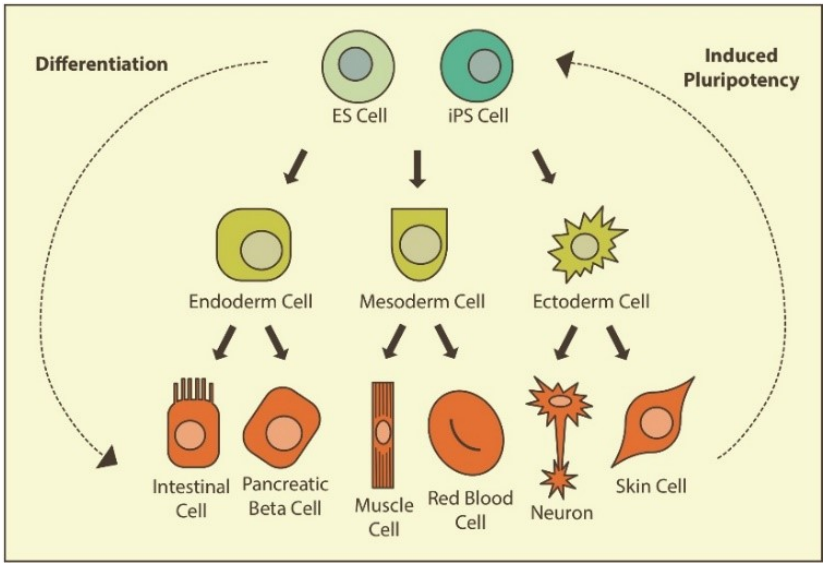

Fig. 3. Embryonic stem cells (light green) are pluripotent, meaning they have the potential to form all cell types of an organism. As an embryo develops, the ES cells differentiate, forming intermediate cell types (yellow) like endoderm, mesoderm, and ectoderm cells, and eventually differentiated cell types (orange) that have a specialized role, but no potential to form other cell types. An iPS cell (dark green) is an engineered cell that is generated via reprogramming of somatic cells using specific transcription factors (http://sitn.hms.harvard.edu/flash/2014/do-it-yourself-stem-cells-the-story-of-induced-pluripotency/).

In 2006, Kazutoshi Takahashi and Shinya Yamanaka opened a new door for stem cell research and regenerative medicine with the discovery that mature cells can be reprogrammed to become pluripotent (Takahashi and Yamanaka, 2006). Following the concept of cell fate reversibility developed by Sir John B. Gurdon few decades before them (Gurdon, 1962, Gurdon et al., 1958), Takahashi and Yamanaka identified the set of genes (octamer-binding transcription factor 4 (Oct3/4), sex determining region Y-box 2 (Sox2), kruppel like factor 4 (Klf4), and c-Myc named “Yamanaka factors”) required to reprogram mouse embryonic or adult fibroblasts into induced pluripotent stem cells. These non-specialized cells can subsequently be differentiated to all types of cells of the three primary germ layers. Gurdon and Yamanaka received the Nobel Prize of Medicine in 2012 for their discovery. Since this breakthrough, iPS cells have been generated from various species and used for many applications including drug discovery, disease modeling, and cell therapy development. Progressively, the reprogramming conditions

were improved to increase efficiency and limit the risk of tumorigenicity (Okita et al., 2007). Here, we used Sendai virus vectors to reprogram cynomolgus monkey fibroblasts into iPS cells. These negative strand RNA viruses replicate in the cytoplasm of infected cells, avoiding any introduction of viral transgenes into the host genome (Li et al., 2000). IPS technology became very popular due to the numerous advantages of these engineered cells compared to the traditional cell lines used in research: accessibility, scalability, adaptability (2D/3D models and co-culture systems), high differentiation potential, reduction of ethical concerns associated with human ES cells, and the access to personalized medicine via the generation of iPS cells derived from patients. More recently, the development of CRISPR-Cas9 (clustered regularly interspaced short palindromic repeats and CRISPR-associated protein 9) technology allowed gene editing in iPS cells, providing a straightforward method for disease modelling using genetically modified iPS cells (Hotta and Yamanaka, 2015, Li et al., 2015, Sontag et al., 2017).

7. Generation of iPS cells from cynomolgus monkey

The generation of iPS cells from non-human primates was reported for the first time in 2008 in a study describing the successful reprogramming of rhesus macaque fibroblasts (Liu et al., 2008). Shortly after, iPS cells were generated from different monkey species including marmoset (Wu et al., 2010), gorilla, bonobo (Wunderlich et al., 2014), and cynomolgus monkey (Coppiello et al., 2017, Deleidi et al., 2011, Okahara-Narita et al., 2012, Okamoto and Takahashi, 2011, Onozato et al., 2018, Shimozawa et al., 2013, Thoma et al., 2016, Wunderlich et al., 2012). Most of the studies describing the generation of cynomolgus monkey iPS (cynIPS) cells used the traditional "Yamanaka factors" for reprogramming. Except from Shimozawa et al., which used allogeneic genes to increase reprogramming efficiency (Shimozawa et al., 2013), cynIPS cells were produced with the human orthologues of the Yamanaka transcription factors. Mostly maintained on feeder cells, the generated monkey iPS cells expressed pluripotency markers similar to their human counterparts (Nanog, Oct3/4, and stage-specific embryonic antigen-4 (SSEA-4), TRA-1-60, and TRA-1-81) and were able to form teratoma in mice (Okahara-Narita et al., 2012, Shimozawa et al., 2013). As cynomolgus monkeys are relevant models for drug efficacy testing and disease modeling, several differentiation protocols were developed towards endothelial cells (Thoma et al., 2016), midbrain dopaminergic neurons (Deleidi et al., 2011), intestinal cells (Onozato et al., 2018), and retinal pigment epithelial cells (Okamoto and Takahashi, 2011). Yet, most of the available methods for cynomolgus monkey iPS cell generation use feeder cells such as irradiated mouse embryonic fibroblasts to support undifferentiated stem cell growth. However, transferring iPS cells to a feeder-less system

presents several advantages compared to the classical feeder layer system (i.e. no exposure to animal pathogens, enables large-scale cell production, less time consuming) when developing cellular models to understand diseases.

8. Hepatocyte generation from iPS cells

There is a need for hepatocyte surrogates as the demand in liver and liver tissues is very high to be covered by primary cells. As a solution to this lack of hepatic cells, researchers have generated iPS-derived hepatocyte-like cells first from mouse and then from humans (Sekiya and Suzuki, 2011, Huang et al., 2011, Huang et al., 2014). Two major approaches are commonly used in the field to generate hepatocyte-like cells. The first consists of adding factors related to the mechanisms underlying mouse embryogenesis to mimic the growth factor signaling environment that developing hepatocytes of the endoderm experience during embryonic development. This includes factors that contribute to endoderm formation (activin A) and factors specific to hepatoblasts (bone morphogenetic protein 4 (BMP4)/basic fibroblast growth factor (bFGF)) and differentiated hepatocytes (hepatocyte growth factor (HGF)/oncostatin M) (Si-Tayeb et al., 2010). In the second approach, induced hepatocyte-like cells are generated via overexpression of transcription factors that are essential for hepatic lineage formation such as hepatocyte nuclear factor 1 homeobox A (HNF1A), hepatocyte nuclear factor 4 alpha (HNF4A) and forkhead box protein A3 (FOXA3) (Huang et al., 2014, Kang et al., 2018, Yoon et al., 2018). Both the stepwise and the transcription factor methods are efficient in producing cells displaying a hepatic signature with a high conversion rate (Goldring et al., 2017, Du et al., 2014, Gao et al., 2017). Nevertheless, the transcription factor approach is faster and less expensive. In this thesis, we tested both differentiation approaches to generate cynomolgus monkey hepatocyte-like cells for the first time.

9. Aims and objectives of the thesis

The overall goal of this thesis was to develop an iPS-based in vitro model for malaria liver stages that allows producing and studying hypnozoites.

The first goal of this project was the generation of iPS cells and hepatocytes from cynomolgus monkey cells. This included the establishment of cynIPS cells from cynomolgus monkey fibroblasts, the transfer of cynIPS cells from feeder cells onto Matrigel (i.e. feeder-free conditions), and the generation of cynomolgus monkey hepatocyte-like cells (cynHLCs) via overexpression of transcription factors for direct hepatocyte differentiation.

The second part of this thesis was dedicated to the development of an infection model using cynHLCs and *P. cynomolgi* sporozoites. First, a protocol for cynHLC infection and subsequent production of *P. cynomolgi* liver-stage parasites was established. Then, both hypnozoites and liver schizonts were characterized via immunofluorescence analysis with antibodies specific to *P. cynomolgi.* Finally, a quantification method for *P. cynomolgi* liver-stage parasites was developed on a high-content imaging system and cynHLC production was scaled up to increase the throughput of a future drug-screening platform.

References

ANSARI, H. R., TEMPLETON, T. J., SUBUDHI, A. K., RAMAPRASAD, A., TANG, J., LU, F., NAEEM, R., HASHISH, Y., OGUIKE, M. C., BENAVENTE, E. D., CLARK, T. G., SUTHERLAND, C. J., BARNWELL, J. W., CULLETON, R., CAO, J. & PAIN, A. 2016. Genome-scale comparison of expanded gene families in Plasmodium ovale wallikeri and Plasmodium ovale curtisi with Plasmodium malariae and with other Plasmodium species. *International Journal for Parasitology,* 46**,** 685-696.

ANTINORI, S., GALIMBERTI, L., MILAZZO, L. & CORBELLINO, M. 2013. Plasmodium knowlesi: The emerging zoonotic malaria parasite. *Acta Tropica,* 125**,** 191-201.

ASHLEY, E. A., DHORDA, M., FAIRHURST, R. M., AMARATUNGA, C., LIM, P., SUON, S., SRENG, S., ANDERSON, J. M., MAO, S., SAM, B., SOPHA, C., CHUOR, C. M., NGUON, C., SOVANNAROTH, S., PUKRITTAYAKAMEE, S., JITTAMALA, P., CHOTIVANICH, K., CHUTASMIT, K., SUCHATSOONTHORN, C., RUNCHAROEN, R., HIEN, T. T., THUY-NHIEN, N. T., THANH, N. V., PHU, N. H., HTUT, Y., HAN, K. T., AYE, K. H., MOKUOLU, O. A., OLAOSEBIKAN, R. R., FOLARANMI, O. O., MAYXAY, M., KHANTHAVONG, M., HONGVANTHONG, B., NEWTON, P. N., ONYAMBOKO, M. A., FANELLO, C. I., TSHEFU, A. K., MISHRA, N., VALECHA, N., PHYO, A. P., NOSTEN, F., YI, P., TRIPURA, R., BORRMANN, S., BASHRAHEIL, M., PESHU, J., FAIZ, M. A., GHOSE, A., HOSSAIN, M. A., SAMAD, R., RAHMAN, M. R., HASAN, M. M., ISLAM, A., MIOTTO, O., AMATO, R., MACINNIS, B., STALKER, J., KWIATKOWSKI, D. P., BOZDECH, Z., JEEYAPANT, A., CHEAH, P. Y., SAKULTHAEW, T., CHALK, J., INTHARABUT, B., SILAMUT, K., LEE, S. J., VIHOKHERN, B., KUNASOL, C., IMWONG, M., TARNING, J., TAYLOR, W. J., YEUNG, S., WOODROW, C. J., FLEGG, J. A., DAS, D., SMITH, J., VENKATESAN, M., PLOWE, C. V., STEPNIEWSKA, K., GUERIN, P. J., DONDORP, A. M., DAY, N. P. & WHITE, N. J. 2014. Spread of artemisinin resistance in Plasmodium falciparum malaria. *N Engl J Med,* 371**,** 411-23.

BAIRD, J. K., BATTLE, K. E. & HOWES, R. E. 2018. Primaquine ineligibility in anti-relapse therapy of Plasmodium vivax malaria: the problem of G6PD deficiency and cytochrome P-450 2D6 polymorphisms. *Malar J,* 17**,** 42.

BERMUDEZ, M., MORENO-PEREZ, D. A., AREVALO-PINZON, G., CURTIDOR, H. & PATARROYO, M. A. 2018. Plasmodium vivax in vitro continuous culture: the spoke in the wheel. *Malar J,* 17**,** 301.

BERTSCHI, N. L., VOORBERG-VAN DER WEL, A., ZEEMAN, A. M., SCHUIERER, S., NIGSCH, F., CARBONE, W., KNEHR, J., GUPTA, D. K., HOFMAN, S. O., VAN DER WERFF, N., NIEUWENHUIS, I., KLOOSTER, E., FABER, B. W., FLANNERY, E. L., MIKOLAJCZAK, S. A., CHUENCHOB, V., SHRESTHA, B., BEIBEL, M., BOUWMEESTER, T., KANGWANRANGSAN, N., SATTABONGKOT, J., DIAGANA, T. T., KOCKEN, C. H. & ROMA, G. 2018. Transcriptomic analysis reveals reduced transcriptional activity in the malaria parasite Plasmodium cynomolgi during progression into dormancy. *Elife,* 7.

BILLKER, O., LINDO, V., PANICO, M., ETIENNE, A. E., PAXTON, T., DELL, A., ROGERS, M., SINDEN, R. E. & MORRIS, H. R. 1998. Identification of xanthurenic acid as the putative inducer of malaria development in the mosquito. *Nature,* 392**,** 289-92.

BILLKER, O., SHAW, M. K., MARGOS, G. & SINDEN, R. E. 1997. The roles of temperature, pH and mosquito factors as triggers of male and female gametogenesis of Plasmodium berghei in vitro. *Parasitology,* 115 (Pt 1)**,** 1-7.

BRANCUCCI, N. M. B., GERDT, J. P., WANG, C., DE NIZ, M., PHILIP, N., ADAPA, S. R., ZHANG, M., HITZ, E., NIEDERWIESER, I., BOLTRYK, S. D., LAFFITTE, M.-C., CLARK, M. A., GRÜRING, C., RAVEL, D., BLANCKE SOARES, A., DEMAS, A., BOPP, S., RUBIO-RUIZ, B., CONEJO-GARCIA, A., WIRTH, D. F., GENDASZEWSKA-DARMACH, E., DURAISINGH, M. T., ADAMS, J. H., VOSS, T. S., WATERS, A. P., JIANG, R. H. Y., CLARDY, J. & MARTI, M. 2017. Lysophosphatidylcholine Regulates Sexual Stage Differentiation in the Human Malaria Parasite Plasmodium falciparum. *Cell,* 171**,** 1532-1544.e15.

BRAY, R. S., KROTOSKI, W. A., COGSWELL, F. B., GARNHAM, P. C., RODRIGUEZ, M., GUY, M. W., GWADZ, R. W., SINDEN, R. E., TARGETT, G. A., DRAPER, C. C. & ET AL. 1985. Observations on early and late post-sporozoite tissue stages in primate malaria. III. Further attempts to find early forms and to correlate hypnozoites with growing exo-erythrocytic schizonts and parasitaemic relapses in Plasmodium cynomolgi bastianellii infections. *Trans R Soc Trop Med Hyg,* 79**,** 269-73.

CHUA, A. C. Y., ANANTHANARAYANAN, A., ONG, J. J. Y., WONG, J. Y., YIP, A., SINGH, N. H., QU, Y., DEMBELE, L., MCMILLIAN, M., UBALEE, R., DAVIDSON, S., TUNGTAENG, A., IMERBSIN, R., GUPTA, K., ANDOLINA, C., LEE, F., K, S. W. T., NOSTEN, F., RUSSELL, B., LANGE, A., DIAGANA, T. T., RENIA, L., YEUNG, B. K. S., YU, H. & BIFANI, P. 2019a. Hepatic spheroids used as an in vitro model to study malaria relapse. *Biomaterials,* 216**,** 119221.

CHUA, A. C. Y., ONG, J. J. Y., MALLERET, B., SUWANARUSK, R., KOSAISAVEE, V., ZEEMAN, A.-M., COOPER, C. A., TAN, K. S. W., ZHANG, R., TAN, B. H., ABAS, S. N., YIP, A., ELLIOT, A., JOYNER, C. J., CHO, J. S., BREYER, K., BARAN, S., LANGE, A., MAHER, S. P., NOSTEN, F., BODENREIDER, C., YEUNG, B. K. S., MAZIER, D., GALINSKI, M. R., DEREUDDRE-BOSQUET, N., LE GRAND, R., KOCKEN, C. H. M., RÉNIA, L., KYLE, D. E., DIAGANA, T. T., SNOUNOU, G., RUSSELL, B. & BIFANI, P. 2019b. Robust continuous in vitro culture of the Plasmodium cynomolgi erythrocytic stages. *Nature Communications,* 10**,** 3635.

COPPIELLO, G., ABIZANDA, G., AGUADO, N., IGLESIAS, E., ARELLANO-VIERA, E., RODRIGUEZ-MADOZ, J. R., CARVAJAL-VERGARA, X., PROSPER, F. & ARANGUREN, X. L. 2017. Generation of Macaca fascicularis iPS cell line ATCi-MF1 from adult skin fibroblasts using non-integrative Sendai viruses. *Stem Cell Res,* 21**,** 1-4.

CUBI, R., VEMBAR, S. S., BITON, A., FRANETICH, J. F., BORDESSOULLES, M., SOSSAU, D., ZANGHI, G., BOSSON-VANGA, H., BENARD, M., MORENO, A., DEREUDDRE-BOSQUET, N., LE GRAND, R., SCHERF, A. & MAZIER, D. 2017. Laser capture microdissection enables transcriptomic analysis of dividing and quiescent liver stages of Plasmodium relapsing species. *Cell Microbiol,* 19.

DELEIDI, M., HARGUS, G., HALLETT, P., OSBORN, T. & ISACSON, O. 2011. Development of histocompatible primate-induced pluripotent stem cells for neural transplantation. *Stem Cells,* 29**,** 1052-63.

DEMBELE, L., FRANETICH, J. F., LORTHIOIS, A., GEGO, A., ZEEMAN, A. M., KOCKEN, C. H., LE GRAND, R., DEREUDDRE-BOSQUET, N., VAN GEMERT, G. J., SAUERWEIN, R., VAILLANT, J. C., HANNOUN, L., FUCHTER, M. J., DIAGANA, T. T., MALMQUIST, N. A., SCHERF, A., SNOUNOU, G. & MAZIER, D. 2014. Persistence and activation of malaria hypnozoites in long-term primary hepatocyte cultures. *Nat Med,* 20**,** 307-12.

DU, Y., WANG, J., JIA, J., SONG, N., XIANG, C., XU, J., HOU, Z., SU, X., LIU, B. & JIANG, T. 2014. Human hepatocytes with drug metabolic function induced from fibroblasts by lineage reprogramming. *Cell stem cell,* 14**,** 394-403.

ELDERFIELD, R. C., MERTEL, H. E., MITCH, R. T., WEMPEN, I. M. & WERBLE, E. 1955. Synthesis of Primaquine and Certain of its Analogs1. *Journal of the American Chemical Society,* 77**,** 4816-4819.

GAO, Y., ZHANG, X., ZHANG, L., CEN, J., NI, X., LIAO, X., YANG, C., LI, Y., CHEN, X., ZHANG, Z., SHU, Y., CHENG, X., HAY, D. C., LAI, D., PAN, G., WEI, G. & HUI, L. 2017. Distinct Gene Expression and Epigenetic Signatures in Hepatocyte-like Cells Produced by Different Strategies from the Same Donor. *Stem Cell Reports,* 9**,** 1813-1824.

GETHING, P. W., ELYAZAR, I. R., MOYES, C. L., SMITH, D. L., BATTLE, K. E., GUERRA, C. A., PATIL, A. P., TATEM, A. J., HOWES, R. E., MYERS, M. F., GEORGE, D. B., HORBY, P., WERTHEIM, H. F., PRICE, R. N., MUELLER, I., BAIRD, J. K. & HAY, S. I. 2012. A long neglected world malaria map: Plasmodium vivax endemicity in 2010. *PLoS Negl Trop Dis,* 6**,** e1814.

GOLDRING, C., ANTOINE, D. J., BONNER, F., CROZIER, J., DENNING, C., FONTANA, R. J., HANLEY, N. A., HAY, D. C., INGELMAN-SUNDBERG, M., JUHILA, S., KITTERINGHAM, N., SILVA-LIMA, B., NORRIS, A., PRIDGEON, C., ROSS, J. A., YOUNG, R. S., TAGLE, D., TORNESI, B., VAN DE WATER, B., WEAVER, R. J., ZHANG, F. & PARK, B. K. 2017. Stem cell-derived models to improve mechanistic understanding and prediction of human drug-induced liver injury. *Hepatology,* 65**,** 710-721.

GOUGOUTSI, A., KARAGEORGOPOULOS, D. E., DIMITRIADOU, A., MELAS, N., KRANIDIOTIS, G., VOUTSINAS, D. & MELIDONIS, A. 2014. Severe Plasmodium vivax malaria complicated with acute respiratory distress syndrome: a case associated with focal autochthonous transmission in Greece. *Vector Borne Zoonotic Dis,* 14**,** 378-81.

GUNALAN, K., NIANGALY, A., THERA, M. A., DOUMBO, O. K. & MILLER, L. H. 2018. Plasmodium vivax Infections of Duffy-Negative Erythrocytes: Historically Undetected or a Recent Adaptation? *Trends Parasitol,* 34**,** 420-429.

GURAL, N., MANCIO-SILVA, L., MILLER, A. B., GALSTIAN, A., BUTTY, V. L., LEVINE, S. S., PATRAPUVICH, R., DESAI, S. P., MIKOLAJCZAK, S. A., KAPPE, S. H. I., FLEMING, H. E., MARCH, S., SATTABONGKOT, J. & BHATIA, S. N. 2018. In Vitro Culture, Drug Sensitivity, and Transcriptome of Plasmodium Vivax Hypnozoites. *Cell Host Microbe,* 23**,** 395-406 e4.

GURDON, J. B. 1962. The Developmental Capacity of Nuclei taken from Intestinal Epithelium Cells of Feeding Tadpoles. *Journal of Embryology and Experimental Morphology,* 10**,** 622.

GURDON, J. B., ELSDALE, T. R. & FISCHBERG, M. 1958. Sexually Mature Individuals of Xenopus laevis from the Transplantation of Single Somatic Nuclei. *Nature,* 182**,** 64-65.

HOLLINGDALE, M. R., COLLINS, W. E., CAMPBELL, C. C. & SCHWARTZ, A. L. 1985. In vitro culture of two populations (dividing and nondividing) of exoerythrocytic parasites of Plasmodium vivax. *Am J Trop Med Hyg,* 34**,** 216-22.

HOTTA, A. & YAMANAKA, S. 2015. From Genomics to Gene Therapy: Induced Pluripotent Stem Cells Meet Genome Editing. *Annu Rev Genet,* 49**,** 47-70.

HOWES, R. E., BATTLE, K. E., SATYAGRAHA, A. W., BAIRD, J. K. & HAY, S. I. 2013. G6PD deficiency: global distribution, genetic variants and primaquine therapy. *Adv Parasitol,* 81**,** 133-201.

HUANG, P., HE, Z., JI, S., SUN, H., XIANG, D., LIU, C., HU, Y., WANG, X. & HUI, L. 2011. Induction of functional hepatocyte-like cells from mouse fibroblasts by defined factors. *nature,* 475**,** 386.

HUANG, P., ZHANG, L., GAO, Y., HE, Z., YAO, D., WU, Z., CEN, J., CHEN, X., LIU, C., HU, Y., LAI, D., HU, Z., CHEN, L., ZHANG, Y., CHENG, X., MA, X., PAN, G., WANG, X. & HUI, L. 2014. Direct reprogramming of human fibroblasts to functional and expandable hepatocytes. *Cell Stem Cell,* 14**,** 370-84.

INGELMAN-SUNDBERG, M. 2004. Genetic polymorphisms of cytochrome P450 2D6 (CYP2D6): clinical consequences, evolutionary aspects and functional diversity. *The Pharmacogenomics Journal,* 5**,** 6.

KAFSACK, B. F., ROVIRA-GRAELLS, N., CLARK, T. G., BANCELLS, C., CROWLEY, V. M., CAMPINO, S. G., WILLIAMS, A. E., DROUGHT, L. G., KWIATKOWSKI, D. P. & BAKER, D. A. 2014. A transcriptional switch underlies commitment to sexual development in malaria parasites. *Nature,* 507**,** 248.

KANG, K., KIM, Y., JEON, H., LEE, S. B., KIM, J. S., PARK, S. A., KIM, W. D., YANG, H. M., KIM, S. J., JEONG, J. & CHOI, D. 2018. Three-Dimensional Bioprinting of Hepatic Structures with Directly Converted Hepatocyte-Like Cells. *Tissue Eng Part A,* 24**,** 576-583.

KROTOSKI, W. A., GARNHAM, P. C., BRAY, R. S., KROTOSKI, D. M., KILLICK-KENDRICK, R., DRAPER, C. C., TARGETT, G. A. & GUY, M. W. 1982. Observations on early and late post-sporozoite tissue stages in primate malaria. I. Discovery of a new latent form of Plasmodium cynomolgi (the hypnozoite), and failure to detect hepatic forms within the first 24 hours after infection. *Am J Trop Med Hyg,* 31**,** 24-35.

LACERDA, M. V., LLANOS-CUENTAS, A., KRUDSOOD, S., LON, C., SAUNDERS, D. L., MOHAMMED, R., YILMA, D., BATISTA PEREIRA, D., ESPINO, F. E. & MIA, R. Z. 2019. Single-dose tafenoquine to prevent relapse of Plasmodium vivax malaria. *New England Journal of Medicine,* 380**,** 215-228.

LI, H. L., FUJIMOTO, N., SASAKAWA, N., SHIRAI, S., OHKAME, T., SAKUMA, T., TANAKA, M., AMANO, N., WATANABE, A., SAKURAI, H., YAMAMOTO, T., YAMANAKA, S. & HOTTA, A. 2015. Precise correction of the dystrophin gene in duchenne muscular dystrophy patient induced pluripotent stem cells by TALEN and CRISPR-Cas9. *Stem Cell Reports,* 4**,** 143-154.

LI, H. O., ZHU, Y. F., ASAKAWA, M., KUMA, H., HIRATA, T., UEDA, Y., LEE, Y. S., FUKUMURA, M., IIDA, A., KATO, A., NAGAI, Y. & HASEGAWA, M. 2000. A cytoplasmic RNA vector derived from nontransmissible Sendai virus with efficient gene transfer and expression. *J Virol,* 74**,** 6564-9.

LIU, H., ZHU, F., YONG, J., ZHANG, P., HOU, P., LI, H., JIANG, W., CAI, J., LIU, M., CUI, K., QU, X., XIANG, T., LU, D., CHI, X., GAO, G., JI, W., DING, M. & DENG, H. 2008. Generation of induced pluripotent stem cells from adult rhesus monkey fibroblasts. *Cell Stem Cell,* 3**,** 587-90.

LIU, W., LI, Y., SHAW, K. S., LEARN, G. H., PLENDERLEITH, L. J., MALENKE, J. A., SUNDARARAMAN, S. A., RAMIREZ, M. A., CRYSTAL, P. A., SMITH, A. G., BIBOLLET-RUCHE, F., AYOUBA, A., LOCATELLI, S., ESTEBAN, A., MOUACHA, F., GUICHET, E., BUTEL, C., AHUKA-MUNDEKE, S., INOGWABINI, B. I., NDJANGO, J. B., SPEEDE, S., SANZ, C. M., MORGAN, D. B., GONDER, M. K., KRANZUSCH, P. J., WALSH, P. D., GEORGIEV, A. V., MULLER, M. N., PIEL, A. K., STEWART, F. A., WILSON, M. L., PUSEY, A. E., CUI, L., WANG, Z., FARNERT, A., SUTHERLAND, C. J., NOLDER, D., HART, J. A., HART, T. B., BERTOLANI, P., GILLIS, A., LEBRETON, M., TAFON, B., KIYANG, J., DJOKO, C. F., SCHNEIDER, B. S., WOLFE, N. D., MPOUDI-NGOLE, E., DELAPORTE, E., CARTER, R., CULLETON, R. L., SHAW, G. M., RAYNER, J.

C., PEETERS, M., HAHN, B. H. & SHARP, P. M. 2014. African origin of the malaria parasite Plasmodium vivax. *Nat Commun,* 5**,** 3346.

LOY, D. E., LIU, W., LI, Y., LEARN, G. H., PLENDERLEITH, L. J., SUNDARARAMAN, S. A., SHARP, P. M. & HAHN, B. H. 2017. Out of Africa: origins and evolution of the human malaria parasites Plasmodium falciparum and Plasmodium vivax. *Int J Parasitol,* 47**,** 87-97.

MARCH, S., NG, S., VELMURUGAN, S., GALSTIAN, A., SHAN, J., LOGAN, D. J., CARPENTER, A. E., THOMAS, D., SIM, B. K., MOTA, M. M., HOFFMAN, S. L. & BHATIA, S. N. 2013. A microscale human liver platform that supports the hepatic stages of Plasmodium falciparum and vivax. *Cell Host Microbe,* 14**,** 104-15.

MARCH, S., RAMANAN, V., TREHAN, K., NG, S., GALSTIAN, A., GURAL, N., SCULL, M. A., SHLOMAI, A., MOTA, M. M., FLEMING, H. E., KHETANI, S. R., RICE, C. M. & BHATIA, S. N. 2015. Micropatterned coculture of primary human hepatocytes and supportive cells for the study of hepatotropic pathogens. *Nat Protoc,* 10**,** 2027-53.

MATUSCHEWSKI, K. 2006. Getting infectious: formation and maturation of Plasmodium sporozoites in the Anopheles vector. *Cellular Microbiology,* 8**,** 1547-1556.

MENDIS, K., SINA, B. J., MARCHESINI, P. & CARTER, R. 2001. The neglected burden of Plasmodium vivax malaria. *Am J Trop Med Hyg,* 64**,** 97-106.

MIKOLAJCZAK, S. A., VAUGHAN, A. M., KANGWANRANGSAN, N., ROOBSOONG, W., FISHBAUGHER, M., YIMAMNUAYCHOK, N., REZAKHANI, N., LAKSHMANAN, V., SINGH, N., KAUSHANSKY, A., CAMARGO, N., BALDWIN, M., LINDNER, S. E., ADAMS, J. H., SATTABONGKOT, J. & KAPPE, S. H. 2015. Plasmodium vivax liver stage development and hypnozoite persistence in human liver-chimeric mice. *Cell Host Microbe,* 17**,** 526-35.

MUELLER, I., GALINSKI, M. R., BAIRD, J. K., CARLTON, J. M., KOCHAR, D. K., ALONSO, P. L. & DEL PORTILLO, H. A. 2009. Key gaps in the knowledge of Plasmodium vivax, a neglected human malaria parasite. *Lancet Infect Dis,* 9**,** 555-66.

NG, S., SCHWARTZ, R. E., MARCH, S., GALSTIAN, A., GURAL, N., SHAN, J., PRABHU, M., MOTA, M. M. & BHATIA, S. N. 2015. Human iPSC-derived hepatocyte-like cells support Plasmodium liver-stage infection in vitro. *Stem Cell Reports,* 4**,** 348-59.

NOULIN, F., BORLON, C., VAN DEN ABBEELE, J., D'ALESSANDRO, U. & ERHART, A. 2013. 1912-2012: a century of research on Plasmodium vivax in vitro culture. *Trends Parasitol,* 29**,** 286-94.

OKAHARA-NARITA, J., UMEDA, R., NAKAMURA, S., MORI, T., NOCE, T. & TORII, R. 2012. Induction of pluripotent stem cells from fetal and adult cynomolgus monkey fibroblasts using four human transcription factors. *Primates,* 53**,** 205-13.

OKAMOTO, S. & TAKAHASHI, M. 2011. Induction of retinal pigment epithelial cells from monkey iPS cells. *Invest Ophthalmol Vis Sci,* 52**,** 8785-90.

OKITA, K., ICHISAKA, T. & YAMANAKA, S. 2007. Generation of germline-competent induced pluripotent stem cells. *Nature,* 448**,** 313-7.

ONOZATO, D., YAMASHITA, M., FUKUYAMA, R., AKAGAWA, T., KIDA, Y., KOEDA, A., HASHITA, T., IWAO, T. & MATSUNAGA, T. 2018. Efficient Generation of Cynomolgus Monkey Induced Pluripotent Stem Cell-Derived Intestinal Organoids with Pharmacokinetic Functions. *Stem Cells Dev,* 27**,** 1033-1045.

PEWKLIANG, Y., RUNGIN, S., LERDPANYANGAM, K., DUANGMANEE, A., KANJANASIRIRAT, P., SUTHIVANICH, P., SA-NGIAMSUNTORN, K., BORWORNPINYO, S., SATTABONGKOT, J., PATRAPUVICH, R. & HONGENG, S. 2018. A novel immortalized hepatocyte-like cell line (imHC) supports in vitro liver stage development of the human malarial parasite Plasmodium vivax. *Malar J,* 17**,** 50.

PYBUS, B. S., MARCSISIN, S. R., JIN, X., DEYE, G., SOUSA, J. C., LI, Q., CARIDHA, D., ZENG, Q., REICHARD, G. A., OCKENHOUSE, C., BENNETT, J., WALKER, L. A., OHRT, C. & MELENDEZ, V. 2013. The metabolism of primaquine to its active metabolite is dependent on CYP 2D6. *Malaria Journal,* 12**,** 212.

RABINOVICH, R. N., DRAKELEY, C., DJIMDE, A. A., HALL, B. F., HAY, S. I., HEMINGWAY, J., KASLOW, D. C., NOOR, A., OKUMU, F., STEKETEE, R., TANNER, M., WELLS, T. N. C., WHITTAKER, M. A., WINZELER, E. A., WIRTH, D. F., WHITFIELD, K. & ALONSO, P. L. 2017. malERA: An updated research agenda for malaria elimination and eradication. *PLoS Med,* 14**,** e1002456.

ROTH, A., MAHER, S. P., CONWAY, A. J., UBALEE, R., CHAUMEAU, V., ANDOLINA, C., KABA, S. A., VANTAUX, A., BAKOWSKI, M. A., LUQUE, R. T., ADAPA, S. R., SINGH, N., BARNES, S. J., COOPER, C. A., ROUILLIER, M., MCNAMARA, C. W., MIKOLAJCZAK, S. A., SATHER, N., WITKOWSKI, B., CAMPO, B., KAPPE, S. H. I., LANAR, D. E., NOSTEN, F., DAVIDSON, S., JIANG, R. H. Y., KYLE, D. E. & ADAMS, J. H. 2018. A comprehensive model for assessment of liver stage therapies targeting Plasmodium vivax and Plasmodium falciparum. *Nat Commun,* 9**,** 1837.

SATTABONGKOT, J., YIMAMNUAYCHOKE, N., LEELAUDOMLIPI, S., RASAMEESORAJ, M., JENWITHISUK, R., COLEMAN, R. E., UDOMSANGPETCH, R., CUI, L. & BREWER, T. G. 2006. Establishment of a human hepatocyte line that supports in vitro development of the exo-erythrocytic stages of the malaria parasites Plasmodium falciparum and P. vivax. *Am J Trop Med Hyg,* 74**,** 708-15.

SEKIYA, S. & SUZUKI, A. 2011. Direct conversion of mouse fibroblasts to hepatocyte-like cells by defined factors. *Nature,* 475**,** 390.

SHIMOZAWA, N., ONO, R., SHIMADA, M., SHIBATA, H., TAKAHASHI, I., INADA, H., TAKADA, T., NOSAKA, T. & YASUTOMI, Y. 2013. Cynomolgus monkey induced pluripotent stem cells established by using exogenous genes derived from the same monkey species. *Differentiation,* 85**,** 131-9.

SI-TAYEB, K., NOTO, F. K., NAGAOKA, M., LI, J., BATTLE, M. A., DURIS, C., NORTH, P. E., DALTON, S. & DUNCAN, S. A. 2010. Highly efficient generation of human hepatocyte-like cells from induced pluripotent stem cells. *Hepatology,* 51**,** 297-305.

SINHA, A., HUGHES, K. R., MODRZYNSKA, K. K., OTTO, T. D., PFANDER, C., DICKENS, N. J., RELIGA, A. A., BUSHELL, E., GRAHAM, A. L. & CAMERON, R. 2014. A cascade of DNA-binding proteins for sexual commitment and development in Plasmodium. *Nature,* 507**,** 253.

SOKHNA, C., NDIATH, M. O. & ROGIER, C. 2013. The changes in mosquito vector behaviour and the emerging resistance to insecticides will challenge the decline of malaria. *Clin Microbiol Infect,* 19**,** 902-7.

SONTAG, S., FORSTER, M., QIN, J., WANEK, P., MITZKA, S., SCHULER, H. M., KOSCHMIEDER, S., ROSE-JOHN, S., SERE, K. & ZENKE, M. 2017. Modelling IRF8 Deficient Human Hematopoiesis and Dendritic Cell Development with Engineered iPS Cells. *Stem Cells,* 35**,** 898-908.

TACHIBANA, M., SATO, C., OTSUKI, H., SATTABONGKOT, J., KANEKO, O., TORII, M. & TSUBOI, T. 2012. Plasmodium vivax gametocyte protein Pvs230 is a transmission-blocking vaccine candidate. *Vaccine,* 30**,** 1807-1812.

TAKAHASHI, K. & YAMANAKA, S. 2006. Induction of pluripotent stem cells from mouse embryonic and adult fibroblast cultures by defined factors. *Cell,* 126**,** 663-76.

THOMA, E. C., HECKEL, T., KELLER, D., GIROUD, N., LEONARD, B., CHRISTENSEN, K., ROTH, A., BERTINETTI-LAPATKI, C., GRAF, M. & PATSCH, C. 2016.

Establishment of a translational endothelial cell model using directed differentiation of induced pluripotent stem cells from Cynomolgus monkey. *Sci Rep,* 6**,** 35830.

TRAGER, W. & JENSEN, J. B. 1976. Human malaria parasites in continuous culture. *Science,* 193**,** 673-675.

TWOHIG, K. A., PFEFFER, D. A., BAIRD, J. K., PRICE, R. N., ZIMMERMAN, P. A., HAY, S. I., GETHING, P. W., BATTLE, K. E. & HOWES, R. E. 2019. Growing evidence of Plasmodium vivax across malaria-endemic Africa. *PLoS Negl Trop Dis,* 13**,** e0007140.

UDOMSANGPETCH, R., KANEKO, O., CHOTIVANICH, K. & SATTABONGKOT, J. 2008. Cultivation of Plasmodium vivax. *Trends in Parasitology,* 24**,** 85-88.

VOORBERG-VAN DER WEL, A., ZEEMAN, A. M., VAN AMSTERDAM, S. M., VAN DEN BERG, A., KLOOSTER, E. J., IWANAGA, S., JANSE, C. J., VAN GEMERT, G. J., SAUERWEIN, R., BEENHAKKER, N., KOOPMAN, G., THOMAS, A. W. & KOCKEN, C. H. 2013. Transgenic fluorescent Plasmodium cynomolgi liver stages enable live imaging and purification of Malaria hypnozoite-forms. *PLoS One,* 8**,** e54888.

WHO 2018. World Malaria Report 2018. Geneva: World Health Organization. Licence: CC BY-NC-SA 3.0 IGO.

WU, Y., ZHANG, Y., MISHRA, A., TARDIF, S. D. & HORNSBY, P. J. 2010. Generation of induced pluripotent stem cells from newborn marmoset skin fibroblasts. *Stem Cell Res,* 4**,** 180-8.

WUNDERLICH, S., HAASE, A., MERKERT, S., BEIER, J., SCHWANKE, K., SCHAMBACH, A., GLAGE, S., GOHRING, G., CURNOW, E. C. & MARTIN, U. 2012. Induction of pluripotent stem cells from a cynomolgus monkey using a polycistronic simian immunodeficiency virus-based vector, differentiation toward functional cardiomyocytes, and generation of stably expressing reporter lines. *Cell Reprogram,* 14**,** 471-84.

WUNDERLICH, S., KIRCHER, M., VIETH, B., HAASE, A., MERKERT, S., BEIER, J., GOHRING, G., GLAGE, S., SCHAMBACH, A., CURNOW, E. C., PAABO, S., MARTIN, U. & ENARD, W. 2014. Primate iPS cells as tools for evolutionary analyses. *Stem Cell Res,* 12**,** 622-9.

XIANG, C., DU, Y., MENG, G., SOON YI, L., SUN, S., SONG, N., ZHANG, X., XIAO, Y., WANG, J., YI, Z., LIU, Y., XIE, B., WU, M., SHU, J., SUN, D., JIA, J., LIANG, Z., SUN, D., HUANG, Y., SHI, Y., XU, J., LU, F., LI, C., XIANG, K., YUAN, Z., LU, S. & DENG, H. 2019. Long-term functional maintenance of primary human hepatocytes in vitro. *Science,* 364**,** 399-402.

YOON, S., KANG, K., CHO, Y. D., KIM, Y., BUISSON, E. M., YIM, J. H., LEE, S. B., RYU, K. Y., JEONG, J. & CHOI, D. 2018. Nonintegrating Direct Conversion Using mRNA into Hepatocyte-Like Cells. *Biomed Res Int,* 2018**,** 8240567.

ZEEMAN, A. M., VAN AMSTERDAM, S. M., MCNAMARA, C. W., VOORBERG-VAN DER WEL, A., KLOOSTER, E. J., VAN DEN BERG, A., REMARQUE, E. J., PLOUFFE, D. M., VAN GEMERT, G. J., LUTY, A., SAUERWEIN, R., GAGARING, K., BORBOA, R., CHEN, Z., KUHEN, K., GLYNNE, R. J., CHATTERJEE, A. K., NAGLE, A., ROLAND, J., WINZELER, E. A., LEROY, D., CAMPO, B., DIAGANA, T. T., YEUNG, B. K., THOMAS, A. W. & KOCKEN, C. H. 2014. KAI407, a potent non-8-aminoquinoline compound that kills Plasmodium cynomolgi early dormant liver stage parasites in vitro. *Antimicrob Agents Chemother,* 58**,** 1586-95.

ZIMMERMAN, P. A. 2017. Plasmodium vivax Infection in Duffy-Negative People in Africa. *Am J Trop Med Hyg,* 97**,** 636-638.

Chapter II

Persistence of *Plasmodium cynomolgi* hypnozoites in cynomolgus monkey iPS-derived hepatocytes

Submitted manuscript

Persistence of *Plasmodium cynomolgi* hypnozoites in cynomolgus monkey iPS-derived hepatocytes

Mélanie Pellisson[1,2,3], Anne-Marie Zeeman[4], Thierry Doll[3], Lucy Kirchhofer-Allan[5], Sven Schuierer[3], Guglielmo Roma[3], Erika Flannery[5], Sebastian Mikolajczak[5], Clemens H. M. Kocken[4], Pascal Mäser[1,2], Matthias Rottmann[1,2*], Matthias Müller[3*]

Affiliations

[1]Swiss Tropical and Public Health Institute (SwissTPH), Basel, Switzerland.

[2]University of Basel, Basel, Switzerland.

[3]Novartis Institutes for Biomedical Research, Novartis Pharma AG, Basel, Switzerland.

[4]Biomedical Primate Research Centre, Department of Parasitology, Rijswijk, The Netherlands.

[5]Novartis Institute for Tropical Diseases, Novartis Pharma AG, Emeryville, United States.

*Correspondence to: matthias.mueller@novartis.com or matthias.rottmann@swisstph.ch

Abstract

Plasmodium cynomolgi (P. cynomolgi) is one of the few parasite species that forms quiescent liver stage parasites known as hypnozoites and is therefore a suitable model for *Plasmodium vivax*. Very little is known about liver stage dormancy, which hampers the search for compounds with anti-hypnozoite activity. Here, we present the development of a *P. cynomolgi* in vitro infection model using stem cell-derived hepatocytes from *Macaca fascicularis.* IPS cells were established on feeder free condition and differentiated into hepatocytes via inducible overexpression of key transcription factors. The generated hepatocytes were infected with *P. cynomolgi* sporozoites and hypnozoite formation as well as schizont development were confirmed by immunofluorescence. This system is a promising tool to study the mechanisms underlying liver stage dormancy and facilitate drug discovery against hypnozoites.

Introduction

In 2017, malaria had an estimated global incidence of 219,000,000 and a death toll of 435,000 (WHO, 2018). Thus, in spite of the recent successes in the fight against malaria (Rabinovich et al., 2017), the disease remains to be a main killer in the tropics. Malaria being anthroponotic, elimination and even eradication are theoretically possible. However, in addition to drug-resistant *Plasmodium* parasites and insecticide-resistant *Anopheles* mosquitoes (Ashley et al., 2018), there is an ultimate hindrance to malaria eradication: the hypnozoites (Campo et al., 2015). Hypnozoites are small, uninucleated, intracellular stages that stay dormant for months or even years in the liver of infected carriers (Krotoski et al., 1982, Dembele et al., 2014), building a hidden reservoir of parasites that, upon reactivation, causes relapsing malaria. Primaquine and tafenoquine are the only drugs that eliminate hypnozoites (Llanos-Cuentas et al., 2019), but their use is limited due to severe side effects in glucose-6-phosphate dehydrogenase-deficient patients (a common genetic trait in malaria endemic countries). Therefore, new molecules with anti-hypnozoite activity are needed.

Very little is known about the biology of hypnozoites, and the mechanisms underlying dormancy and reactivation remain to be elucidated. Most studies on *Plasmodium vivax* (*P. vivax)* hypnozoites have been conducted with human primary hepatocytes as host cells. These, however, present problems regarding quality, donor-to-donor variability, and ethical considerations. Moreover, working with *P. vivax* is challenging as there is no long term in vitro culture system and sporozoite sourcing is extremely limited (Tachibana et al., 2012). The best surrogate organism for *P. vivax* is *P. cynomolgi*, a closely related and more accessible malaria parasite of non-human primates that also produces hypnozoites (Krotoski et al., 1980). Here we present for the first time a solution that overcomes the limitations of both *P. vivax* in vitro work and primary host cell usage by establishing an in vitro system for *P. cynomolgi* hypnozoites that uses cynomolgus monkey hepatocyte-like cells generated by induced pluripotent stem (iPS) cells technology.

Methods

Primary cells

Cynomolgus monkey fibroblasts used for iPS cell generation were obtained from ZenBio (monkey PDF091812) and Novartis (monkey 5501). Cynomolgus monkey primary hepatocytes were purchased from Biopredic. Human dermal fibroblasts used for iPS and hepatocyte generation were purchased from Invitrogen and human primary hepatocytes from KaLy-Cell. The donors provided written informed consents.

Cynomolgus monkey iPS (cynIPS) cell generation

Primary cynomolgus monkey dermal fibroblasts were reprogrammed using Sendai viruses of CytoTune-iPS 2.0 Sendai Reprogramming Kit (Life Technologies, A16517) according to the standard protocol. Cells and viruses were plated on irradiated mouse embryonic fibroblasts (Merck Millipore, PMEF-CF1) and cultivated with human embryonic stem cell (hESC) medium [KnockOut DMEM; 4.5 g/L glucose, 0.11 g/L sodium pyruvate, without glutamine (Gibco, 10829018), 20% KnockOut Serum Replacement (Gibco, 10828028), 1% glutaMAX (Gibco, 35050038), 1% MEM Non-Essential Amino Acids (NEAA) (Gibco, 11140035), 1% penicillin/streptomycin (Gibco, 15140-122), 10 ng/mL human basic fibroblast growth factor (bFGF) (Invitrogen, 13256029), and 0.1% β-mercaptoethanol (Gibco, 31350010)]. Colonies with hallmark of pluripotent morphology were readily visible between 2-3 weeks after transduction. These pluripotent colonies were picked and subcloned multiple times either on feeder cells or on Matrigel (BD Biosciences, 354277) coated plates in hESC or mTeSR1 medium (Stem Cell Technologies, 05850). This serial subcloning was performed until remnants of Sendai virus RNA were no longer detected and the morphology looked stable. As constant bFGF activity is essential for cynIPS maintenance, mTeSR1 medium was progressively replaced by StemFlex medium (Gibco, A3349401) which allows maintenance of bFGF levels over time. Pluripotency was assessed by immunofluorescence staining, fluorescence-activated cell sorting (FACS) analysis, and differentiation potential in all three germ layers (see sections below). Karyotype of each selected line was checked by array Comparative Genomic Hybridization (aCGH method) (Cell Line Genetics) and all showed a normal karyotype.

Flow cytometry analysis for bFGF experiment and iPS characterization

CynIPS cells were dissociated with TryplE (Invitrogen, 12604), followed by fixation and permeabilization using Cytofix/Cytoperm reagent (BD Biosciences, 554655 and 51-20S1KZ) according to the manufacturer. Cells were stained with Nanog-PE (BD Biosciences, 560589a), Oct3/4-PerCP (BD Biosciences, 560794) and Sox2-A647 (BD Biosciences, 562139) intracellular primary antibodies for 45 min at 4 °C, washed twice with ice cold Cytoperm reagent and re-suspended in 1% fetal calf serum (FCS) in phosphate buffered saline (PBS) (Invitrogen, 14190). Cells were subsequently analyzed on a CyAn flow cytometer (Beckmann Coulter).

Karyotyping

For each tested cell line, 1.5E05 cells were seeded onto a T25 Matrigel coated flask in StemFlex medium supplemented with 10 µM rock inhibitor (Merck Millipore, Y-27632). Medium was refreshed the following day without rock inhibitor and lived cells were sent over to Cell Line Genetics when 20-30% confluence was reached. Karyotype of each selected line was checked by aCGH method.

Differentiation potential

1. Endoderm differentiation

Endodermal cells were induced from cynIPS cells using STEMdiff Definitive Endoderm (DE) Kit (Stem Cell Technologies, 05110). CynIPS cells were seeded onto a 24-well plate (TPP, 92024) coated with Matrigel and cultivated with StemFlex medium until culture reached 95-100% confluence. Cells were washed with PBS and medium was switched to STEMdiff medium with 1% DE supplements A and B. The next day, medium was switched to STEMdiff medium with 1% DE supplement B. Medium was changed every day. Cells were fixed after 5 days of differentiation with 4% paraformaldehyde (Electron Microscopy Sciences, 15714) in PBS and immunofluorescence staining was performed with forkhead box A2 (FoxA2) (1:50 dilution, Abcam, ab60721) and Oct4 (1:1,000 dilution, Stemgent, 09-0023) primary antibodies.

2. Ectoderm differentiation

Neuronal precursors were differentiated from cynIPS cells using a modified dual Smad inhibition protocol. 6E04 undifferentiated iPS cells were seeded onto a 96-well ultra-low attachment (ULA) plate (Costar, 7007) in 0.1 mL StemFlex medium with 10 ng/mL penicillin/streptomycin and 10 µM rock inhibitor to prevent apoptosis. 24 hours after seeding, Embryoid Bodies (EBs) were formed and 0.1 mL fresh StemFlex medium were added to the wells. The next day, 30 EBs were transferred to a 4-well Matrigel coated plate with StemFlex medium (7 or 8 EBs seeded per well). 6 hours later, StemFlex medium was replaced by neural induction medium (20% KnockOut™ Serum Replacement, 0.1 mM MEM NEAA, 0.1 mM β-mercaptoethanol, 75% DMEM/F12/glutaMAX; 1% penicillin/streptomycin, 10 ng/mL human bFGF, 10 µM SB431542 (Tocris, 1614), and 1 µM LDN193189 (Stemgent, 04-0074). Medium was changed every other day until day 13. Cells were fixed after 14 days of differentiation with 4% paraformaldehyde in PBS for 10 min at room temperature and immunofluorescence staining was performed with βIII-tubulin (1:5,000 dilution, Sigma, T8660), 200 kDa neurofilament

(NF200) (1:6,000 dilution, Abcam, ab72996), neuronal nuclei (NeuN) (1:500 dilution, Merck Millipore, ABN78), and Oct4 (1:1,000 dilution, Stemgent, 09-0023) primary antibodies.

3. Mesoderm differentiation

6E04 undifferentiated cynIPS cells were seeded onto a 96-well ULA plate in 0.1 mL StemFlex medium with 10 ng/mL penicillin/streptomycin and 10 µM rock inhibitor to prevent apoptosis. 24 hours after seeding, EBs were formed and 0.1 mL fresh StemFlex medium were added to the wells. The next day, medium was replaced by STEMdiff Mesoderm Induction Medium (Stem Cell Technologies, 05220). Medium was refreshed daily until spontaneous EB contraction was observed after 10 days of differentiation (Movie S1).

Generation of cynomolgus monkey hepatocyte-like cells (cynHLCs)

CynIPS cells were harvested and seeded (1.1E05 cells/well) onto a 96-well plate (Greiner, 655090) coated with Laminin 521 (Biolamina, LN521) in StemFlex medium supplemented with 100 µg/mL geneticin (G418) (Gibco, 10131035), and 10 µM rock inhibitor. The next day, cells were washed with PBS and differentiation was started (day 0) in Chemically Defined Medium (CDM) [50% IMDM (Invitrogen, 31980030), 50% DMEM/F12 (HAM) (Invitrogen, A14625DJ), 1% Insulin-Transferrin-Selenium (ITS) (Invitrogen, 51500056), 0.1% CD Lipid Concentrate (Invitrogen, 11905031) and 2% bovine serum albumin (BSA) (Sigma, A7979)] supplemented with 1 µg/mL doxycycline (Dox). The next day, medium was changed with CDM supplemented with 1 µg/mL Dox. On day 2, medium was switched to William's E medium (no phenol red, Gibco, A1217601) with Primary Hepatocyte Maintenance Supplements (Gibco, CM4000) and 1 µg/mL Dox. Medium was refreshed the next day. On day 4, Dox induction was stopped and William's E medium containing Primary Hepatocyte Maintenance Supplements was supplemented with 5 µM of a combination of compounds (doramapimod, dihydroorotate dehydrogenase (DHODH) inhibitor, and rapidly accelerated fibrosarcoma (Raf) inhibitor) to maintain cynHLCs until 17 days of differentiation. Medium was refreshed daily.

Generation of human hepatocyte-like cells (HLCs)

Human iPS cells were harvested and seeded onto a 96-well Laminin 521 coated plate (8E04 cells/well) in mTeSR1 medium supplemented with 100 µg/mL G418 and 10 µM rock inhibitor. The next day (day 0), cells were washed with PBS and differentiated for 3 days in CDM supplemented with 1 µg/mL Dox (medium was refreshed daily). On day 3, medium was switched to William's E medium with Primary Hepatocyte Maintenance Supplements and 1

µg/mL Dox. Medium was refreshed on day 4 and 5. On day 6, Dox induction was stopped and cells were further differentiated in William's E medium containing Primary Hepatocyte Maintenance Supplements until day 25. Medium was refreshed every other day.

Immunofluorescence analysis

Cells were fixed with 4% paraformaldehyde in PBS, permeabilized with Triton X-100 (Sigma, T8787) in PBS and stained with primary antibodies visualized with appropriate fluorescently labeled secondary antibodies (Alexa Fluor®). Cultures were counterstained with the nuclear marker Hoechst (Invitrogen, 33342) and immunostained samples were imaged using a Zeiss LSM 700 microscope. Primary and secondary antibodies references can be found in Table S1.

Periodic Acid Schiff (PAS) staining (Sigma, 395-1KT)

Fixed samples were rinsed with deionized water and then placed in 0.5% periodic acid aqueous solution for 5 min at room temperature. Samples were then rinsed with running tap water for 3 min and quickly rinsed with deionized water before being placed in Schiff reagent solution for 15 min. The same rinsing steps as described above were used and samples were then counterstained with hematoxylin for 2 min. Samples were rinsed with deionized water for 3 min. Samples were rinsed twice with 70% ethanol, twice with 96% ethanol and twice with 100% ethanol for 1 min each. Samples were covered with PBS before imaging.

Oil Red O staining

Fixed samples were washed twice with deionized water and placed in 60% isopropanol for 5 min. 30 mL Oil Red O stock solution (60 mg Oil Red O (BioVision, K580-24-3) in 20 mL 100% isopropanol) was mixed with 20 mL deionized water and filtered using a 0.2 µm syringe filter to make Oil Red O working solution. Samples were incubated with working solution for 15 min and then washed two to five times with deionized water until excess stain was no longer apparent. Samples were counterstained with hematoxylin (BioVision, K580-24-2) for 1 min. Samples were washed two to five times with deionized water before imaging.

Enzyme-linked immunosorbent assay (ELISA)

To assess albumin secretion capacity of hepatocytes, cynIPS cells were harvested and seeded onto a 24-well Laminin 521 coated plate (7.5E05 cells/well) and differentiated as previously described. Culture medium was collected every 24 hours before the next medium change. ELISA assay was performed with the collected supernatants according to the provider standard protocol (Immunology Consultants Laboratory, E-80AL).

Hepatocyte survival screen

CynIPS cells were harvested and 2.5E04 cells/well were seeded using a multidrop dispenser onto 384-well Laminin 521 coated plates (Corning, 3712) in StemFlex medium supplemented with 100 µg/mL G418, and 10 µM rock inhibitor. Cells were differentiated as described above until day 4. At day 4, Dox induction was stopped, medium was replaced by William's E medium with Primary Hepatocyte Maintenance Supplements and cells were treated with the Novartis compound library in the Echo® Liquid Handling platform (Labcyte Inc.). Cells were returned to overnight incubation at 37 °C, 5% CO_2. Cells were treated with the Novartis compound library every other day after medium change. At day 13, bright field images of all plates were acquired with a high-throughput high-content imaging system (Operetta, PerkinElmer) and CellTiter-Glo luminescent cell viability assay (Promega, G7570) was performed. Luminescent readings were obtained using an EnVision multilabel plate reader (PerkinElmer) after 10 min incubation at room temperature. Generated data were analyzed in TIBCO Spotfire® (TIBCO Software Inc.).

RNA sequencing

Total RNA was isolated using the Direct-zol RNA MiniPrep Kit (Zymo Research, R2071) including on-column deoxyribonuclease (DNase) digestion according to the manufacturer's instructions. RNA sequencing libraries were prepared using the Illumina TruSeq RNA Sample Prep kit v2 (Illumina, RS-122-2001) and sequenced using the Illumina HiSeq2500 platform. Samples were sequenced to a length of 2 x 76 base pairs. Read pairs from cynomolgus iPS cells, HLCs, and primary hepatocytes were mapped to the *Macaca fascicularis* genome and the cynomolgus gene transcripts from Refseq by using an in-house gene quantification pipeline (Schuierer and Roma, 2016). The human genome (hg38) was used for the mapping of human HLCs, primary hepatocytes, and liver related cancer cell lines. Genome and transcript alignments were used to calculate gene counts based on Ensembl gene IDs.

Generation of *P. cynomolgi* sporozoites

The Biomedical Primate Research Centre (BPRC) is an AAALAC-certified institute. All rhesus macaques (*Macaca mulatta*) used in this study were captive bred for research purposes and were housed at the BPRC facilities in compliance with the Dutch law on animal experiments, European directive 2010/63/EU, and with the Standard for Human Care and Use of Laboratory Animals by Foreign institutions, identification number A5539-01, provided by the National Institutes of Health (NIH). Prior to the start of experiments, all protocols were approved by the local independent ethical committee, according to Dutch law. For each batch of infected mosquitoes, one rhesus macaque was infected with 1E06 *P. cynomolgi* M strain blood stage parasites and bled at peak parasitaemia, after which the monkey was cured from the malaria infection by intramuscular injection of 7.5 mg/kg chloroquine on three consecutive days. Approximately 1,200 female *Anopheles stephensi* mosquitoes strain Sind-Kasur Nijmegen (Nijmegen University Medical Centre St. Radboud, Department of Medical Microbiology) were fed with this blood using an ex vivo glass feeder system.

Sporozoite inoculation of cynHLCs

Sporozoite inoculation of cynHLCs was performed at Novartis according to the methods of Dembélé et al. (Dembele et al., 2014). *P. cynomolgi* sporozoites were isolated at the BPRC and shipped to Novartis in Leibovitz L15 medium (Invitrogen, 11415-056) with 3% FCS and 2% penicillin/streptomycin at 4 °C to ensure good sporozoite infectiousness. Upon arrival, 4-days differentiated cynHLCs were infected with different sporozoite densities in 96-well plates. Cultures were kept at 37 °C in 5% CO_2 with daily medium changes. To evaluate the development of *P. cynomolgi* liver stages, cultures were fixed with 4% paraformaldehyde at the indicated time points.

Immunofluorescence staining of liver stage parasites

Infected hepatocytes were fixed with 4% paraformaldehyde for 30 min, followed by overnight incubation at 4 °C with rabbit primary antibodies against *P. cynomolgi* 70 kilodalton heat shock proteins (Hsp70) and rat primary antibodies against *P. cynomolgi* upregulated in infective sporozoites gene 4 protein (UIS4) both diluted in 1% BSA and 0.3% Triton X-100 in PBS solution. Subsequently, donkey secondary immunoglobulin G (IgG) Alexa Fluor® 555-conjugated anti-rabbit antibodies (1:1,000 dilution, Invitrogen, A31572), chicken secondary IgG Alexa Fluor® 594-conjugated anti-rat antibodies (1:1,000 dilution, Invitrogen, A21471)

were added for three hours at room temperature. Nuclei were counterstained with Hoechst for 10 min at room temperature, samples were finally covered with PBS and viewed under an inverted microscope (Leica DMI6000 or Zeiss LSM 700). Image acquisition and post processing were performed with proprietary Leica or Zeiss software, LAS X or Zen 2012 respectively. Primary and secondary antibodies references can be found in Table S1.

Statistical analysis

Data are presented as mean ± standard deviation (Stdev). "n" refers to biological replicates. $P < 0.05$ was considered statistically significant (ns, not significant ($P > 0.05$); $^{*}P < 0.05$; $^{**}P < 0.01$; $^{***}P < 0.001$; $^{****}P < 0.0001$). GraphPad Prism 7 (GraphPad Software) was used for statistical analyses. In Fig. 13C, one-way analysis of variance (ANOVA) was used to compare the groups followed by Dunnett post hoc test.

Results

CynIPS cells were generated from dermal skin fibroblasts from two different monkeys by reprogramming, using Sendai viruses bearing the transcription factors Oct3/4, Sox2, Klf4, and c-Myc (Takahashi and Yamanaka, 2006). Pluripotent colonies appeared two to three weeks after infection and were kept on irradiated mouse embryonic fibroblasts. After several passages, the iPS cells were transferred on Matrigel, but spontaneous differentiation occurred on this feeder-less system (Fig. 1A). Further investigations showed that a higher concentration of basic fibroblast growth factor (bFGF) was essential to maintain these cynomolgus cells in an undifferentiated state (Fig. 1B).

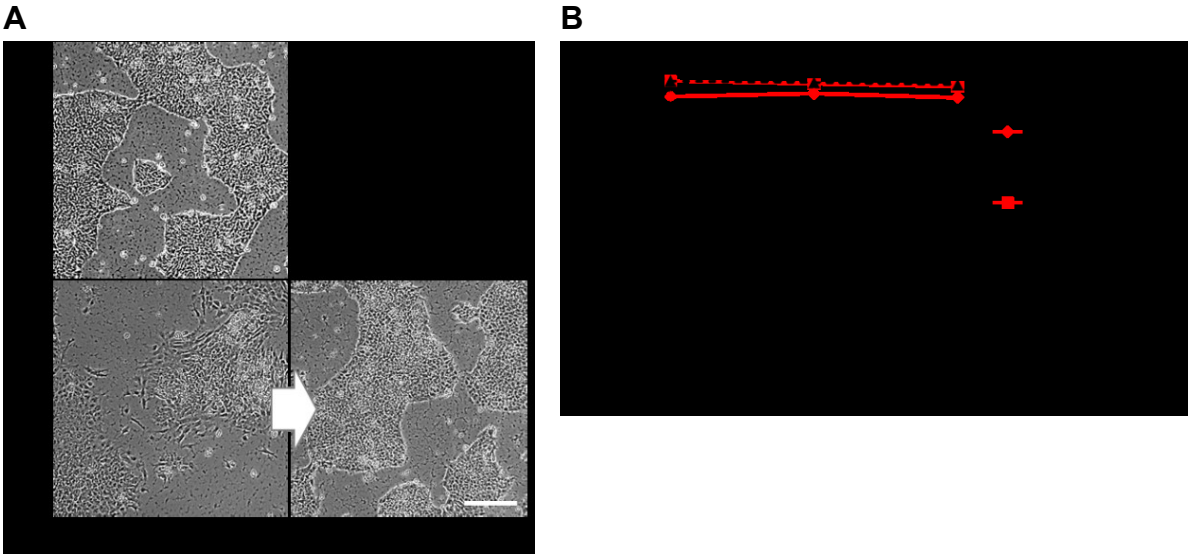

Fig. 1. Cynomolgus vs. human iPS cell maintenance after generation. A, Brightfield images of human (h) and cynomolgus (cyn) iPS cells. CynIPS spontaneously differentiated when cultivated with mTeSR1 medium. Switching to StemFlex medium with stabilized bFGF was essential for cynIPS cell maintenance. Scale bar, 200 µm. **B,** FACS analysis of human and cynomolgus iPS cells (cultivation +/- bFGF) with Oct4 and Sox2 pluripotent markers.

Following the clonal expansion phase, clones exhibiting typical human embryonic stem cell-like morphology (flat and tightly packed colonies of round cells with large nuclei) were selected and fully characterized by immunofluorescence (Figs. 2 and 3). Based on this result the best clone (#13) was selected and checked for karyotype (Fig. 4), and differentiation potential into the three germ layers (Fig. 5 and Movie S1).

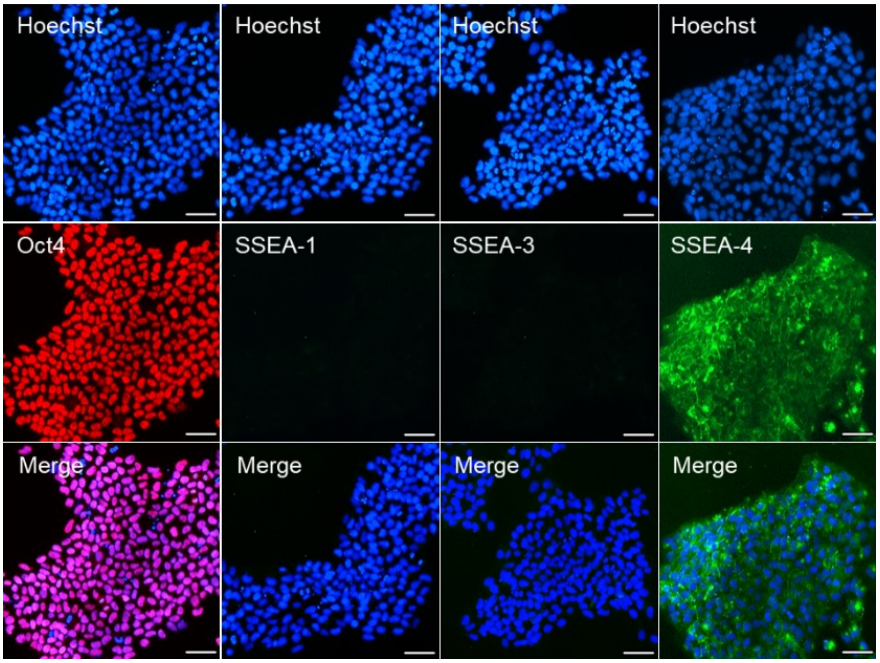

Fig. 2. Selected clone #13 from monkey PDF091812. Immunofluorescence analysis of Oct4 (red), and stage-specific embryonic antigens (SSEA-1, SSEA-3, and SSEA-4) (green) in cynIPS cells. Nuclei were counterstained with Hoechst (blue). Scale bars, 50 µm.

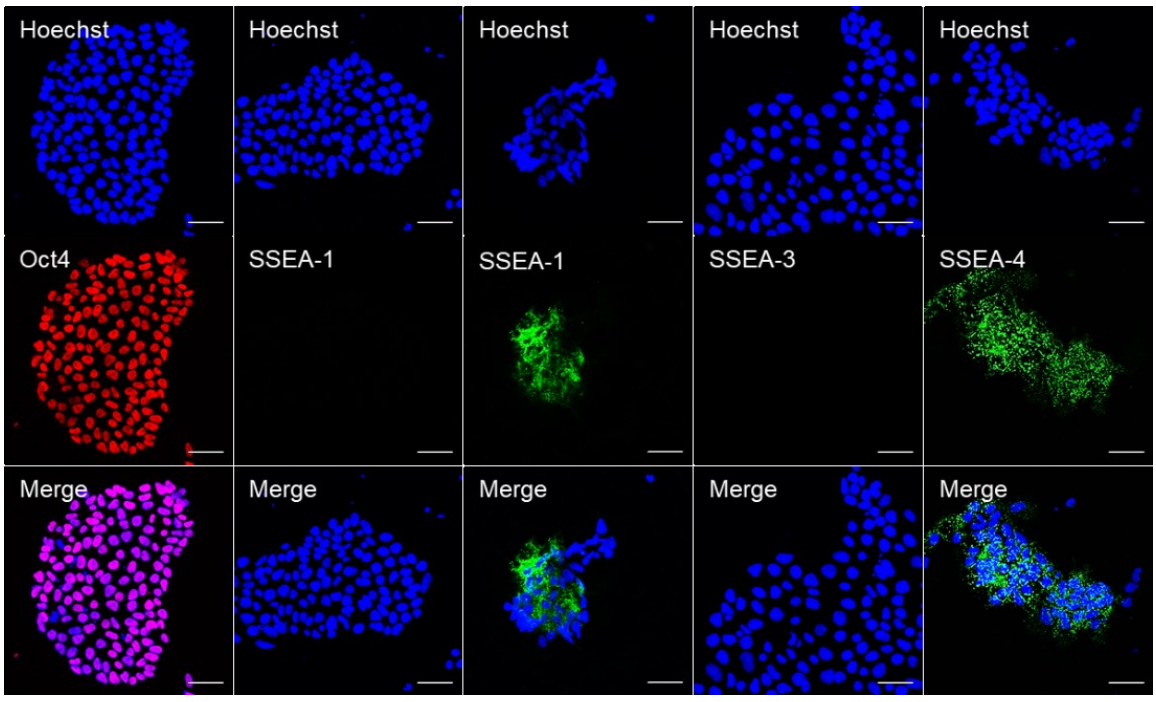

Fig. 3. Example of a clone not selected based on SSEA-1 expression. Immunofluorescence analysis of an iPS clone from monkey 5501 of Oct4 (red), SSEA-1, SSEA-3, and SSEA-4 (green). Nuclei were counterstained with Hoechst (blue). Scale bars, 50 µm.

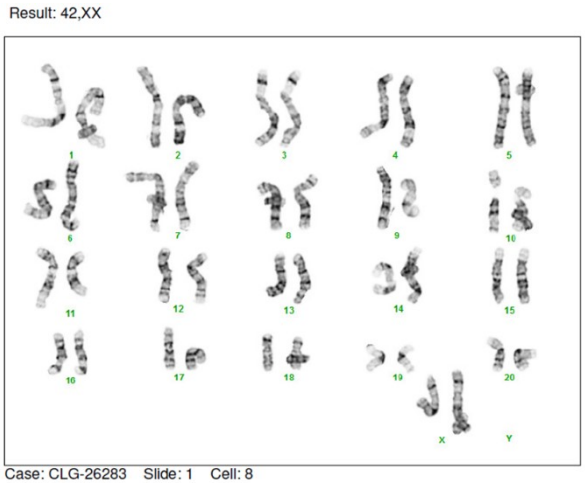

Fig. 4. Karyotype analysis of cynIPS cells from clone #13 by array Comparative Genomic Hybridization method.

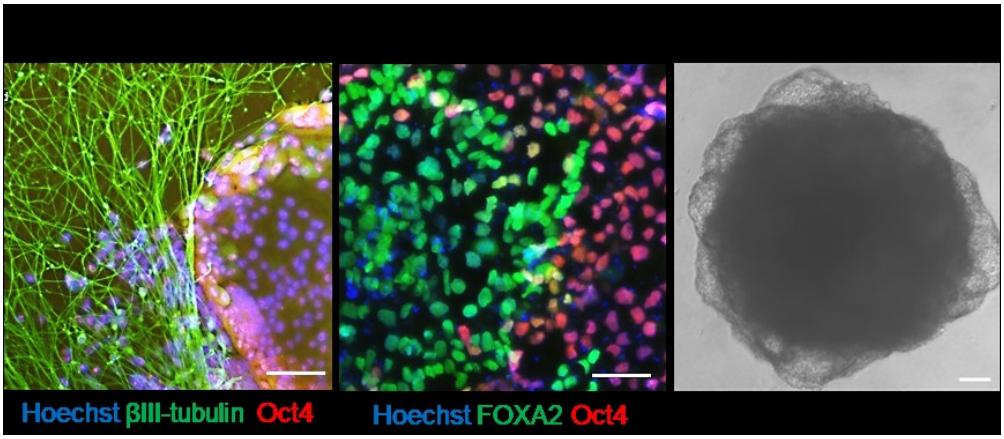

Fig. 5. Differentiation potential of cynIPS cells from clone #13. Upon stimulation, cells expressed βIII-tubulin (green, ectoderm marker), FOXA2 (green, endoderm marker) and contracted spontaneously after EB formation (mesoderm). Non-responsive cells remained pluripotent and expressed Oct4 (red). Nuclei were counterstained with Hoechst (blue). Scale bars, 100 µm.

The generation of human hepatocytes from stem cells is a well-known process and diverse protocols have been developed (Chen et al., 2012, Gao et al., 2017, Si-Tayeb et al., 2010), but the translation of this process to cynomolgus cells required extensive tailoring. The stepwise approach, which consists of adding growth factors mimicking liver embryogenesis, was not robust and reproducible enough (data not shown). Therefore, we used a direct differentiation approach to generate cynomolgus monkey hepatocyte-like cells (cynHLCs) by overexpressing essential transcription factors for hepatic lineage formation (Huang et al., 2014). Using an inducible construct based on a tetracycline ON/OFF system (Fig. 6), hepatocyte nuclear factor 4 homeobox A (HNF4A) and forkhead box protein A3 (FOXA3) were overexpressed in cynIPS cells to drive endoderm formation and hepatocyte maturation (Kang et al., 2018, Yoon et al., 2018).

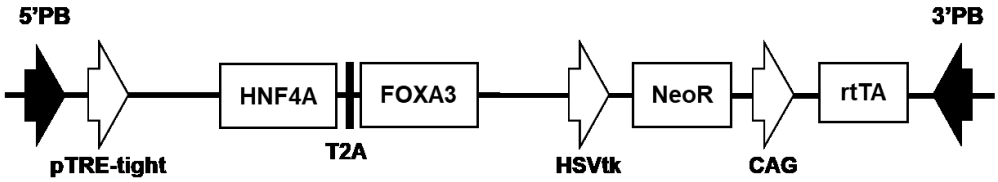

Fig. 6. Schematic representation of the Dox-inducible construct. PB: PiggyBac DNA transposon; TRE: TET responsive element; HNF4A: Coding sequence of hepatocyte nuclear factor 4 alpha; FOXA3: Coding sequence forkhead box protein A3); T2A: self-cleavage peptides from *Thosea asigna* virus; HSVtk: Minimal promoter fragment from the HSV thymidine kinase promoter; NeoR: neomycin resistance gene; CAG: chicken β-actin promoter; rtTA: TET transactivator protein gene.

Briefly, a confluent pluripotent cell population was induced for 4 days with doxycycline (Dox), and hepatic progenitor cells were further matured for 2 days to generate cynHLCs (Fig. 7). CynHLCs produced from clone HNF4A/FOXA3-#13.5 displayed the best hepatic characteristics, such as albumin (ALB), hepatocyte nuclear factor 1 homeobox A (HNF1A), HNF4A, α1-antitrypsin (A1AT), cytokeratin 18 (KRT18), α-fetoprotein (AFP), and forkhead box A2 (FOXA2) expression (Figs. 8A and B) and high levels of albumin secretion (Fig. 9A). Additional characterization methods revealed accumulation of lipid droplets (Oil Red O staining) and glycogen storage (Periodic Acid Schiff staining), which are attributes of hepatocytes (Fig. 9B).

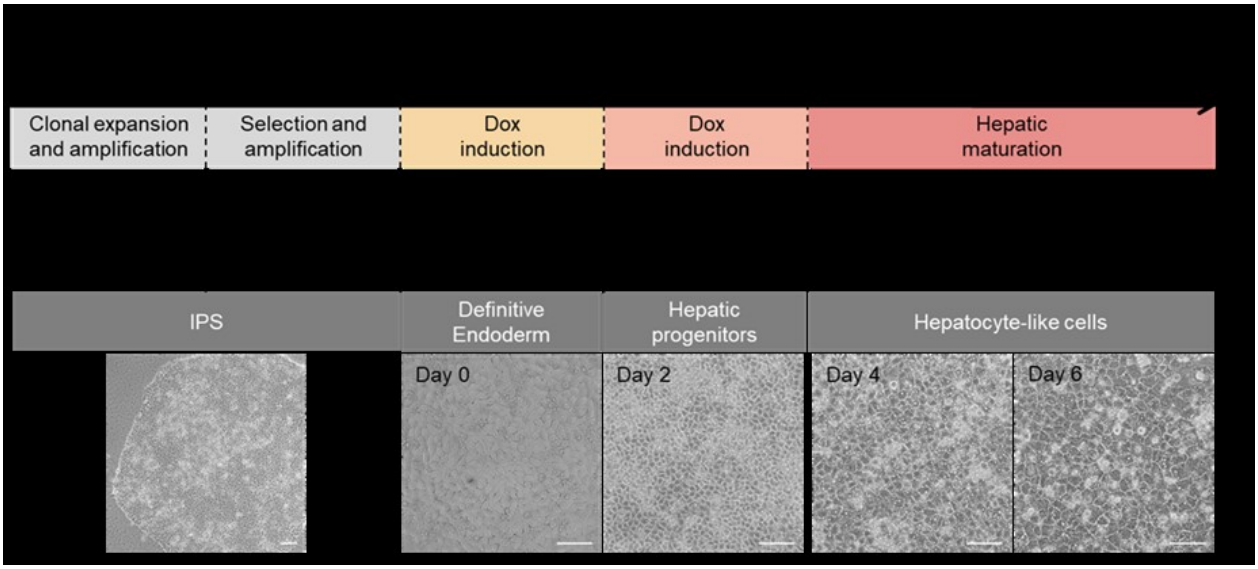

Fig. 7. CynHLCs generation from iPS cells. Schematic representation of the differentiation protocol and brightfield images of differentiating cynIPS cells at the indicated time points. G418: geneticin; Dox: doxycycline. Scale bars, 100 µm.

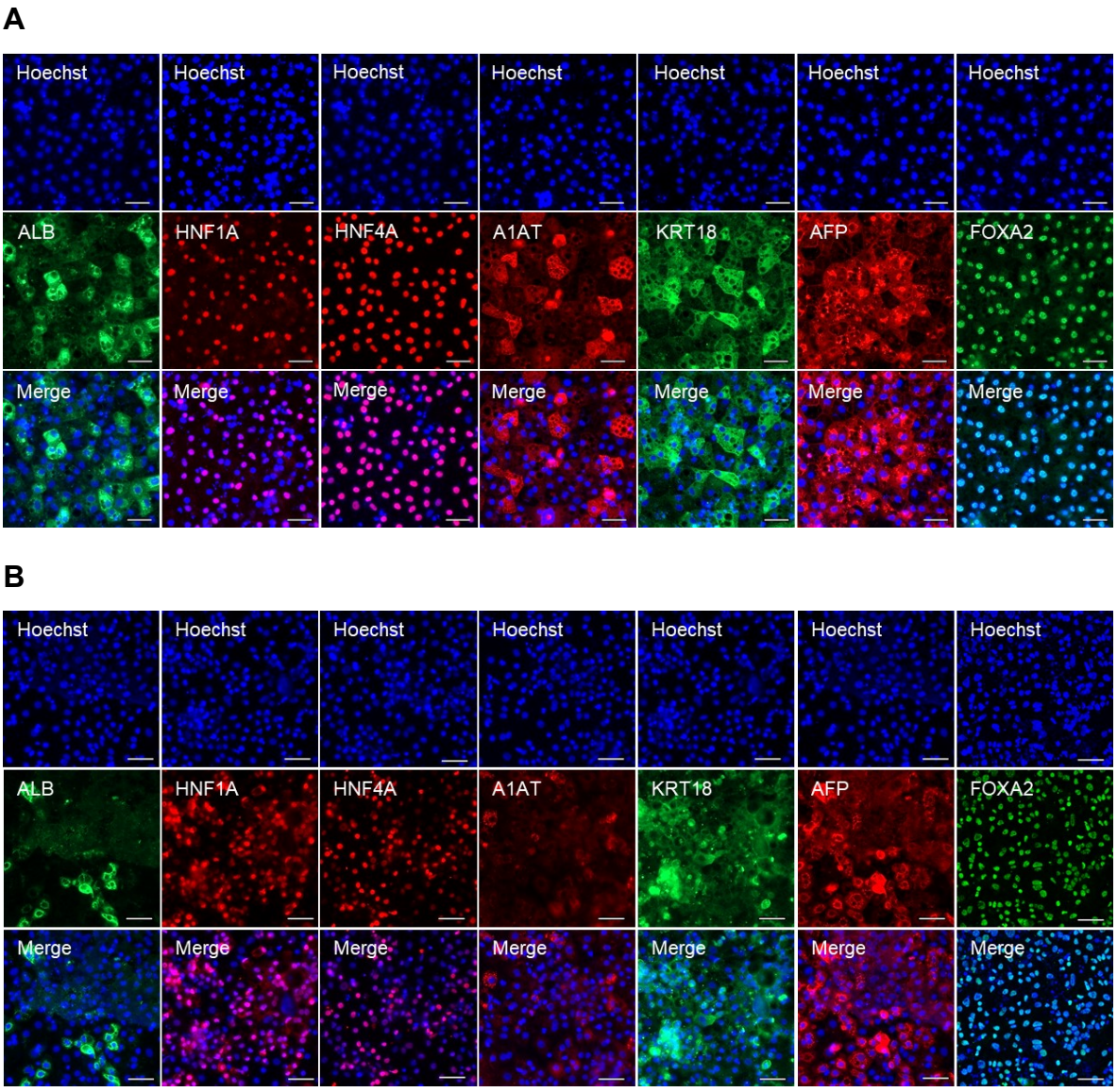

Fig. 8. Immunofluorescence of cynHLCs at day 6 of selected clone #13.5 (**A**) and clone #13.6 (**B**) with antibodies to HNF1A, HNF4A, AFP, A1AT (red), ALB, KRT18, and FOXA2 (green). Nuclei were visualized with Hoechst (blue). Scale bars, 50 µm.

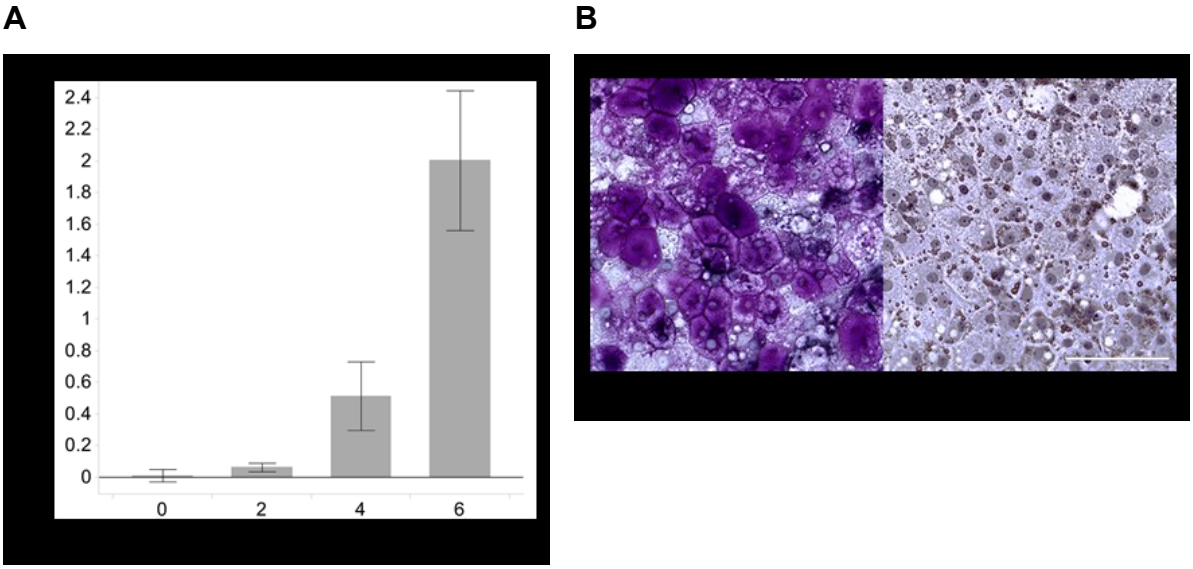

Fig. 9. A, Enzyme-linked immunosorbent assay (ELISA) for ALB in the supernatants at indicated time points. n=3. **B,** Periodic Acid Schiff (PAS) and Oil Red O staining of cynHLCs after 10 days of differentiation. Scale bar, 100 μm.

RNA-seq analysis of cynHLCs confirmed the hepatic signature of the generated cells (Fig. 10). Comparison with human HLCs as well as liver cancer cell lines (HepG2 and Huh7) showed a very high similarity on the mRNA expression profile. While differentiating, the obtained cynHLCs lost expression of pluripotent markers and expressed typical hepatic progenitor genes and mature hepatic genes including efflux transporters at day 7. We also assessed the expression of known *Plasmodium* host entry receptors such as cluster of differentiation 81 (CD81) and scavenger receptor class B type 1 (SRB1) in the generated cynHLCs. Expression of SRB1 and CD81 was confirmed in cynHLCs at the mRNA level during the differentiation process (Fig. 11A). CD81 was gradually expressed in iPS (day 0) and differentiating cells. In contrast, SRB1 was weakly expressed in iPS cells but highly and constantly after day 3, suggesting that cynHLCs become permissive to *Plasmodium* only when they acquire a hepatic signature (Ng et al., 2015). CynHLCs were infected after 4 days of differentiation, when they expressed hallmark hepatic markers like ALB, HNF4A, and AFP in addition to the host entry receptors SRB1 and CD81 (Fig. 11B). Although SRB1 was already highly expressed at day 3, *P. cynomolgi* sporozoite inoculation was performed at day 4 to avoid potential parasite inhibition due to doxycycline (Gaillard et al., 2015, Pang et al., 1988).

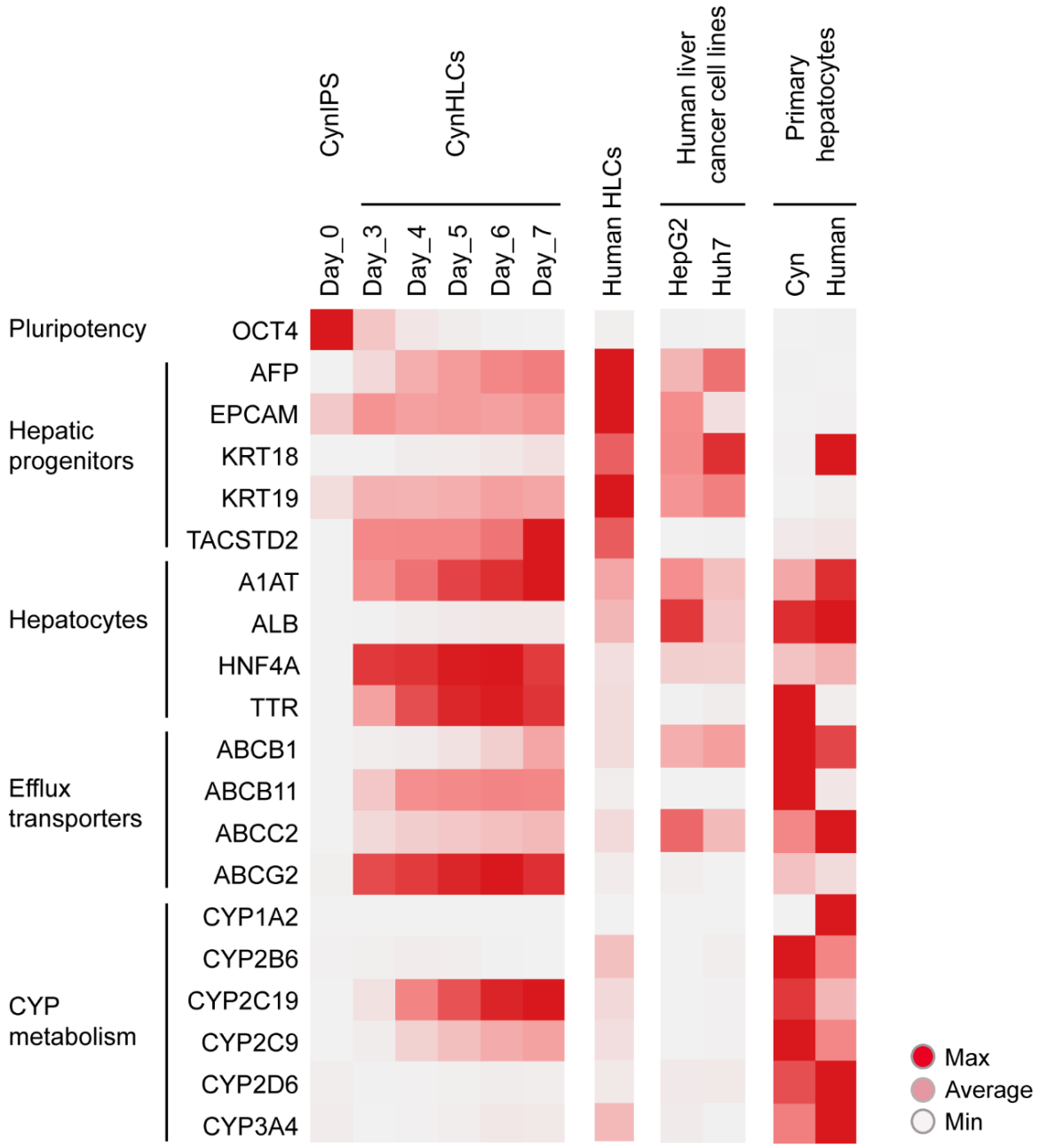

Fig. 10. Heatmap of the RNA-seq based mean expression of cynIPS cells (Day_0), cynHLCs (Day_3 to Day_7), human HLCs, human liver cancer cell lines (HepG2 and Huh7), and primary hepatocytes for selected genes indicative of cell types (pluripotency, hepatic progenitors, and hepatocytes) or cellular processes (efflux transporters and CYP metabolism). Expression values in transcripts per million (tpm) are colored relative to the maximum (red) and minimum (white) expression value for each gene.

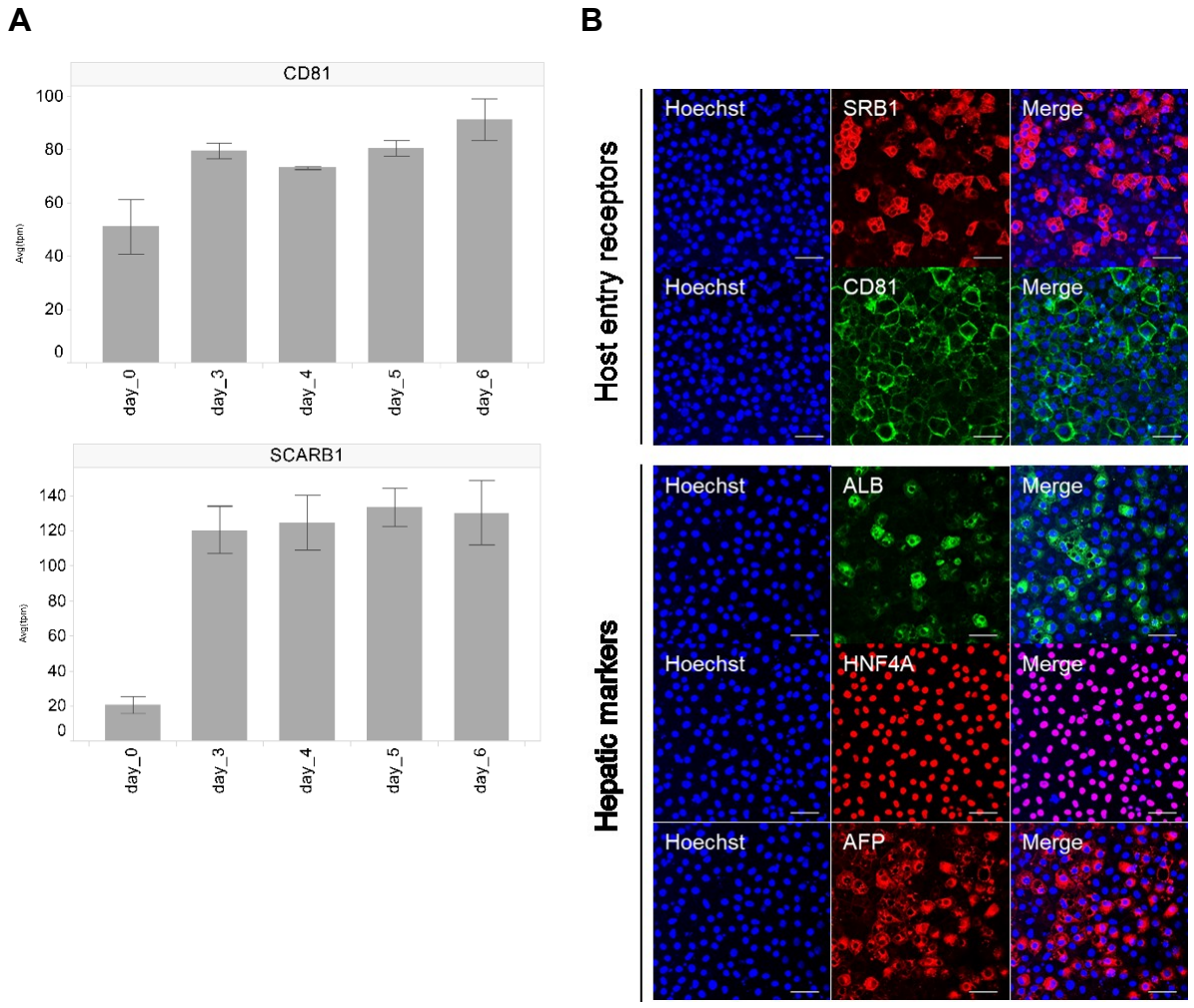

Fig. 11. Hepatic signature and expression of host entry receptors indicate permissiveness of cynHLCs to *Plasmodium* parasite. A, Bar charts representing mRNA levels in tpm of SRB1 (SCARB1) and CD81 at day 0, 3, 4, 5, and 6. Error bars represent standard deviation. n=3. **B,** Immunofluorescence of cynHLCs at day 4 with antibodies to the hepatic markers ALB (green), HNF4A (red), and AFP (red) and to the host entry receptors SRB1 (red) and CD81 (green). Nuclei were visualized with Hoechst (blue). Scale bars, 50 µm.

While the differentiation process was extremely fast with the cynomolgus cells, the maintenance of the hepatic stage was challenging. After 8 days of differentiation, cynHLCs started to detach and died. In order to improve cell survival, we conducted a screen against an in-house chemical library of well-characterized compounds. Three hit compounds that improved cell viability were identified: a stress-activated protein kinase 2/p38β (SAPK2/p38β) inhibitor named doramapimod, a dihydroorotate dehydrogenase (DHODH) inhibitor, and a rapidly accelerated fibrosarcoma (Raf) inhibitor (Fig. 12).

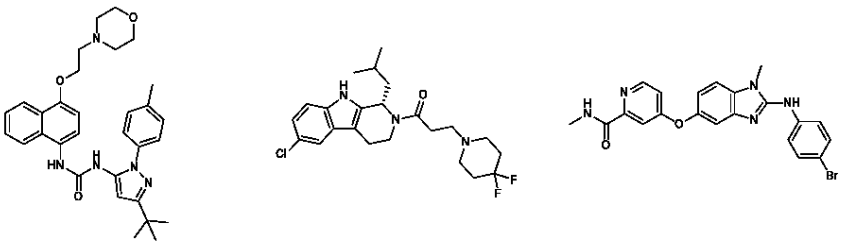

Doramapimod DHODH inhibitor Raf inhibitor

Compound name	IUPAC name	Canonical Smiles
Doramapimod	1-[5-tert-butyl-2-(4-methylphenyl)pyrazol-3-yl]-3-[4-(2-morpholin-4-ylethoxy)naphthalen-1-yl]urea	CC1=CC=C(C=C1)N2C(=CC(=N2)C(C)(C)C)NC(=O)NC3=CC=C(C4=CC=CC=C43)OCCN5CCOCC5
DHODH inhibitor	1-[(1S)-6-chloro-1-(2-methylpropyl)-1,3,4,9-tetrahydropyrido[3,4-b]indol-2-yl]-3-(4,4-difluoropiperidin-1-yl)propan-1-one	CC(C)CC1C2=C(CCN1C(=O)CCN3CCC(CC3)(F)F)C4=C(N2)C=CC(=C4)Cl
Raf inhibitor	4-[2-(4-bromoanilino)-1-methylbenzimidazol-5-yl]oxy-N-methylpyridine-2-carboxamide	CNC(=O)C1=NC=CC(=C1)OC2=CC3=C(C=C2)N(C(=N3)NC4=CC=C(C=C4)Br)C

Fig. 12. Chemical structures of the hit compounds identified in survival screen (doramapimod, DHODH inhibitor, and Raf inhibitor) and table displaying the International Union of Pure and Applied Chemistry (IUPAC) names and the canonical smiles of each compound.

Daily treatment with a mix containing the three hits enhanced hepatocyte survival up to 17 days of differentiation (Fig. 13A) and maintained ALB and HNF4 expression (Fig. 13B). With the triple combination, cell viability remained constant from day 6 to day 12 whereas it dramatically decreased when cells were not treated (DMSO control) or treated with only one hit compound (Fig. 13C). Although the treated cynHLCs showed a more precursor-like mRNA signature than untreated cynHLCs (Fig. 14), the triple combination allows now to study liver stage parasite development for at least 12 days, a timeframe necessary to investigate the dormant stage of malaria.

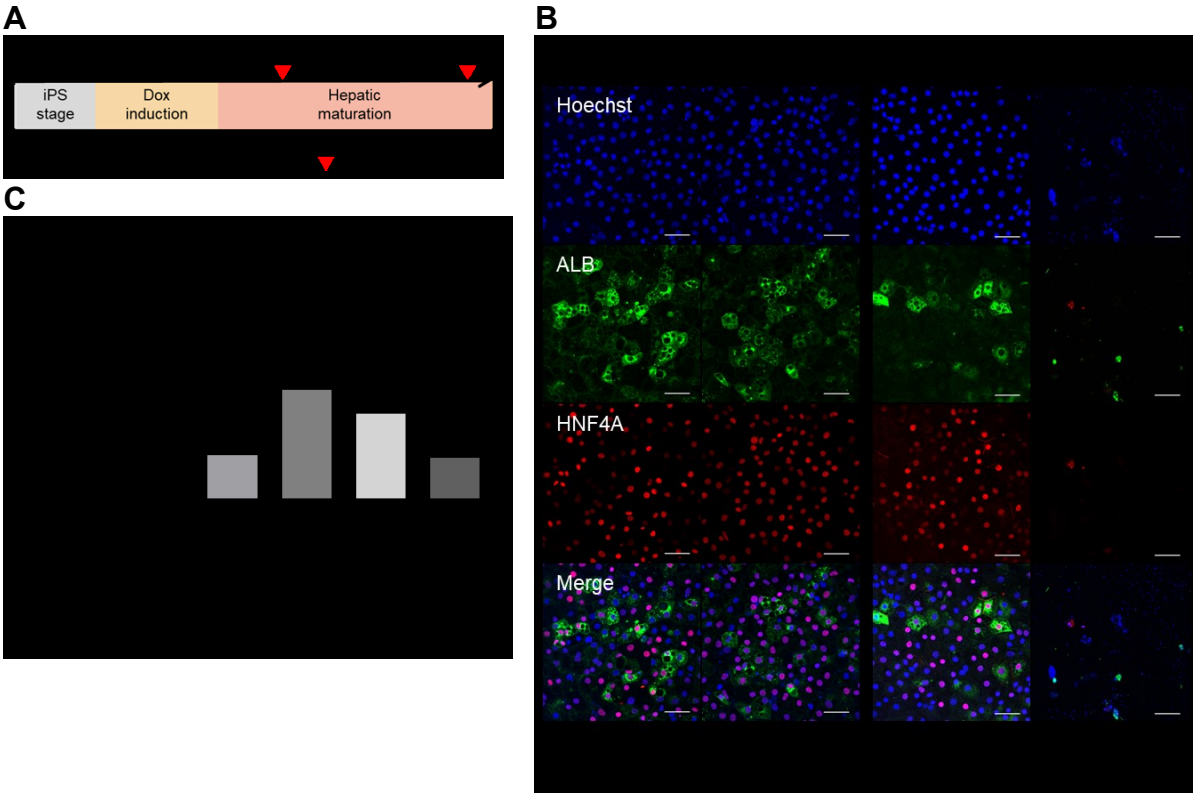

Fig. 13. Survival screen allows identification of compounds that improve cynHLCs longevity. A, Schematic representation of the experiment conducted to assess the effect of hit compounds identified to promote cynHLCs survival. Cells were treated daily from day 4 (D4) to day 12 (D12). **B,** Immunofluorescence at day 6 and 12 of treated (triple combination) and untreated (DMSO control) cynHLCs with antibodies to ALB (green) and HNF4A (red). Nuclei were visualized with Hoechst (blue). Scale bars, 50 µm. **C,** Bar chart representing the nuclei counts of treated and untreated cynHLCs at day 12. Error bars represent standard deviation. n=3.

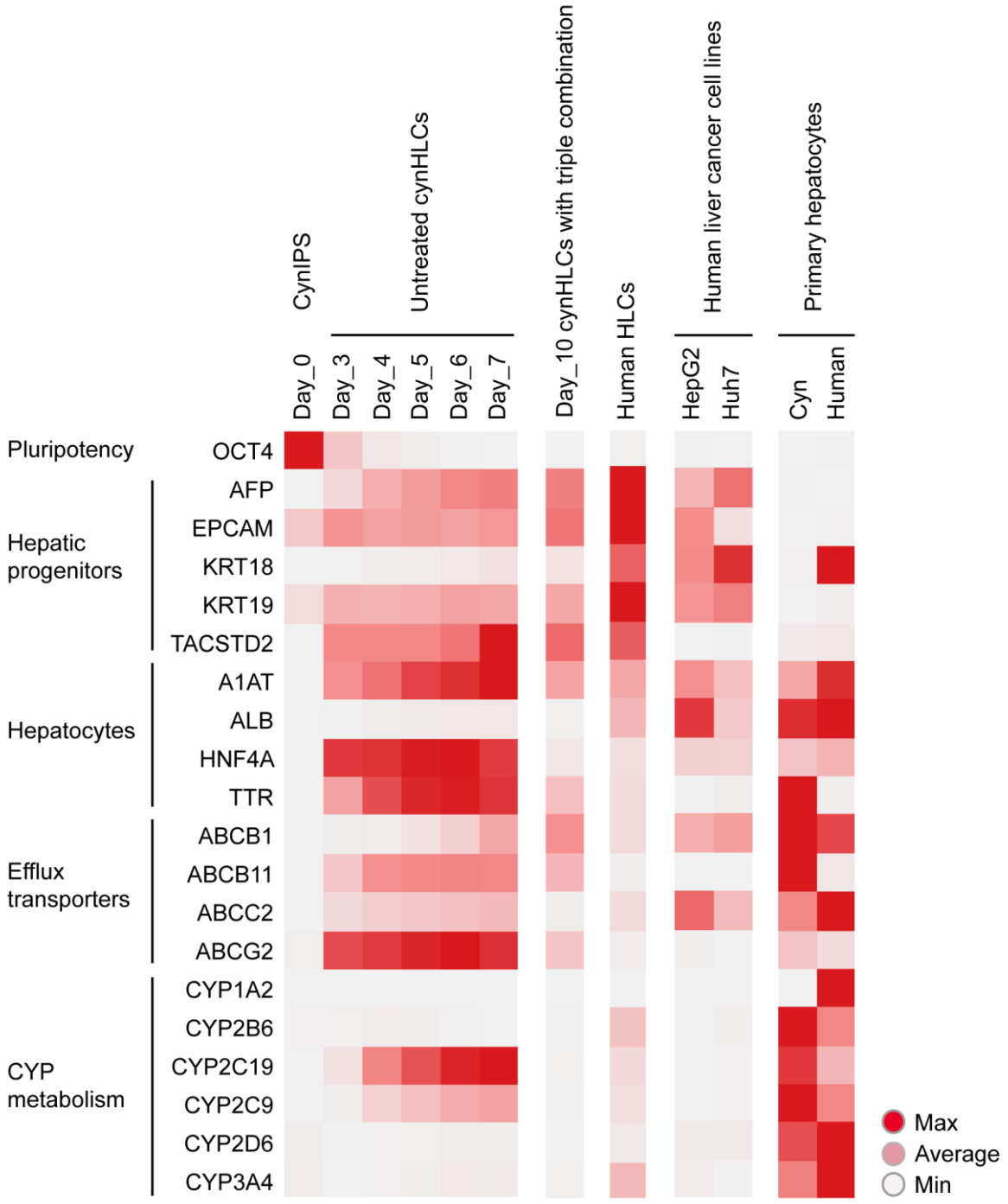

Fig. 14. Heatmap of the RNA-seq based mean expression of cynIPS cells (Day_0), cynHLCs (Day_7 untreated and Day_10 triple combination), and human HLCs for selected genes indicative of cell types (pluripotency, hepatic progenitors, and hepatocytes) or cellular processes (efflux transporters and CYP metabolism). Expression values in transcripts per million (tpm) are colored relative to the maximum (red) and minimum (white) expression value for each gene.

Infection of 4-days differentiated cynHLCs was performed with freshly isolated *P. cynomolgi* sporozoites from *Anopheles stephensi* mosquitoes. We detected the first liver stage parasites at 2 days post-infection (dpi) after fixation and staining with *P. cynomolgi* anti-Hsp70 (70 kilodalton heat shock proteins) antibodies. An additional staining with antibodies against UIS4 (up regulated in infective sporozoites gene 4) confirmed that the parasitophorous vacuole membrane (PVM) of liver stage parasites was formed (Bertschi et al., 2018). At 2 dpi, we observed a uniform population of uninucleated parasites with a size of 3 µm (Fig. 15A). Despite the low infection rate of less than 10 parasites per well in a 96-well plate, two populations of liver stage parasites were clearly distinguishable by 4 dpi. The first (Fig. 15B) was composed of stationary parasites that stayed uninucleated over time (Dembele et al., 2014). The second population (Fig. 15C) was composed of growing and multinucleated forms, which would lead to the formation of liver schizonts. It is currently unclear if a PVM prominence detected by anti-UIS4 antibodies would be a reliable hypnozoite-specific marker (Gural et al., 2018, Mikolajczak et al., 2015, Schafer et al., 2018). In our system, PVM prominence was found in a subset of developing liver stage parasites (Fig. 16) which would suggest that PVM prominence is not sufficient to discriminate between dormant and developing liver stage parasites. Therefore, in the absence of a *P. cynomolgi* hypnozoite-specific marker, we defined a hypnozoite as a small, round liver stage parasite (diameter <8 µm) containing a single nucleus. In comparison, a developing schizont is bigger in size and contains at least two nuclei. Small and uninucleated forms were observed until 12 dpi. As previously described (Mikolajczak et al., 2015), the dormant parasites were slightly increasing in size (from 3 µm at 4 dpi to 5 µm at 12 dpi), but the single nucleus observed by Hoechst staining confirmed the quiescent state of these liver stage parasites. The current conditions did not allow us to visualize hypnozoite reactivation and subsequent development into mature liver schizonts as described for *P. cynomolgi* in primary cynomolgus monkey hepatocytes (Dembele et al., 2014).

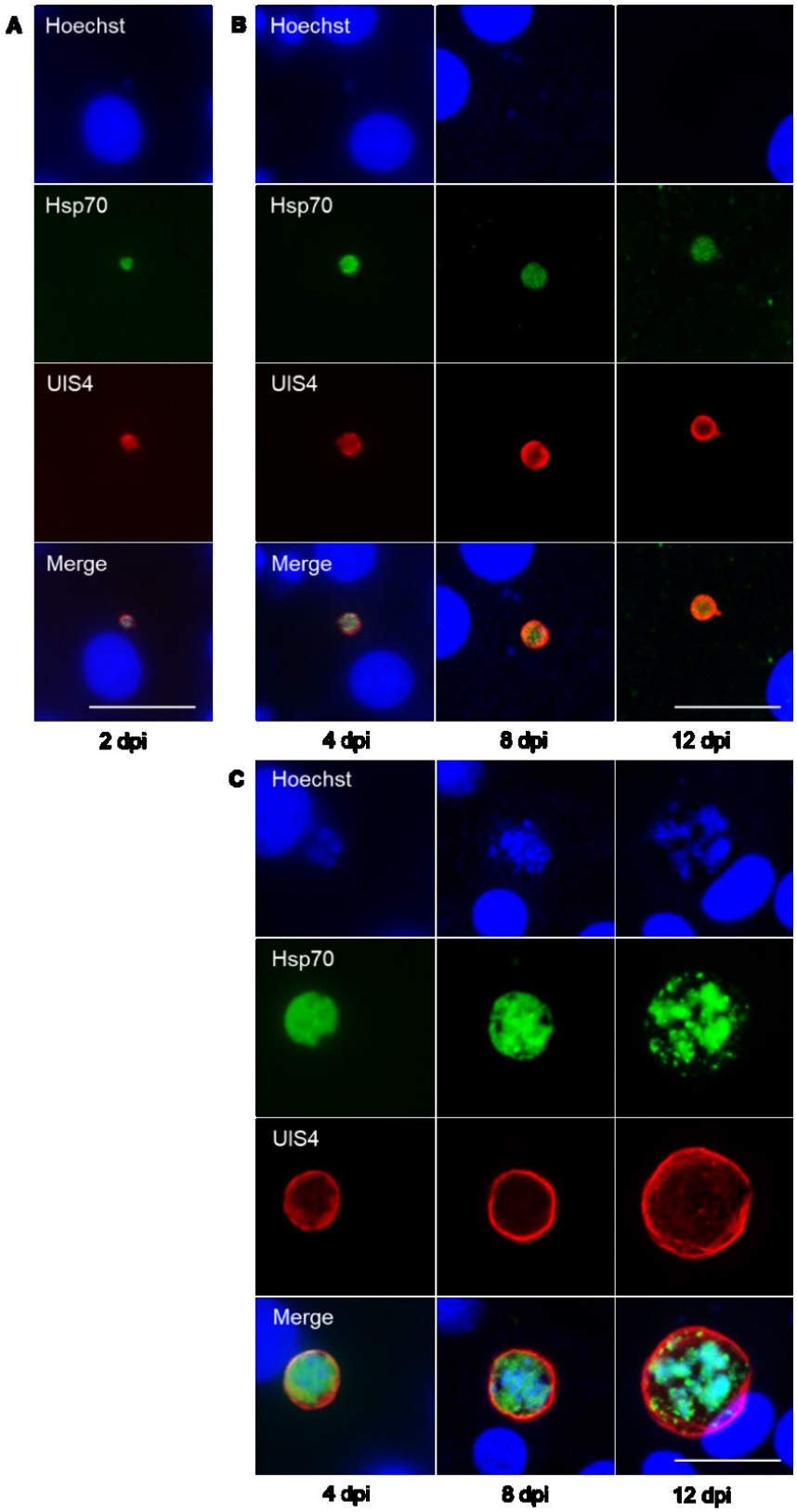

Fig. 15. Infection of cynHLCs with *P. cynomolgi* sporozoites. Immunofluorescence of liver stage parasites with antibodies specific for *P. cynomolgi*-Hsp70 (green) and *P. cynomolgi*-UIS4 (red) at 2 dpi (**A**), 4-12 dpi small forms (**B**) and 4-12 dpi large forms (**C**). Cell nuclei and parasite DNA were visualized with Hoechst (blue). Scale bars, 20 µm.

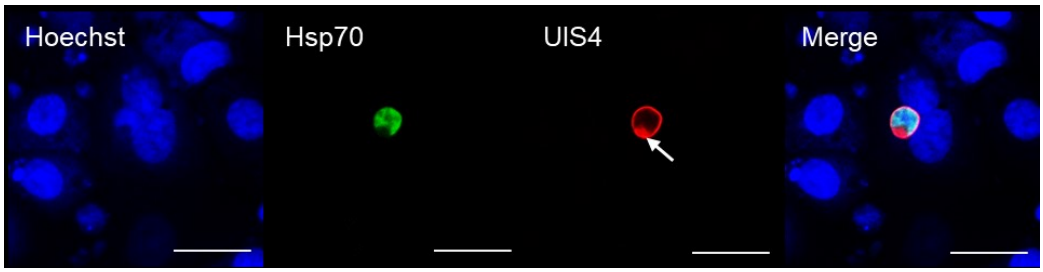

Fig. 16. Prominence (white arrow) observed in a subset of schizonts. All liver stage parasites were visualized with antibodies specific for *P. cynomolgi* Hsp70 (green) and UIS4 (red). Host cell nuclei and parasite DNA content were visualized with Hoechst (blue). Scale bars, 20 µm.

In summary, we report for the first time the generation of cynHLCs from the *P. cynomolgi* natural host *Macaca fascicularis*. Infection of these host cells with *P. cynomolgi* sporozoites resulted in successful formation of hypnozoites and persistence until 12 dpi. Moreover, combining the iPS technology with in vitro cultured *P. cynomolgi* erythrocytic stages would make the *P. cynomolgi* system more accessible and more importantly, largely independent of primates. In conclusion, this iPS-based in vitro system provides a promising alternative to investigate the dormant stage of malaria in the liver and may facilitate drug screening for compounds with activity against hypnozoites.

Acknowledgments: We thank Isabelle Fruh, Bettina Leonhard, Carole Manneville, and Annick Werner for continuous support with iPS technology; Nicole van der Werff, Ivonne Nieuwenhuis, and Lars Vermaat for mosquito dissection and sporozoite preparation; Annemarie Voorberg-van der Wel for helpful discussions regarding infection assay and critical reading of the manuscript; Isabelle Claerr for technical assistance with high content imaging; Olaf Galuba for support in conducting the survival screen; Dominic Trojer for help in microscopy; Volker Heussler for insightful discussions; Benoit Fischer and Marianne Uteng for providing RNA samples from cynomolgus monkey primary hepatocytes; Judith Knehr and Walter Carbone for RNA-sequencing; and the Walter Fischli-Foundation, the Bill and Melinda Gates Foundation and the Medicines for Malaria Venture for financial support. **Funding:** This work was supported by the Walter Fischli-Foundation, the Bill and Melinda Gates Foundation (OPP1141292) and the Medicines for Malaria Venture. **Author contributions:** M.M., M.R., and P.M.: Conception and design, data analysis and interpretation, manuscript writing; M.P.: Conception and design, collection and assembly of data, data analysis and interpretation, manuscript writing; A.M.Z.: Provision of sporozoites, data analysis and interpretation; G.R., S.S.: Analysis of RNA-seq experiment; A.M.Z., C.H.M.K., E.F., G.R., L.K.A., M.M., M.R., P.M., S.M., S.S., and T.D.: Final approval of manuscript. **Competing interests:** E.F., G.R., L.K.A., M.M., S.M., S.S., and T.D. are employed by and/or shareholders of Novartis Pharma AG. The authors declare no competing interests. **Data and materials availability:** All data are available in the main text or the supplementary materials.

References

ASHLEY, E. A., PYAE PHYO, A. & WOODROW, C. J. 2018. Malaria. *Lancet,* 391**,** 1608-1621.

BERTSCHI, N. L., VOORBERG-VAN DER WEL, A., ZEEMAN, A. M., SCHUIERER, S., NIGSCH, F., CARBONE, W., KNEHR, J., GUPTA, D. K., HOFMAN, S. O., VAN DER WERFF, N., NIEUWENHUIS, I., KLOOSTER, E., FABER, B. W., FLANNERY, E. L., MIKOLAJCZAK, S. A., CHUENCHOB, V., SHRESTHA, B., BEIBEL, M., BOUWMEESTER, T., KANGWANRANGSAN, N., SATTABONGKOT, J., DIAGANA, T. T., KOCKEN, C. H. & ROMA, G. 2018. Transcriptomic analysis reveals reduced transcriptional activity in the malaria parasite Plasmodium cynomolgi during progression into dormancy. *Elife,* 7.

CAMPO, B., VANDAL, O., WESCHE, D. L. & BURROWS, J. N. 2015. Killing the hypnozoite--drug discovery approaches to prevent relapse in Plasmodium vivax. *Pathog Glob Health,* 109**,** 107-22.

CHEN, Y. F., TSENG, C. Y., WANG, H. W., KUO, H. C., YANG, V. W. & LEE, O. K. 2012. Rapid generation of mature hepatocyte-like cells from human induced pluripotent stem cells by an efficient three-step protocol. *Hepatology,* 55**,** 1193-203.

DEMBELE, L., FRANETICH, J. F., LORTHIOIS, A., GEGO, A., ZEEMAN, A. M., KOCKEN, C. H., LE GRAND, R., DEREUDDRE-BOSQUET, N., VAN GEMERT, G. J., SAUERWEIN, R., VAILLANT, J. C., HANNOUN, L., FUCHTER, M. J., DIAGANA, T. T., MALMQUIST, N. A., SCHERF, A., SNOUNOU, G. & MAZIER, D. 2014. Persistence and activation of malaria hypnozoites in long-term primary hepatocyte cultures. *Nat Med,* 20**,** 307-12.

GAILLARD, T., MADAMET, M. & PRADINES, B. 2015. Tetracyclines in malaria. *Malaria Journal,* 14**,** 445.

GAO, Y., ZHANG, X., ZHANG, L., CEN, J., NI, X., LIAO, X., YANG, C., LI, Y., CHEN, X., ZHANG, Z., SHU, Y., CHENG, X., HAY, D. C., LAI, D., PAN, G., WEI, G. & HUI, L. 2017. Distinct Gene Expression and Epigenetic Signatures in Hepatocyte-like Cells Produced by Different Strategies from the Same Donor. *Stem Cell Reports,* 9**,** 1813-1824.

GURAL, N., MANCIO-SILVA, L., MILLER, A. B., GALSTIAN, A., BUTTY, V. L., LEVINE, S. S., PATRAPUVICH, R., DESAI, S. P., MIKOLAJCZAK, S. A., KAPPE, S. H. I., FLEMING, H. E., MARCH, S., SATTABONGKOT, J. & BHATIA, S. N. 2018. In Vitro Culture, Drug Sensitivity, and Transcriptome of Plasmodium Vivax Hypnozoites. *Cell Host Microbe,* 23**,** 395-406 e4.

HUANG, P., ZHANG, L., GAO, Y., HE, Z., YAO, D., WU, Z., CEN, J., CHEN, X., LIU, C., HU, Y., LAI, D., HU, Z., CHEN, L., ZHANG, Y., CHENG, X., MA, X., PAN, G., WANG, X. & HUI, L. 2014. Direct reprogramming of human fibroblasts to functional and expandable hepatocytes. *Cell Stem Cell,* 14**,** 370-84.

KANG, K., KIM, Y., JEON, H., LEE, S. B., KIM, J. S., PARK, S. A., KIM, W. D., YANG, H. M., KIM, S. J., JEONG, J. & CHOI, D. 2018. Three-Dimensional Bioprinting of Hepatic Structures with Directly Converted Hepatocyte-Like Cells. *Tissue Eng Part A,* 24**,** 576-583.

KROTOSKI, W. A., GARNHAM, P. C., BRAY, R. S., KROTOSKI, D. M., KILLICK-KENDRICK, R., DRAPER, C. C., TARGETT, G. A. & GUY, M. W. 1982. Observations on early and late post-sporozoite tissue stages in primate malaria. I. Discovery of a new latent form of Plasmodium cynomolgi (the hypnozoite), and failure to detect hepatic forms within the first 24 hours after infection. *Am J Trop Med Hyg,* 31**,** 24-35.

KROTOSKI, W. A., KROTOSKI, D. M., GARNHAM, P. C., BRAY, R. S., KILLICK-KENDRICK, R., DRAPER, C. C., TARGETT, G. A. & GUY, M. W. 1980. Relapses in primate malaria: discovery of two populations of exoerythrocytic stages. Preliminary note. *Br Med J,* 280**,** 153-4.

LLANOS-CUENTAS, A., LACERDA, M. V. G., HIEN, T. T., VÉLEZ, I. D., NAMAIK-LARP, C., CHU, C. S., VILLEGAS, M. F., VAL, F., MONTEIRO, W. M., BRITO, M. A. M., COSTA, M. R. F., CHUQUIYAURI, R., CASAPÍA, M., NGUYEN, C. H., ARUACHAN, S., PAPWIJITSIL, R., NOSTEN, F. H., BANCONE, G., ANGUS, B., DUPARC, S., CRAIG, G., ROUSELL, V. M., JONES, S. W., HARDAKER, E., CLOVER, D. D., KENDALL, L., MOHAMED, K., KOH, G. C. K. W., WILCHES, V. M., BRETON, J. J. & GREEN, J. A. 2019. Tafenoquine versus Primaquine to Prevent Relapse of Plasmodium vivax Malaria. *New England Journal of Medicine,* 380**,** 229-241.

MIKOLAJCZAK, S. A., VAUGHAN, A. M., KANGWANRANGSAN, N., ROOBSOONG, W., FISHBAUGHER, M., YIMAMNUAYCHOK, N., REZAKHANI, N., LAKSHMANAN, V., SINGH, N., KAUSHANSKY, A., CAMARGO, N., BALDWIN, M., LINDNER, S. E., ADAMS, J. H., SATTABONGKOT, J. & KAPPE, S. H. 2015. Plasmodium vivax liver stage development and hypnozoite persistence in human liver-chimeric mice. *Cell Host Microbe,* 17**,** 526-35.

NG, S., SCHWARTZ, R. E., MARCH, S., GALSTIAN, A., GURAL, N., SHAN, J., PRABHU, M., MOTA, M. M. & BHATIA, S. N. 2015. Human iPSC-derived hepatocyte-like cells support Plasmodium liver-stage infection in vitro. *Stem Cell Reports,* 4**,** 348-59.

PANG, L., LIMSOMWONG, N. & SINGHARAJ, P. 1988. Prophylactic treatment of vivax and falciparum malaria with low-dose doxycycline. *J Infect Dis,* 158**,** 1124-7.

RABINOVICH, R. N., DRAKELEY, C., DJIMDE, A. A., HALL, B. F., HAY, S. I., HEMINGWAY, J., KASLOW, D. C., NOOR, A., OKUMU, F., STEKETEE, R., TANNER, M., WELLS, T. N. C., WHITTAKER, M. A., WINZELER, E. A., WIRTH, D. F., WHITFIELD, K. & ALONSO, P. L. 2017. malERA: An updated research agenda for malaria elimination and eradication. *PLoS Med,* 14**,** e1002456.

SCHAFER, C., DAMBRAUSKAS, N., STEEL, R. W., CARBONETTI, S., CHUENCHOB, V., FLANNERY, E. L., VIGDOROVICH, V., OLIVER, B. G., ROOBSOONG, W., MAHER, S. P., KYLE, D., SATTABONGKOT, J., KAPPE, S. H. I., MIKOLAJCZAK, S. A. & SATHER, D. N. 2018. A recombinant antibody against Plasmodium vivax UIS4 for distinguishing replicating from dormant liver stages. *Malar J,* 17**,** 370.

SCHUIERER, S. & ROMA, G. 2016. The exon quantification pipeline (EQP): a comprehensive approach to the quantification of gene, exon and junction expression from RNA-seq data. *Nucleic Acids Res,* 44**,** e132.

SI-TAYEB, K., NOTO, F. K., NAGAOKA, M., LI, J., BATTLE, M. A., DURIS, C., NORTH, P. E., DALTON, S. & DUNCAN, S. A. 2010. Highly efficient generation of human hepatocyte-like cells from induced pluripotent stem cells. *Hepatology,* 51**,** 297-305.

TACHIBANA, M., SATO, C., OTSUKI, H., SATTABONGKOT, J., KANEKO, O., TORII, M. & TSUBOI, T. 2012. Plasmodium vivax gametocyte protein Pvs230 is a transmission-blocking vaccine candidate. *Vaccine,* 30**,** 1807-1812.

TAKAHASHI, K. & YAMANAKA, S. 2006. Induction of pluripotent stem cells from mouse embryonic and adult fibroblast cultures by defined factors. *Cell,* 126**,** 663-76.

WHO 2018. World Malaria Report 2018. Geneva: World Health Organization. Licence: CC BY-NC-SA 3.0 IGO.

YOON, S., KANG, K., CHO, Y. D., KIM, Y., BUISSON, E. M., YIM, J. H., LEE, S. B., RYU, K. Y., JEONG, J. & CHOI, D. 2018. Nonintegrating Direct Conversion Using mRNA into Hepatocyte-Like Cells. *Biomed Res Int,* 2018**,** 8240567.

Supplementary Materials

Table S1

Caption for Movie S1

Name	Symbol	Provider	Reference	Specie	Dilution
Alpha-1-antitrypsin	A1AT	Dako	A0012	Rabbit	1:10,000
Alpha-1-Fetoprotein	AFP	Dako	A0008	Rabbit	1:500
Albumin	ALB	Bethyl	A80-129A	Goat	1:500
Class III β-tubulin	βIII-tubulin	Sigma	T8660	Mouse	1:5'000
Cluster of Differentiation 81	CD81	Invitrogen	MA5-13548	Mouse	1:100
Forkhead box protein A2	FOXA2	Abcam	ab60721	Mouse	1:50
Cytokeratin 18	KRT18	Abcam	ab82254	Mouse	1:100
Hepatocyte nuclear factor 1A	HNF1A	Cell Signaling Technologies	12425	Rabbit	1:100
Hepatocyte nuclear factor 4A	HNF4A	Cell Signaling Technologies	3113	Rabbit	1:100
Octamer-4	Oct4	Stemgent	09-0023	Rabbit	1:1,000
P. cynomolgi 70 kilodalton heat shock proteins	Pc-Hsp70	Anne-Marie Zeeman, BPRC	20285	Rabbit	1:1,000
P. cynomolgi up-regulated in infective sporozoites gene 4	Pc-UIS4	Anne-Marie Zeeman, BPRC	5262527	Rat	1:400
Scavenger Receptor class B member 1	SRB1	Novus Biologicals	NB400-104	Rabbit	1:100
Stage-specific embryonic antigen-1	SSEA-1	Chemicon/Milipore	MAB4301	Mouse	1:200
Stage-specific embryonic antigen-3	SSEA-3	Stemgent	09-0014	Rat	1:200
Stage-specific embryonic antigen-4	SSEA-4	Stemgent	09-0006	Mouse	1:1,000
Alexa Fluor 555 donkey anti-rabbit	Dk@Rb	Invitrogen	A31572	Donkey	1:1,000
Alexa Fluor 488 donkey anti-goat	Dk@Gt	Invitrogen	A11055	Donkey	1:1,000
Alexa Fluor 488 goat anti-mouse	Gt@Ms	Invitrogen	A10667	Goat	1:1,000
Alexa Fluor 594 chicken anti-rat	Ch@Rt	Invitrogen	A21471	Chicken	1:1,000
Goat anti-rabbit IgG-FITC	Gt@Rb	Anne-Marie Zeeman, BPRC		Goat	1:200
Hoechst	Hoechst	Invitrogen	33342	N.A.	1:10,000

Table S1. Primary and secondary antibodies used for immunofluorescence analysis.

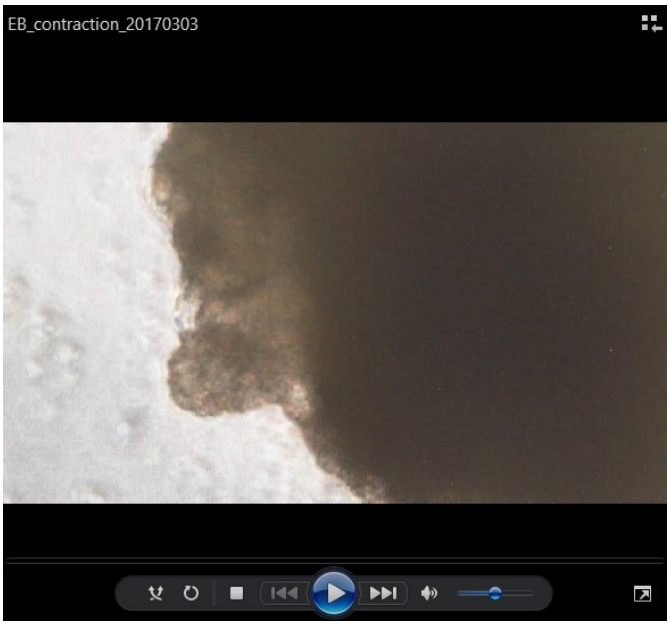

Movie S1. Embryoid body (EB) contraction occurred spontaneously after 10 days of differentiation in ultra low attachment plate.

Own contribution

This manuscript is the result of a collaborative effort between the SwissTPH, Novartis, the Biomedical Primate Research Center (BPRC) and the Novartis Institute for Tropical Diseases (NITD).

Trained by Thierry Doll in the lab of Matthias Müller at Novartis (Basel), I have generated the iPS cells from cynomolgus monkey fibroblasts and characterized the different clones. I have adapted protocols established for human iPS cells to generate hepatocyte-like cells from cynIPS cells and proceeded with the characterization of the best clone. Supported by Olaf Galuba and Isabelle Fruh (Novartis), I have conducted a mode of action screen with 4'000 compounds from the Novartis library on a semi-automated platform.

Anne-Marie Zeeman and Clemens Kocken (BPRC) provided the *P. cynomolgi* sporozoites for infection assays I conducted and subsequently analyzed at Novartis.

Once the system was established, we initiated the transfer of the iPS technology to the BPRC and the NITD. In this regard, I visited the BPRC for a month and trained three technicians on the iPS technology and the hepatocyte generation procedure. This experience also allowed me to perform two infection assays on cynHLCs in parallel with simian primary hepatocytes prepared by Anne-Marie Zeeman's team. The iPS technology was also transferred to the NITD and I trained a scientist, Lucy Kirchoffer-Allan, via email exchange and videoconference meetings. Both the BPRC and the NITD are now able to generate cynHLCs and conduct infection assays with this source of cells.

During the project, Matthias Müller provided supervision and guidance on stem cell-related topics, Matthias Rottmann and Pascal Mäser on malaria-related topics. International partners from the BPRC and the NITD provided expertise and advice on the infection part of this project.

Chapter III

Live imaging of malaria liver stage development in iPS-derived hepatocytes infected with a transgenic *Plasmodium cynomolgi* reporter line

Working manuscript

submission after publication of Voorberg-van der Wel et al. (under review)

Live imaging of malaria liver stage development in iPS-derived hepatocytes infected with a transgenic *Plasmodium cynomolgi* reporter line

Mélanie Pellisson[1,2,3], Annemarie Voorberg-van der Wel[4], Anne-Marie Zeeman[4], Clemens H. M. Kocken[4], Pascal Mäser[1,2], Matthias Müller[3], Matthias Rottmann[1,2*]

Affiliations

[1]Swiss Tropical and Public Health Institute (SwissTPH), Basel, Switzerland.

[2]University of Basel, Basel, Switzerland.

[3]Novartis Institutes for Biomedical Research, Novartis Pharma AG, Basel, Switzerland.

[4]Biomedical Primate Research Centre, Department of Parasitology, Rijswijk, The Netherlands.

*Correspondence to: matthias.rottmann@swisstph.ch

Abstract

Hypnozoites of *Plasmodium vivax* are the ultimate hindrance to malaria elimination. Our limited knowledge of these dormant parasites and the lack of a specific hypnozoite marker severely hampers drug discovery in this field. Recently, the liver specific protein 2 (LISP2) was identified as a marker of activated liver schizonts (Gupta et al., 2019). Based on these findings, a transgenic parasite line stably expressing the fluorescent reporter proteins GFP and mCherry in liver stage parasites was established (Voorberg-van der Wel et al., under review). Driven by Hsp70 and LISP2 promoters, GFP and mCherry expression enabled monitoring the hypnozoites and schizont morphogenesis by live imaging of rhesus monkey primary hepatocytes infected with *Plasmodium cynomolgi* sporozoites. Here, we further demonstrate the potential of this transgenic parasite line in cynomolgus monkey iPS-derived hepatocytes. Live imaging confirmed that all the liver stage parasites that harbored the construct expressed GFP over time, and the liver schizonts additionally expressed mCherry once activated. Therefore, this molecular tool corroborated hypnozoite persistence as well as schizont emergence and development in iPS-derived hepatocytes.

Introduction

Plasmodium vivax (P. vivax) has always been the second priority for malaria control programmes after the more virulent *Plasmodium falciparum*. Nevertheless, *P. vivax* puts more people at risk of disease every year and is geographically more widespread than *P. falciparum* (Guerra et al., 2010). One of the major obstacles to *P. vivax* malaria elimination is the presence of quiescent forms named hypnozoites, which can reside for months or even years in the liver of asymptomatic carriers. Since the discovery of the dormant liver stage in the 1980's (Krotoski et al., 1982), hypnozoite biology remained elusive. This hampered the search for compounds with anti-hypnozoite activity, which could replace the current drugs primaquine and tafenoquine, which are not safe for glucose-6-phosphate dehydrogenase deficient patients and pregnant or breathfeeding women (Baird et al., 2018, Watson et al., 2018). Moreover, in vitro investigations on *P. vivax* are hardly feasible as no long-term cultivation system exists and access to sporozoites is challenging (Tachibana et al., 2012, Noulin et al., 2013). Recently, progress has been made in the identification of hypnozoite-specific markers via transcriptomic studies (Voorberg-van der Wel et al., 2017, Bertschi et al., 2018, Cubi et al., 2017, Gural et al., 2018). However, the overall shutdown of the metabolic activity observed in hypnozoites is a major roadblock for these investigations (Bertschi et al., 2018). This has prompted the search for genes that are upregulated in activated hypnozoites and/or developing schizonts (Gupta et al., 2019, Voorberg-van der Wel et al., 2017). The liver specific protein 2 (LISP2) was identified as an early marker of liver stage development in both *P. cynomolgi* (PcyM_0307500) and *P. vivax* (PVP01_0304700) (Voorberg-van der Wel et al., 2017, Gural et al., 2018). First identified in *Plasmodium berghei* (Orito et al., 2013), this exported protein composed of an N-terminal signal peptide and a conserved C-terminal 6-cysteine domain plays a critical role in parasite development in host hepatocytes. Indeed, liver stage development is severely impaired or completely arrested upon genetic disruption of LISP2 (Orito et al., 2013, Annoura et al., 2014, Kumar et al., 2016). In order to obtain more biological insights on the LISP2 protein, Gupta et al. followed LISP2 expression over time using antibodies against *P. cynomolgi* and *P. vivax* LISP2. They showed that LISP2 expression marked the initiation of liver stage development at 3 days post infection (dpi). At this early stage, LISP2 expression was characterized by a crescent-shape located on the parasitophorous vacuole membrane (PVM). Then, LISP2 rapidly distributed through the PVM and progressively spread into cytosolic vacuoles during schizont growth. Hypnozoites did not express LISP2 (Gupta et al., 2019). Based on these findings, Voorberg-van der Wel et al. (under review) developed a construct with two reporter genes, GFP and mCherry, under the control of Hsp70 and LISP2 promoters

respectively. Rhesus monkey primary hepatocytes were infected with this transgenic parasite line and live imaging confirmed that all parasites harboring the plasmid expressed Hsp70 and activated schizonts were specifically expressing LISP2.

In Chapter II, we presented the development of an in vitro model for *P. cynomolgi* infection using cynomolgus monkey iPS-derived hepatocytes (cynHLCs). These hepatocytes were successfully infected with *P. cynomolgi* sporozoites and both hypnozoites and liver schizonts were observed until 12 dpi. Here we monitored LISP2 expression over time after sporozoite inoculation in cynHLCs. In line with the previously reported data, hypnozoites did not express LISP2, while activated liver schizonts expressed the gene in cynHLCs.

Methods

Generation of cynomolgus monkey iPS cell (cynIPS) and cynHLCs

CynIPS cells were generated as previously described in Chapter II. CynIPS cells were harvested and seeded (1.1E05 cells/well) onto a 96-well plate (Greiner, 655090) coated with Laminin 521 (Biolamina, LN521) in StemFlex medium (Gibco, A3349401) supplemented with 100 µg/mL G418 (Gibco, 10131035), and 10 µM rock inhibitor (Merck Millipore, Y-27632). The next day, cells were washed with PBS and differentiation was started (day 0) in Chemically Defined Medium (CDM) [50% IMDM (Invitrogen, 31980-030), 50% DMEM/F12 (HAM) (Invitrogen, A14625DJ), 1% Insulin-Transferrin-Selenium (ITS) (Invitrogen, 51500056), 0.1% CD Lipid Concentrate (Invitrogen, 11905031) and 2% BSA (Sigma, A7979)] supplemented with 1 µg/mL doxycycline (Dox) (Sigma, D1822). The next day, medium was changed with CDM supplemented with 1 µg/mL Dox. On day 2, medium was switched to William's E medium (Gibco, A1217601) with Primary Hepatocyte Maintenance Supplements (Gibco, CM4000) or William's B medium [William's E with glutamax (Invitrogen, 32551087) containing 10% human serum (A+), 1% MEM non-essential amino acids (Gibco, 11140035), 2% penicillin/streptomycin (Gibco, 15140122), 1% ITS, 1% sodium pyruvate (Invitrogen, 11360036), 50 µM β-mercaptoethanol (Gibco, 31350010), and 0.05 µM hydrocortisone (Sigma, H0888)] supplemented with 1 µg/mL Dox. Medium was refreshed the next day. On day 4, Dox induction was stopped and William's E medium containing Primary Hepatocyte Maintenance Supplements (cynHLC medium) or William's B medium (I^{ary} hep medium) used for the simian primary hepatocytes maintenance were supplemented with 5 µM of a combination of compounds previously described in Chapter II to maintain cynHLCs until 17 days of differentiation. Medium was refreshed daily.

Production of transgenic *P. cynomolgi* sporozoites

P. cynomolgi M strain pCyCEN_Lisp2mCherry_hsp70_GFP (Voorberg-van der Wel et al., under review) sporozoites were produced as described previously (Voorberg-van der Wel et al., 2017): Blood stage infections were initiated in rhesus monkeys by intravenous injection of 1E06 *P. cynomolgi* M strain pCyCEN_Lisp2mCherry_hsp70_GFP parasites from a cryopreserved stock. To exclude possible wild type contaminant parasites, monkeys were treated with pyrimethamine (1 mg/kg, orally on a biscuit every other day) for 3–4 times starting one day post infection. Parasitaemia was monitored by Giemsa-stained smears prepared from a drop of blood obtained from thigh pricks. Animals were trained to voluntarily present for thigh pricks, and were rewarded afterwards. Around peak parasitaemia, on two consecutive days, generally at days 11 and 12 post-infection, 9 mL of heparin blood was taken to feed mosquitoes and monkeys were cured from *Plasmodium* infection by intramuscular treatment with chloroquine (7.5 mg/kg) on three consecutive days. Typically, ±600 mosquitoes (two to five days old female *Anopheles stephensi* mosquitoes Sind-Kasur strain Nijmegen; Nijmegen UMC St. Radboud, Department of Medical Microbiology) were fed per blood sample using a glass feeder system. Mosquitoes were kept under standard conditions (Voorberg-van der Wel et al., 2013). Approximately one week after feeding, oocysts were counted and mosquitoes were given an uninfected blood meal to promote sporozoite invasion of the salivary glands. Two weeks post mosquito feeding on transgenic *P. cynomolgi* M strain infected blood, salivary gland sporozoites were isolated and used for inoculation.

CynHLCs infection with transgenic sporozoites

Four days after induction, cynHLCs were infected at the Biomedical Primate Research Center (BPRC) according to the methods of Dembélé et al. (Dembele et al., 2014) with *P. cynomolgi* M strain pCyCEN_Lisp2mCherry_hsp70_GFP sporozoites. CynHLCs were infected with 50,000 sporozoites per well. Cultures were kept at 37 °C in 5% CO_2 with daily medium change with cynHLC or I^{ary} hep medium accordingly. To evaluate the development of *P. cynomolgi* liver stage parasites, cultures were imaged with the Operetta system from 5 to 10 dpi every day after media replacement.

Live imaging of liver stage parasites

Image acquisition was performed in the Operetta system (PerkinElmer). Brightfield images were acquired to visualize the hepatocyte monolayer and lived *P. cynomolgi* liver stage parasites were detected with the enhanced green fluorescent protein (EGFP) (excitation 460-490 nm, emission 500-550 nm) and mCherry (excitation 560-580 nm, emission 590-640 nm) channels. The 20x long working distance objective was used with the following exposure times: brightfield (10 ms), EGFP (200 ms), and mCherry (200 ms). Objects were counted as parasites if their mean EGFP intensity was ≥500. Parasites were defined as activated schizonts if the previous criterion was fulfilled and the mean intensity in the mCherry filter was ≥50. Parasites were classified as hypnozoites if their mean mCherry intensity was <50, their diameter was <8 µm and their roundness was >0.8. In the absence of a reliable script, individual exoerythrocytic forms (EEFs) were counted manually and their respective areas and diameters were assessed using the Harmony software.

Results and discussion

Hepatocyte-like cells were obtained from cynomolgus monkey iPS cells by induced expression of the genes hepatocyte nuclear factor 4 alpha (HNF4A) and forkhead box protein A3 (FOXA3) as described in Chapter II. Four days post induction, the differentiated cynHLCs were infected with sporozoites of the *P. cynomolgi* M strain pCyCEN_Lisp2mCherry_hsp70_GFP (Fig. 1). Liver stage development was monitored daily from 5 to 10 dpi with the Operetta system. All the liver stage parasites expressed Hsp70, which triggered GFP expression. Therefore, each individual parasites were observed and tracked based on their GFP signal. In addition, once some liver stage parasites were activated, they started to express LISP2 and this triggered the mCherry signal.

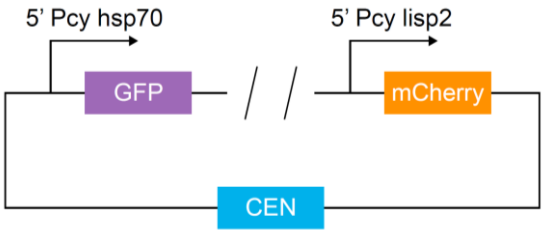

Fig. 1. Schematic representation of the pCyCEN_Lisp2mCherry_hsp70_GFP plasmid. The plasmid contains two expression cassettes for constitutive expression of GFP and mCherry. Additionally, to maintain the plasmid throughout the life cycle, a putative *P. cynomolgi* centromere (CEN) has been included.

GFP positive parasites were first observed at 2 dpi. At this early time point, the localization of the parasites and the invasion rate were difficult to precisely assess (Fig. S1A). Until 4 dpi, all the detected parasites were positive exclusively for GFP, demonstrating that LISP2 was not expressed in early liver-stage parasites residing in cynHLCs (Fig. S1B). From 5 dpi onwards, we observed three distinct parasite populations: (1) parasites that remained small over time and only expressed GFP (LISP2-) (Fig. 2A), (2) parasites that remained small over time and expressed both GFP and mCherry (LISP2+) (Fig. 2B), (3) parasites that grew over time and expressed both GFP and mCherry (LISP2++) (Fig. 2C). These categories were previously described in simian primary hepatocytes based on LISP2 immunostaining from 3 to 21 dpi (Gupta et al., 2019). Notably, the authors had suggested that LISP2+ parasites appeared continuously throughout the culture period and developed progressively into LISP2++ maturing schizonts. Although we could not clearly identify the previously described crescent-shape in LISP2+ parasites by live imaging, we observed that some of the LISP2+ parasites were persistent and remained small over time (Fig. 2B). As these parasites were positive for GFP and mCherry (GFP+/mCherry+), they were different from the LISP2- parasites, which were only GFP positive (GFP+). To the best of our knowledge, the growth arrest or growth delay of liver schizonts has never been described. Therefore, further investigations will be required to test the following possible explanations: (1) the host hepatocyte chosen by the parasite is unable to support the full parasite development; (2) the host cell controls the parasite and prevents its maturation; (3) a subset of activated parasites stays in a “transition” phase before completing their development.

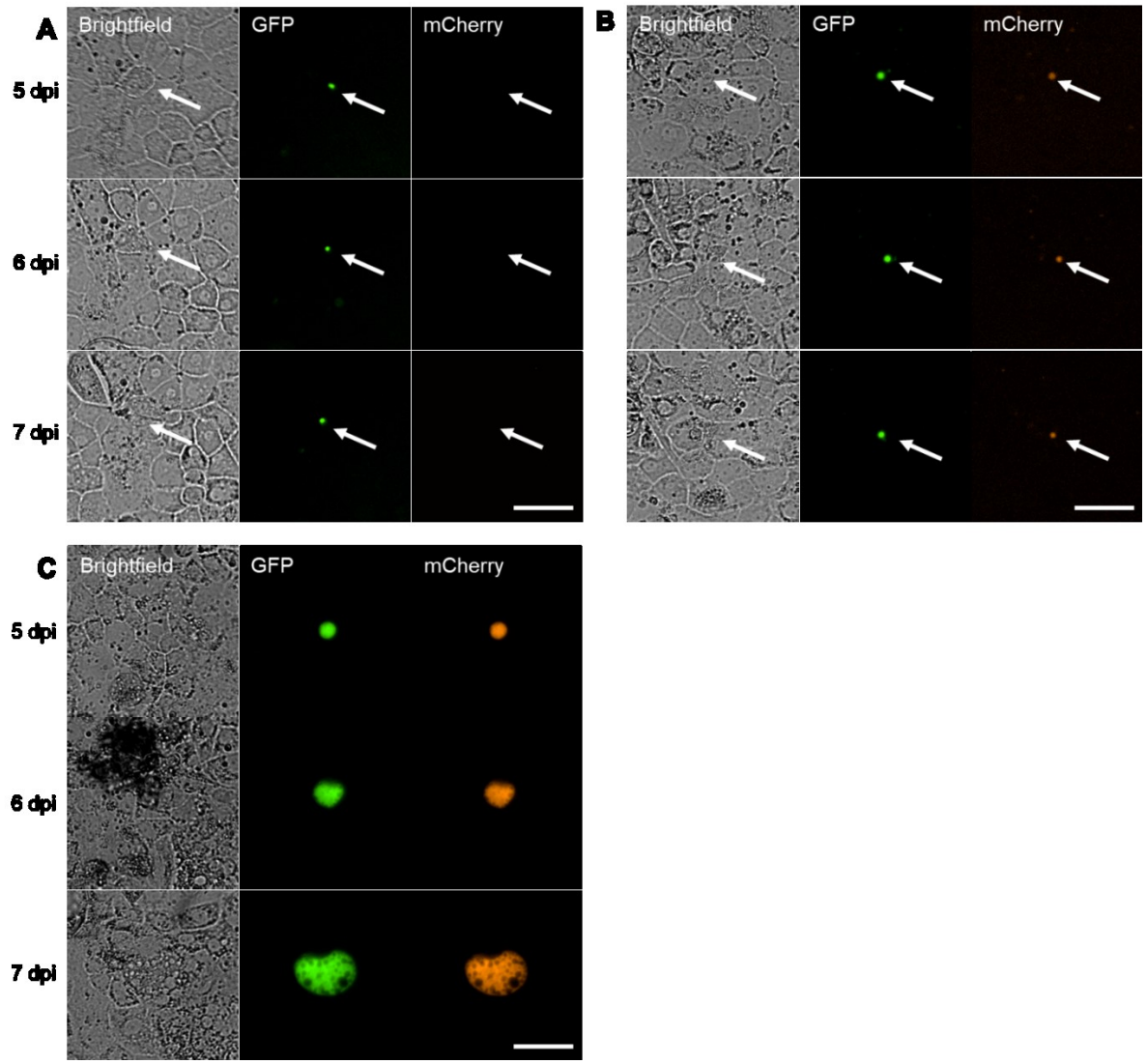

Fig. 2. Real-time monitoring of *P. cynomolgi* liver stage parasites' development. Brightfield, GFP, and mCherry images acquired at 5, 6, and 7 dpi of *P. cynomolgi* liver stage parasites. The top left panel (**A**) displays the presence of a GFP+ parasite, the top right panel (**B**) represents a GFP+/mCherry+ parasite of constant size over time and the lower panel (**C**) shows the development of a GFP+/mCherry+ liver schizont. Scale bars, 50 µm.

As cultivation medium for hepatocyte maintenance may influence parasite development, this experiment was conducted with two different media: the cynHLC maintenance medium (cynHLC) containing dexamethasone and bovine serum albumin and the simian primary hepatocyte maintenance medium (I^{ary} hep) containing 10% human serum. Both media were tested in parallel and we compared the infection rates, hypnozoite:schizont ratios, and parasite growth kinetics. At 6 dpi, we observed more liver stage parasites in cells maintained in cynHLC medium (37 parasites vs. 29 parasites counts in 8 wells, Fig. 3A). In addition, the hepatocytes maintained in cynHLC medium contained more GFP+ parasites than GFP+/mCherry+ parasites (3.6 to 1 ratio). The I^{ary} hep medium, instead, displayed a 1 to 1 ratio for GFP+ vs.

GFP+/mCherry+ parasites (Figs. 3A and 3B). However, the number of parasites in cynHLCs were very low for both tested media compared to primary cells. For these, 60 small and 41 large EEFs (average numbers from 6 individual wells) were counted at 6 dpi with wild-type parasites and 67 small and 42 large EEFs were counted with the transgenic line (Voorberg-van der Wel et al., under review). Therefore, further optimizations and investigations are required to improve infection efficiency with cynHLCs and confirm these findings.

A

Medium	cynHLC		I^{ary} hep	
Parasite category	GFP+	GFP+/ mCherry+	GFP+	GFP+/ mCherry+
Replica 1	4	3	1	2
Replica 2	6	0	2	1
Replica 3	3	2	1	1
Replica 4	3	0	0	3
Replica 5	5	0	3	3
Replica 6	3	2	3	2
Replica 7	3	1	4	2
Replica 8	2	0	1	0
Total	**29**	**8**	**15**	**14**
Mean	**3.6**	**1.0**	**1.9**	**1.8**
Stdev	**1.2**	**1.1**	**1.3**	**1.0**

B

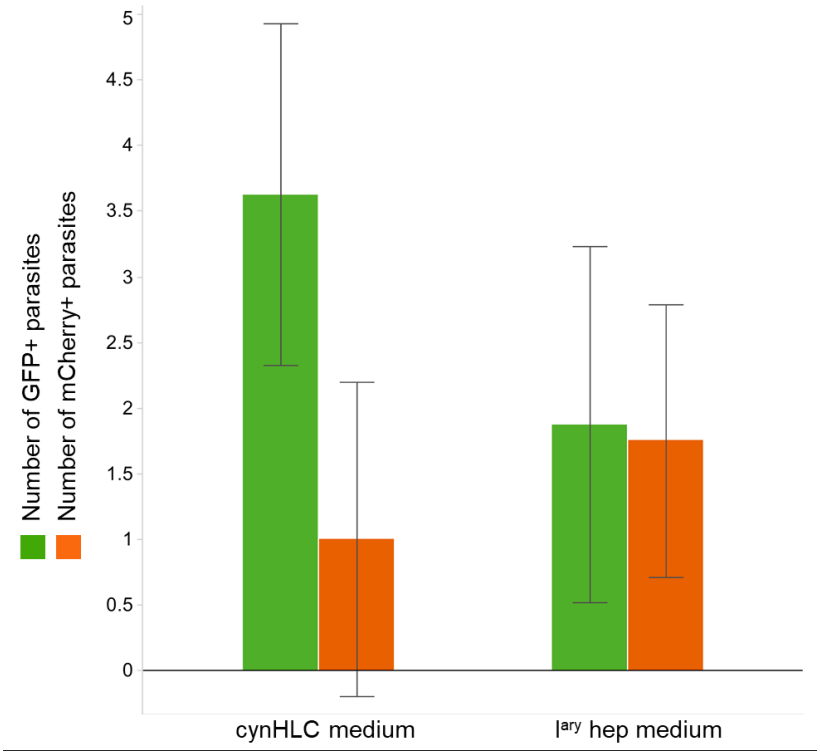

Fig. 3. A, Table displaying the number of GFP+ and GFP+/mCherry+ parasites for both cynHLC and I^{ary} hep media tested at 6 dpi. The total number of parasites, the mean (n=8) and the standard deviation (stdev) of the mean are shown at the bottom of the table. **B,** Bar chart representing the number of GFP+ (green) and GFP+/mCherry+ (orange) parasites at 6 dpi for both cynHLC and I^{ary} hep media. Error bars represent the standard deviation of the mean (n=8).

In addition, we assessed parasite growth kinetics by measuring the size of each individual GFP+/mCherry+ parasite from 5 to 10 dpi (Figs. 4 and 5). From the eight liver schizonts detected at 5 dpi in cells maintained with cynHLC medium, three were growing and were consequently classified as LISP2++ parasites with a size ranging from 7.0 µm up to 16.9 µm in diameter (Figs. 4A and 4B). The other five GFP+/mCherry+ parasites were not growing over time. For the cells maintained in I^{ary} hep medium, we observed different growth kinetics. From the total number of eighteen GFP+/mCherry+ parasites, eight were LISP2++ with a size ranging from 4.5 µm up to 55.5 µm in diameter, five were not growing, and the last five were shrinking in size or even disappearing at 6 dpi (Figs. 4A and 4C). In addition, the median diameter for all GFP+/mCherry+ parasites ranged from 7.9 µm up to 9.4 µm for cynHLC medium (Fig. 5A) and from 8.4 µm up to 14.7 µm for I^{ary} hep medium (Fig. 5C). This is in contrast with the LISP2++ parasites in simian primary hepatocytes, which displayed a median diameter of 9.4 µm at 4 dpi and 21.6 µm by 10 dpi (Gupta et al., 2019). The lower median diameter measured at 10 dpi for both tested media is due to the high percentage of non-growing and disappearing GFP+/mCherry+ parasites (Fig. 4A). Furthermore, the total number of GFP+/mCherry+ parasites decreased over time from eight parasites to three for cynHLC medium (Fig. 5B), and from eighteen parasites to one for I^{ary} hep medium (Fig. 5D). This progressive decrease of activated parasites is expected, as liver schizonts become mature and form merozoite-filled vesicles called merosomes upon completion of the liver stage development (Sturm et al., 2006). Merosome release is an asynchronous event, which occurs between 10 and 14 dpi for *P. vivax* (Gural et al., 2018) and *P. cynomolgi* (Voorber-van der Wel, personal communication). Observation of merosomes and/or merozoites is possible yet challenging due to the rapid merosome detachment and subsequent release of merozoites in the supernatant (Graewe et al., 2011, Baer et al., 2007, Gural et al., 2018). In our setup, we observed disappearance of schizonts between two measurements but no evident schizont rupture followed by merosome detachment. This would suggest that this event occurred between two time points or the liver schizonts were unable to complete their development in the host hepatocytes. Moreover, this decrease in parasite numbers is partially due to cynHLC detachment before the liver schizonts got mature enough to form merosomes. Based on the live imaging analysis we observed the disappearance of some GFP+/mCherry+ parasites with no apparent host cell death (Fig. S2A) but also some with a clear detachment of the region surrounding the infected cynHLC (Fig. S2B).

A

Scatter plot color	Parasite growth profile	All media		cynHLC medium		Iary hep medium	
		Parasite nb	Percentage (%)	Parasite nb	Percentage (%)	Parasite nb	Percentage (%)
	Non-growing	10	38	5	63	5	28
	Growing	11	42	3	38	8	44
	Disappearing after 5 dpi	4	15	0	0.0	4	22
	Shrinking and disappearing	1	4	0	0.0	1	6
	Total	**26**	**100**	**8**	**100**	**18**	**100**

B

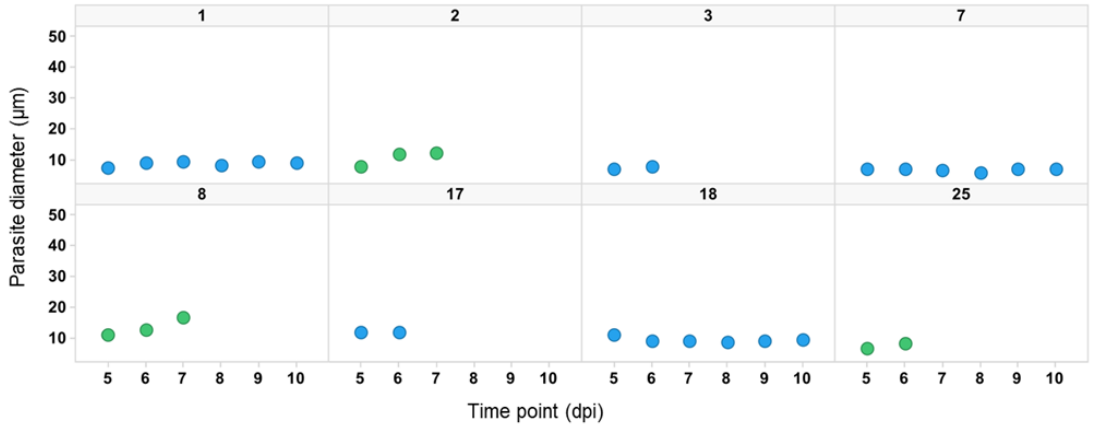

C

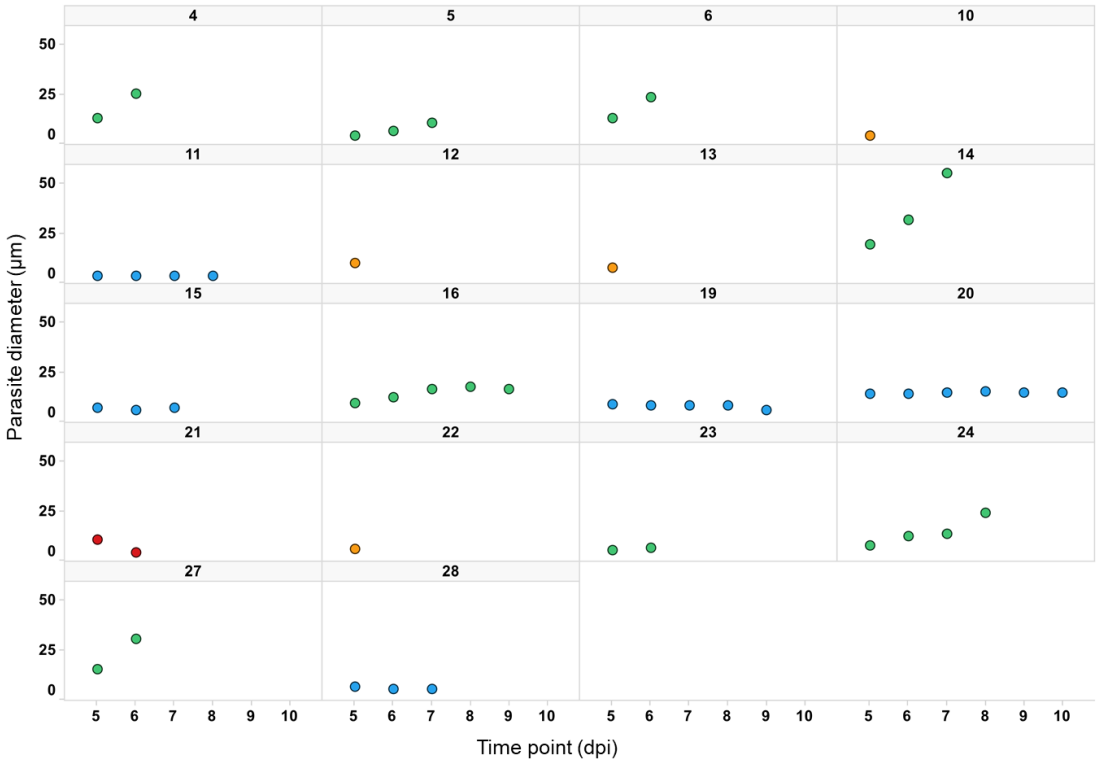

Fig. 4. A, Table showing the growth kinetics of GFP+/mCherry+ parasites for each medium tested. **B,** and **C,** Scatter plots displaying parasite diameter from 5 to 10 dpi of individual non-growing (blue), growing (green), disappearing (orange), and shrinking (red) parasites observed in hepatocytes maintained in cynHLC medium (**B**) and I^{ary} hep medium (**C**).

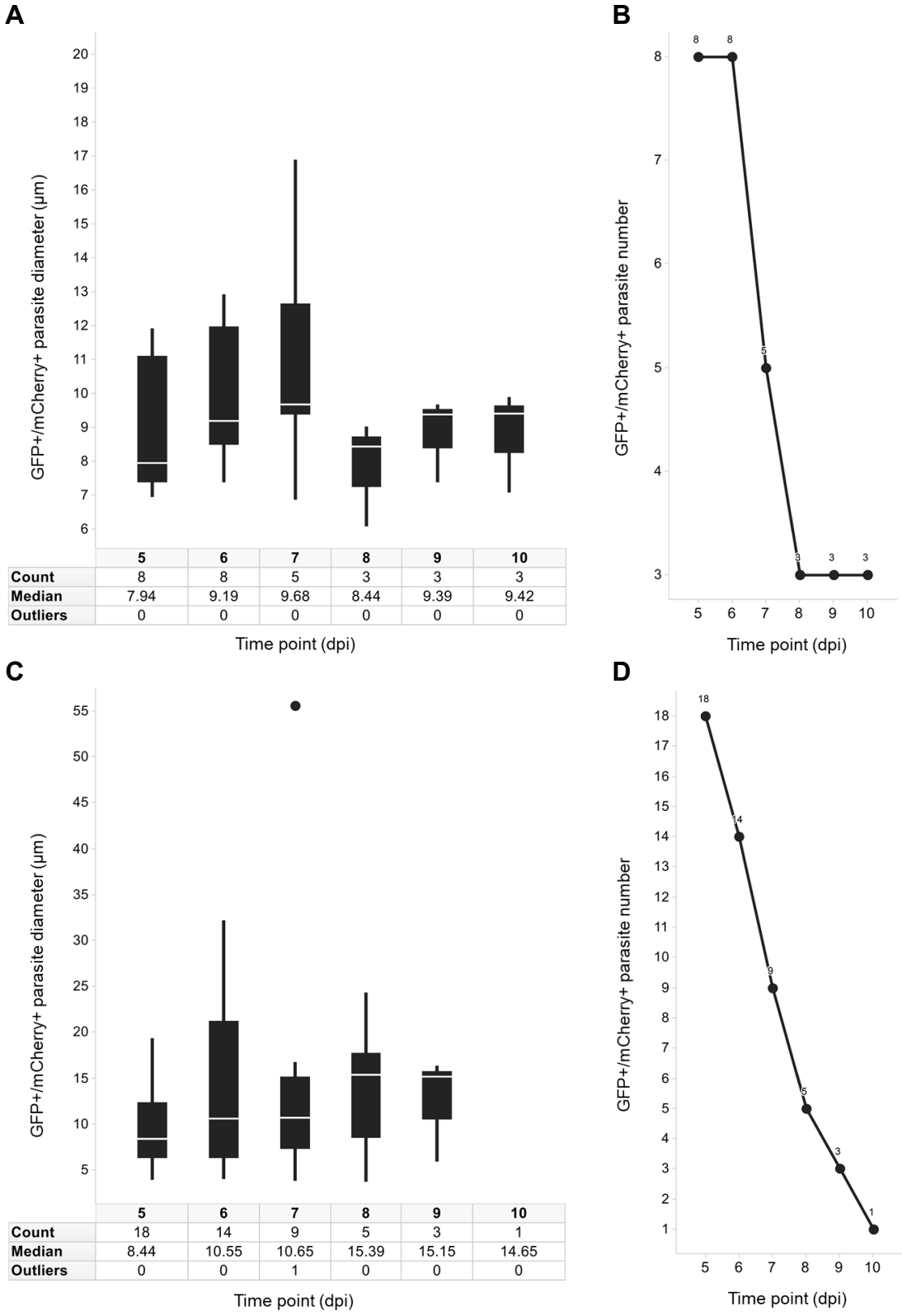

	5	6	7	8	9	10
Count	8	8	5	3	3	3
Median	7.94	9.19	9.68	8.44	9.39	9.42
Outliers	0	0	0	0	0	0

	5	6	7	8	9	10
Count	18	14	9	5	3	1
Median	8.44	10.55	10.65	15.39	15.15	14.65
Outliers	0	0	1	0	0	0

Fig. 5. Box plots representing the size distribution of GFP+/mCherry+ parasites from 5 to 10 dpi in cells maintained with cynHLC medium (**A**) or I^{ary} hep medium (**C**). The bottom tables display the time points (dpi) in bold numbers with the corresponding parasite counts, medians, and outliers. **B,** and **D,** Line charts displaying the parasite counts for each time point (dpi) for cynHLC medium (**B**) and I^{ary} hep medium (**D**).

In summary, we demonstrate that the pCyCEN_Lisp2mCherry_hsp70_GFP parasite line enables live imaging of liver stage parasites in cynHLCs generated from *Macaca fascicularis*. As in simian primary hepatocytes, LISP2 expressing liver schizonts were distinguished from LISP2 negative hypnozoites. Nevertheless, further investigations will be required to understand why a significant proportion of parasites expressing the LISP2 gene did not grow over time in cynHLCs. In addition, further improvement of hepatocyte maintenance would allow us to get more insights on the egress of *P. cynomolgi* parasites from cynHLCs. Compared to primary cells, iPS cells can self-renew, can be derived from any donor and can be easily genetically manipulated. These features make them extremely advantageous for studying the mechanisms underlying parasite development and host-pathogen interactions. The combination of the iPS technology with transgenic parasites will provide a powerful system to get more biological insights on liver stage development and will facilitate screening of drugs with anti-hypnozoite activity.

Acknowledgments: We thank Thierry Doll, Isabelle Fruh, Bettina Leonhard, Carole Manneville, and Annick Werner for continuous support with iPS technology; Nicole van der Werff, Ivonne Nieuwenhuis, and Lars Vermaat for mosquito dissection and sporozoite preparation; Isabelle Claerr for technical assistance with high content imaging; Dominic Trojer for help in microscopy; and the Walter Fischli-Foundation, the Bill and Melinda Gates Foundation and the Medicines for Malaria Venture for financial support. **Funding:** This work was supported by the Walter Fischli-Foundation, the Bill and Melinda Gates Foundation (OPP1141292) and the Medicines for Malaria Venture. **Author contributions:** M.M., M.R., and P.M.: Conception and design, data analysis and interpretation, manuscript writing; M.P.: Conception and design, collection and assembly of data, data analysis and interpretation, manuscript writing; A.V.: Provision of sporozoites, data analysis and interpretation; A.V., A.M.Z., C.H.M.K., M.M., M.R., P.M.: Final approval of manuscript. **Competing interests:** M.M., is employed by and/or shareholder of Novartis Pharma AG. The authors declare no competing interests. **Data and materials availability:** All data are available in the main text or the supplementary materials.

References

ANNOURA, T., VAN SCHAIJK, B. C. L., PLOEMEN, I. H. J., SAJID, M., LIN, J.-W., VOS, M. W., DINMOHAMED, A. G., INAOKA, D. K., RIJPMA, S. R., VAN GEMERT, G.-J., CHEVALLEY-MAUREL, S., KIEŁBASA, S. M., SCHELTINGA, F., FRANKE-FAYARD, B., KLOP, O., HERMSEN, C. C., KITA, K., GEGO, A., FRANETICH, J.-F., MAZIER, D., HOFFMAN, S. L., JANSE, C. J., SAUERWEIN, R. W. & KHAN, S. M. 2014. Two Plasmodium 6-Cys family-related proteins have distinct and critical roles in liver-stage development. *The FASEB Journal,* 28**,** 2158-2170.

BAER, K., KLOTZ, C., KAPPE, S. H. I., SCHNIEDER, T. & FREVERT, U. 2007. Release of Hepatic Plasmodium yoelii Merozoites into the Pulmonary Microvasculature. *PLOS Pathogens,* 3**,** e171.

BAIRD, J. K., BATTLE, K. E. & HOWES, R. E. 2018. Primaquine ineligibility in anti-relapse therapy of Plasmodium vivax malaria: the problem of G6PD deficiency and cytochrome P-450 2D6 polymorphisms. *Malar J,* 17**,** 42.

BERTSCHI, N. L., VOORBERG-VAN DER WEL, A., ZEEMAN, A. M., SCHUIERER, S., NIGSCH, F., CARBONE, W., KNEHR, J., GUPTA, D. K., HOFMAN, S. O., VAN DER WERFF, N., NIEUWENHUIS, I., KLOOSTER, E., FABER, B. W., FLANNERY, E. L., MIKOLAJCZAK, S. A., CHUENCHOB, V., SHRESTHA, B., BEIBEL, M., BOUWMEESTER, T., KANGWANRANGSAN, N., SATTABONGKOT, J., DIAGANA, T. T., KOCKEN, C. H. & ROMA, G. 2018. Transcriptomic analysis reveals reduced transcriptional activity in the malaria parasite Plasmodium cynomolgi during progression into dormancy. *Elife,* 7.

CUBI, R., VEMBAR, S. S., BITON, A., FRANETICH, J. F., BORDESSOULLES, M., SOSSAU, D., ZANGHI, G., BOSSON-VANGA, H., BENARD, M., MORENO, A., DEREUDDRE-BOSQUET, N., LE GRAND, R., SCHERF, A. & MAZIER, D. 2017. Laser capture microdissection enables transcriptomic analysis of dividing and quiescent liver stages of Plasmodium relapsing species. *Cell Microbiol,* 19.

DEMBELE, L., FRANETICH, J. F., LORTHIOIS, A., GEGO, A., ZEEMAN, A. M., KOCKEN, C. H., LE GRAND, R., DEREUDDRE-BOSQUET, N., VAN GEMERT, G. J., SAUERWEIN, R., VAILLANT, J. C., HANNOUN, L., FUCHTER, M. J., DIAGANA, T. T., MALMQUIST, N. A., SCHERF, A., SNOUNOU, G. & MAZIER, D. 2014. Persistence and activation of malaria hypnozoites in long-term primary hepatocyte cultures. *Nat Med,* 20**,** 307-12.

GRAEWE, S., RANKIN, K. E., LEHMANN, C., DESCHERMEIER, C., HECHT, L., FROEHLKE, U., STANWAY, R. R. & HEUSSLER, V. 2011. Hostile Takeover by Plasmodium: Reorganization of Parasite and Host Cell Membranes during Liver Stage Egress. *PLOS Pathogens,* 7**,** e1002224.

GUERRA, C. A., HOWES, R. E., PATIL, A. P., GETHING, P. W., VAN BOECKEL, T. P., TEMPERLEY, W. H., KABARIA, C. W., TATEM, A. J., MANH, B. H., ELYAZAR, I. R., BAIRD, J. K., SNOW, R. W. & HAY, S. I. 2010. The international limits and population at risk of Plasmodium vivax transmission in 2009. *PLoS Negl Trop Dis,* 4**,** e774.

GUPTA, D. K., DEMBELE, L., VOORBERG-VAN DER WEL, A., ROMA, G., YIP, A., CHUENCHOB, V., KANGWANRANGSAN, N., ISHINO, T., VAUGHAN, A. M., KAPPE, S. H., FLANNERY, E. L., SATTABONGKOT, J., MIKOLAJCZAK, S., BIFANI, P., KOCKEN, C. H. & DIAGANA, T. T. 2019. The Plasmodium liver-specific protein 2 (LISP2) is an early marker of liver stage development. *Elife,* 8.

GURAL, N., MANCIO-SILVA, L., MILLER, A. B., GALSTIAN, A., BUTTY, V. L., LEVINE, S. S., PATRAPUVICH, R., DESAI, S. P., MIKOLAJCZAK, S. A., KAPPE, S. H. I., FLEMING, H. E., MARCH, S., SATTABONGKOT, J. & BHATIA, S. N. 2018. In Vitro Culture, Drug Sensitivity, and Transcriptome of Plasmodium Vivax Hypnozoites. *Cell Host Microbe,* 23**,** 395-406 e4.

KROTOSKI, W. A., GARNHAM, P. C., BRAY, R. S., KROTOSKI, D. M., KILLICK-KENDRICK, R., DRAPER, C. C., TARGETT, G. A. & GUY, M. W. 1982. Observations on early and late post-sporozoite tissue stages in primate malaria. I. Discovery of a new latent form of Plasmodium cynomolgi (the hypnozoite), and failure to detect hepatic forms within the first 24 hours after infection. *Am J Trop Med Hyg,* 31**,** 24-35.

KUMAR, H., SATTLER, J. M., SINGER, M., HEISS, K., REINIG, M., HAMMERSCHMIDT-KAMPER, C., HEUSSLER, V., MUELLER, A.-K. & FRISCHKNECHT, F. 2016. Protective efficacy and safety of liver stage attenuated malaria parasites. *Scientific Reports,* 6**,** 26824.

NOULIN, F., BORLON, C., VAN DEN ABBEELE, J., D'ALESSANDRO, U. & ERHART, A. 2013. 1912–2012: a century of research on Plasmodium vivax in vitro culture. *Trends in parasitology,* 29**,** 286-294.

ORITO, Y., ISHINO, T., IWANAGA, S., KANEKO, I., KATO, T., MENARD, R., CHINZEI, Y. & YUDA, M. 2013. Liver-specific protein 2: a Plasmodium protein exported to the hepatocyte cytoplasm and required for merozoite formation. *Mol Microbiol,* 87**,** 66-79.

STURM, A., AMINO, R., VAN DE SAND, C., REGEN, T., RETZLAFF, S., RENNENBERG, A., KRUEGER, A., POLLOK, J. M., MENARD, R. & HEUSSLER, V. T. 2006. Manipulation of host hepatocytes by the malaria parasite for delivery into liver sinusoids. *Science,* 313**,** 1287-90.

TACHIBANA, M., SATO, C., OTSUKI, H., SATTABONGKOT, J., KANEKO, O., TORII, M. & TSUBOI, T. 2012. Plasmodium vivax gametocyte protein Pvs230 is a transmission-blocking vaccine candidate. *Vaccine,* 30**,** 1807-1812.

VOORBERG-VAN DER WEL, A., ROMA, G., GUPTA, D. K., SCHUIERER, S., NIGSCH, F., CARBONE, W., ZEEMAN, A. M., LEE, B. H., HOFMAN, S. O., FABER, B. W., KNEHR, J., PASINI, E., KINZEL, B., BIFANI, P., BONAMY, G. M. C., BOUWMEESTER, T., KOCKEN, C. H. M. & DIAGANA, T. T. 2017. A comparative transcriptomic analysis of replicating and dormant liver stages of the relapsing malaria parasite Plasmodium cynomolgi. *Elife,* 6.

VOORBERG-VAN DER WEL, A., ZEEMAN, A. M., VAN AMSTERDAM, S. M., VAN DEN BERG, A., KLOOSTER, E. J., IWANAGA, S., JANSE, C. J., VAN GEMERT, G. J., SAUERWEIN, R., BEENHAKKER, N., KOOPMAN, G., THOMAS, A. W. & KOCKEN, C. H. 2013. Transgenic fluorescent Plasmodium cynomolgi liver stages enable live imaging and purification of Malaria hypnozoite-forms. *PLoS One,* 8**,** e54888.

WATSON, J., TAYLOR, W. R. J., BANCONE, G., CHU, C. S., JITTAMALA, P. & WHITE, N. J. 2018. Implications of current therapeutic restrictions for primaquine and tafenoquine in the radical cure of vivax malaria. *PLoS Negl Trop Dis,* 12**,** e0006440.

Supplementary Materials

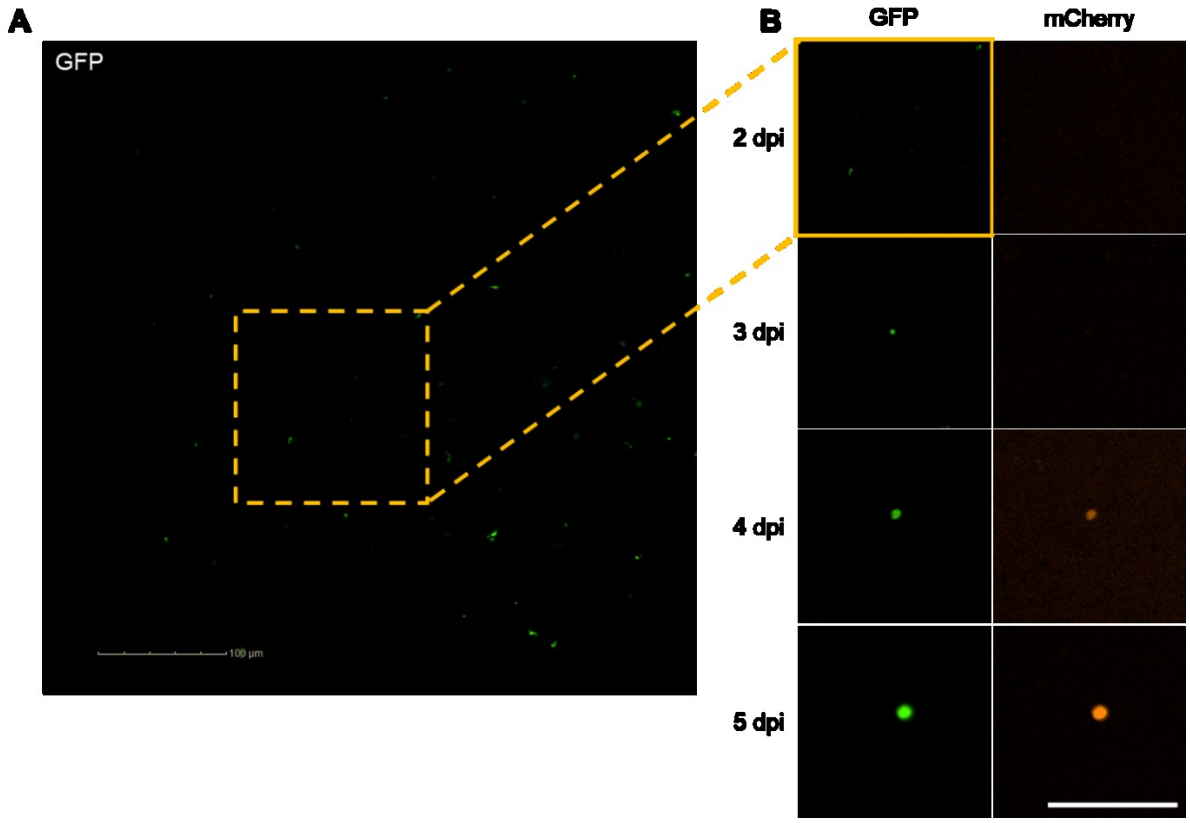

Fig. S1. A, GFP image acquired at 2 dpi of *P. cynomolgi* liver stage parasites. **B,** Real time monitoring of a growing parasite with GFP and mCherry images acquired at 2, 3, 4, and 5 dpi. The parasite was not detected at 2 dpi, expressed GFP from 3 to 5 dpi and mCherry at 4 and 5 dpi. Scale bars, 100 µm.

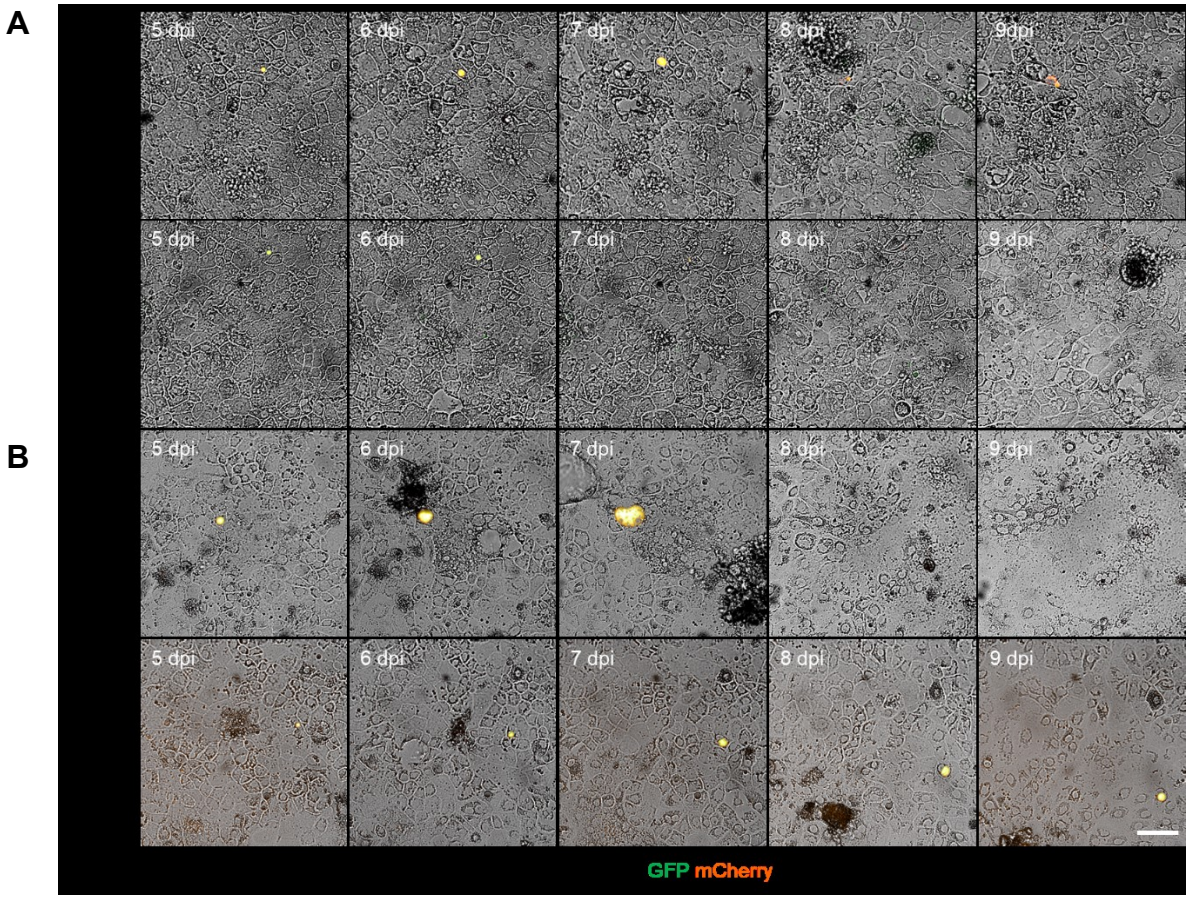

Fig. S2. Real time monitoring of the GFP+/mCherry+ EEFs #8, #14, #16, and #17 (see Figs. 4B and 4C for the growth kinetics of each individual parasite) from 5 to 9 dpi. Overlay of brightfield, GFP, and mCherry images showed parasite disappearance while cynHLC monolayer was maintained (**A**) but also when hepatocytes were detaching (**B**). Scale bar, 100 µm.

Own contribution

For this manuscript, the transgenic parasites were provided by Annemarie Voorberg-van der Wel (BPRC). I have generated the cynHLCs and conducted the infection assay with the transgenic sporozoites at the BPRC during my stay in The Netherlands. Annemarie Voorberg-van der Wel provided guidance for the live imaging of liver stage parasites and I acquired images on the different plates every day. I proceeded with the image analysis at Novartis (Basel) in the Harmony software, which was also the software used by the BPRC. Regular discussions with Annemarie Voorberg-van der Wel facilitated the data analysis and the comparison with simian primary hepatocytes.

Chapter IV

General discussion

General discussion

This chapter discusses the relevance of an iPS-based *P. cynomolgi* infection model to study hypnozoite biology, summarizes results, and provides direction for future work.

In this thesis, we have developed a new in vitro model using iPS cells to study the dormant hypnozoite of the malaria parasite and in the future to test compounds for anti-hypnozoite activity. Although numerous reports exist on the generation of hepatocytes from human or rodent cells (Cai et al., 2007, Han et al., 2012, Hu and Li, 2015, Mallanna and Duncan, 2013, Si-Tayeb et al., 2010, Touboul et al., 2010, Du et al., 2014, Huang et al., 2011, Sekiya and Suzuki, 2011), we have described for the first time a protocol that leads to the generation of iPS-derived hepatocytes from non-human primates (i.e. cynomolgus monkey). Across the differentiation process, the generated cells acquired a hepatic signature and a morphology similar to the human hepatocyte-like cells. These non-human primate hepatocytes will be extremely useful for various areas of research including malaria, as the cynomolgus monkey is the natural host of *P. cynomolgi* (Coatney et al., 1971). The latter is a well-accepted surrogate model for *P. vivax*, which is hardly amenable to in vitro work. We showed that the cynomolgus monkey iPS-derived hepatocytes (cynHLCs) were permissive to *P. cynomolgi* sporozoites and supported hypnozoite formation and persistence as well as schizont development until 12 days post infection (dpi). The cellular model presented in this thesis enables the production of hypnozoites to investigate relapsing malaria and will ultimately allow screening of compounds for anti-hypnozoite activity. In addition, the iPS technology offers the possibility to study host genetic diversity and host-pathogen interactions via genetic manipulation of the cells at the iPS stage, thus making this system advantageous compared to the primary cells.

Although we could successfully developed the iPS-based system, it is important to notice that several roadblocks were encountered and efforts have been made to overcome them and reach the objectives of this thesis. First, the iPS generation from cynomolgus monkey fibroblasts was more challenging than expected. Once transferred on a feeder-less system, the pluripotent cells spontaneously differentiated and could not be maintained for several passages under the conditions used for human iPS maintenance. We showed that a higher concentration of basic fibroblast growth factor (bFGF) was required to maintain the cynomolgus monkey iPS (cynIPS) cells in their pluripotent state (Chapter II). Then, the generation of hepatocyte-like cells was a long and difficult process, which required extensive adaptation from the original human protocol. Optimizing this protocol allowed us to produce hepatocytes within 6 days

with a high efficiency (>50% of the cells expressed albumin (ALB) and >70% expressed hepatocyte nuclear factor 4 alpha (HNF4A)). Nevertheless, the short lifetime of these cells forced us to search for a solution to improve their survival. With the three-compound cocktail identified in a survival screen, cynHLCs can now be maintained for 17 days instead of 8 days, thus enabling observation of liver stage parasite development upon sporozoite inoculation. Finally, the extremely limited number of sporozoites allocated to our experiments was a major hurdle for our investigations towards the establishment of the iPS-based system.

Despite all these challenges, we have demonstrated the successful development of an iPS-based in vitro model for malaria liver stages. The following paragraphs highlight specific leverage parameters from the host cells (i.e. cynHLCs) and the parasite (i.e. *P. cynomolgi*) (Fig. 1) on infection assay outcomes and provides recommendations for further optimization.

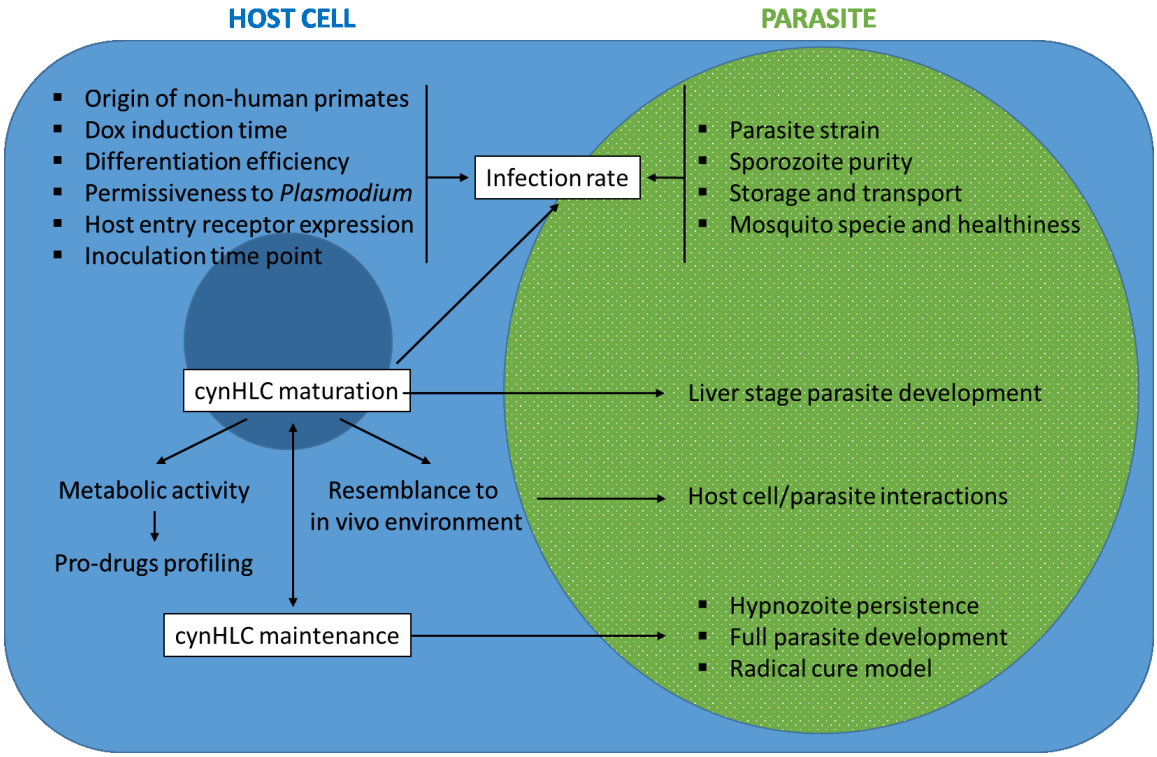

Fig. 1. Schematic representation of the different parameters related to the host cell and/or the parasite influencing infection rate, and their impact on the infection model.

1. Fetal phenotype of stem cell derived hepatocytes

One of the major hurdles in the field of iPS-derived hepatocytes is their lack of maturation. All the different well established protocols to generate hepatocyte-like cells from iPS/ES cells result in immature hepatocytes (Baxter et al., 2015, Jozefczuk et al., 2011, Kia et al., 2013, Schwartz et al., 2014, Si-Tayeb et al., 2010, Song et al., 2015). Although iPS-derived hepatocytes generated from various species display a clear hepatic signature at the end of the differentiation, they are considered as fetal rather than mature, as they more resemble primary hepatocytes from fetal liver tissue. Our effort to generate iPS-derived hepatocytes also confirms this finding. Based on immunofluorescence and RNA-seq analyses, we have observed that human HLCs and cynHLCs generated via the inducible approach have elevated α-fetoprotein (AFP) levels, a low metabolic activity, and a lack of some key efflux transporters (e.g. ATP binding cassette subfamily B member 1 (ABCB1) and ATP binding cassette subfamily C member 2 (ABCC2)). Different approaches have been used to further mature iPS-derived hepatocytes. Shan et al. for instance, conducted a screen to identify compounds that promote the complete differentiation of human hepatocytes (Shan et al., 2013). With the developed screening platform, they identified small molecules (FH1 and FPH1) that induced the proliferation of primary human hepatocytes in vitro and significantly improved the maturation of iPS-derived hepatocytes (Shan et al., 2013). FH1- and FPH1-treated cultures increased ALB, CYP2A6, and CYP3A4 levels and significantly reduced AFP levels compared to untreated iPS-derived hepatocytes. Elevated ATP-binding cassette (ABC) transporter expression levels were also observed in FH1- and FPH1-treated HLCs, and their expression pattern resembled that of adult primary human hepatocytes more than that of fetal hepatocytes. With this chemical approach, iPS-derived cells hold great promise to be used more widely and ultimately replace the primary cells, which are limited in numbers and variable from donor to donor. Recently, a maturation screen for human HLCs was also conducted at Novartis and led to the identification of a four compounds-cocktail containing forskolin, a matrix metalloproteinase-7 (MMP-7) inhibitor, linsitinib (i.e. insulin-like growth factor 1 receptor (IGF-1R) inhibitor), and an activin receptor-like kinase-2 (ALK2) inhibitor. Treating human HLCs with this cocktail significantly increased ALB production and CYP3A4 activity and decreased AFP secretion (Harper et al., in preparation). The small molecules identified in the screens conducted by Shan et al. (Shan et al., 2013) and by our colleagues at Novartis could potentially further mature cynHLCs, improve their permissiveness, and facilitate drug screening for malaria drug discovery. Indeed, untreated human HLCs are unable to metabolize primaquine due to their fetal phenotype (Ng

et al., 2015). However, further maturation of human HLCs using FPH1 improved the metabolic activity of hepatocytes and caused them to activate primaquine (Ng et al., 2015). Thus, hepatocyte maturation is a critical parameter for malaria liver stage drug discovery. Using a system in which hepatocytes are mature enough is essential to sustain key hepatic functions and sufficient metabolic activity to be able to test pro-drugs like 8-aminoquinolines. We performed a pilot experiment to assess the metabolic activity of cynHLCs upon primaquine treatment. Although two metabolites resulting from oxidative deamination of the parental molecule (Pybus et al., 2013) were detected after 24 hours of treatment, CYP activity in cynHLCs was very low, which predicts a poor conversion of primaquine to its active metabolites (data not shown). On the one hand, this characteristic hampers testing of pro-drugs like 8-aminoquinolines in our system. On the other hand, a low metabolic activity enables the testing of compounds that are rapidly cleared from the liver. For instance, assessing the activity of cladosporin analogs in primary hepatocytes is not feasible as these molecules are eliminated within 30 min by the primary cells. In this perspective, cynHLCs would be advantageous due to their low CYP expression levels. Cladosporins were identified as potent and selective lysyl-tRNA synthetase inhibitors and these compounds showed activity against blood and liver stage parasites (Hoepfner et al., 2012). Nevertheless, the potential activity of cladosporins against hypnozoites remains to be elucidated. Therefore, we plan to assess the activity of several cladosporin analogs in our system in the future. If those compounds indeed turn out to be active against hypnozoites, researchers may proceed to a structure-activity-relationship phase to synthesize analogs with a longer hepatic clearance while retaining activity against *Plasmodium* parasites to ultimately lead to the development of a potential drug.

Besides the chemical approach, hepatic functions of iPS-derived hepatocytes can be enhanced via genetic manipulation of the iPS cells. For instance, the overexpression of transcription factors specifically expressed in adult hepatocytes (i.e. activating transcription factor 5 (ATF5), CCAAT/ enhancer-binding protein alpha (c/EBPα), and prospero homeobox protein 1 (PROX1)) resulted in elevated CYP and others liver specific gene expression levels (Nakamori et al., 2016). 3D approaches have also proven efficacy in enhancing the functionality and the metabolic activity of human iPS-derived hepatocytes via 3D cell aggregation and cyclic adenosine monophosphate (cAMP) signaling (Ogawa et al., 2013) or via the in vivo transplantation and vascularization of liver buds generated from iPS cells in vitro (Takebe et al., 2013).

2. Hepatocyte maintenance

In addition to their lack of maturation, cynHLCs are difficult to maintain in in vitro cultures. The generation of hepatocytes from human stem cells is a well-known process, and diverse protocols have been developed (Chen et al., 2012, Gao et al., 2017, Mallanna and Duncan, 2013, Si-Tayeb et al., 2010, Touboul et al., 2010). However, the translation of this process to monkey cells required extensive tailoring. Our investigations led to the observation that the differentiation process in non-human primate cells is faster than in human cells. This finding is extremely advantageous in terms of screening capacity and costs, as cynIPS cells reached the hepatic stage within 6 days as compared to 25 days for their human counterparts (Fig. 2). However, this phenomenon was accompanied by a rapid detachment of the cell monolayer shortly after the hepatic stage had been reached.

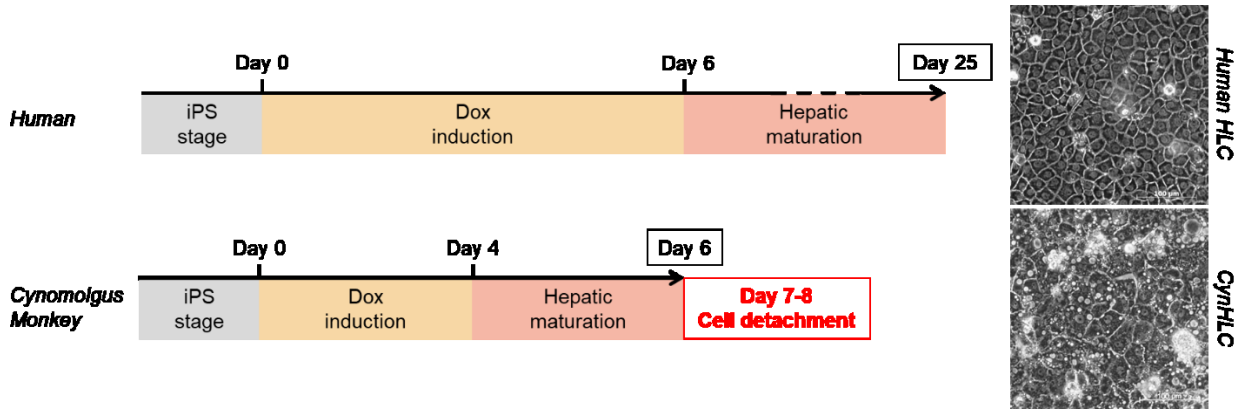

Fig. 2. Schematic representation of HLC generation from human and cynomolgus monkey iPS cells. Morphology of resulting HLCs is shown for human and cynHLC at Day 25 and Day 6 respectively.

Several alternatives were tested to prevent the massive cell loss, including coating and media optimization as well as co-cultivation with other liver cell types (Fig. 3). Unfortunately, none of these attempts improved cell survival.

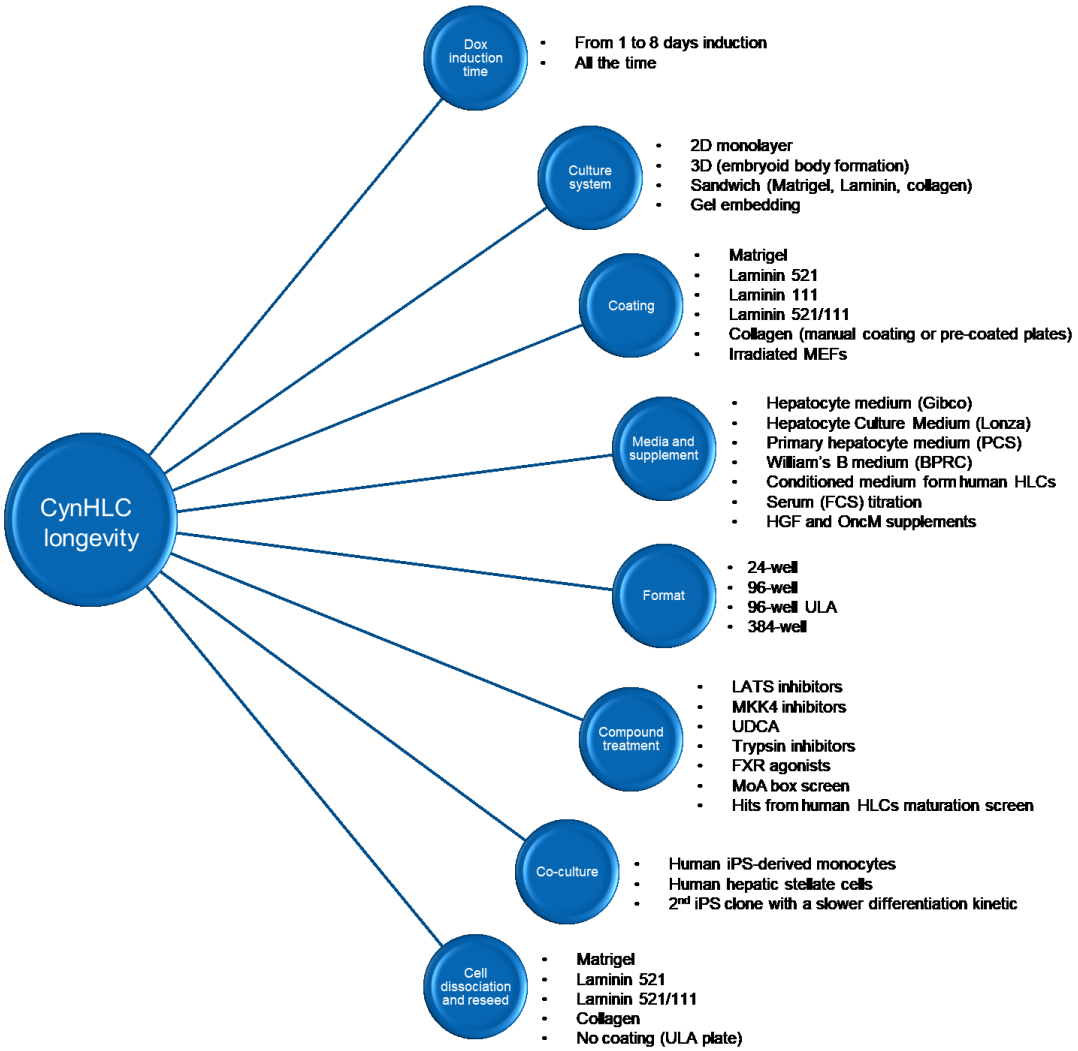

Fig. 3. Alternatives tested in this thesis to improve cynHLC longevity.

Screening the Novartis mode of action (MoA) box library allowed identification of compounds that significantly improved our in vitro system. CynHLCs were maintained for 17 days in culture when treated daily with the identified triple hit-combination cocktail (Chapter II). It is important to stress that treated and untreated cynHLCs were tested in parallel for each infection performed to exclude any potential effect of the compounds on parasite development. No differences in efficiency and parasite development were observed, which suggests that the identified compounds are not affecting the parasite. This finding is a significant improvement for malaria infection assays, as liver stage parasite development can be observed for 12 days instead of 5 days in the untreated cynHLCs. This time window is suitable to observe hypnozoite formation and schizont development until it ruptures but it is not sufficient to observe potential hypnozoite reactivation. As demonstrated in cynomolgus monkey primary hepatocytes maintained in a sandwich culture, this particular event would require a time window of at least 21 days (Dembele et al., 2014).

The first compound identified in the survival screen is an inhibitor of human dihydroorotate dehydrogenase (DHODH). This enzyme, located on the outer surface of the inner mitochondrial membrane, catalyzes the fourth, rate-limiting step of de novo pyrimidine biosynthesis. DHODH inhibitors like brequinar and leflunomide have been used for autoimmune diseases, cancer treatment, and anti-rejection therapy after organ transplantation (Löffler et al., 2005, Peters et al., 1990, Cramer et al., 1992). The mechanisms underlying DHODH inhibition mediated by leflunomide are still not fully understood. It is thought that apoptosis leading to concanavalin A (con A)-induced liver injury is prevented by inhibition of caspase-3-like and caspase-9-like upon leflunomide treatment (Imose et al., 2004). In addition, this pro-drug shuts down c-Jun N-terminal kinase 2 (JNK2) activity in primary hepatocytes (Migita et al., 2005). JNK2 inhibition prevents cells from mitochondrial permeability transition pore opening, which abrogates downstream release of pro-apoptotic factors like cytochrome c. Latchoumycandane et al. confirmed this finding in an acetaminophen-induced cell death model using an immortalized human hepatocyte cell line (Latchoumycandane et al., 2006). They demonstrated that leflunomide counteracts JNK2 activation mediated by acetaminophen, thus promoting hepatocyte survival via mitochondrial permeability transition blockade. Taken together, these results provide evidence on the key role of JNK2 in hepatocyte survival. Assuming that the DHODH inhibitor identified in our screen and leflunomide have a similar mode of action, we suggest that this hit compound prevents mitochondrial release of pro-apoptotic agents in cynHLCs via JNK2 activity inhibition. Thus, the effect of leflunomide on cynHLC survival should be assessed to confirm the mechanism of action. It is important to note that *Plasmodium falciparum* DHODH is an attractive target to eliminate malaria parasites (Coteron et al., 2011, Kokkonda et al., 2016, Phillips et al., 2015, Phillips and Rathod, 2010). Indeed, contrary to mammalian cells, which can obtain pyrimidine via both de novo synthesis and salvage pathway, *Plasmodium* relies exclusively on de novo synthesis to produce pyrimidine stocks. In addition, a study testing several potent human DHODH inhibitors on the *Plasmodium* enzyme showed that all tested compounds were poorly active against *Plasmodium* DHODH (Baldwin et al., 2002). Moreover, the discovery of selective *E. coli* and *Helicobacter pyroli* DHODH inhibitors emphasizes the specie selectivity of these compounds. Taken together, these findings provide evidence that DHODH inhibitors are specie selective and consequently abrogates the concern of using the selected hit compound to improve hepatocyte survival in our system.

The second compound identified in our mode of action screen, doramapimod or BIRB-796, functions as a stress-activated protein kinase 2/p38β (SAPK2/p38β) inhibitor. Although p38 mitogen-activated protein kinases (MAPKs) play a key role in many cellular processes such as cell proliferation, differentiation, survival, migration and invasion, their effect varies depending on the cell type and the stimulus. In particular, MAPK family members were described as modulators of apoptosis (Nebreda and Porras, 2000). Xia et al. showed that activation of c-Jun N-terminal kinase-p38 (JNK-p38) induces apoptosis in rat PC-12 pheochromocytoma cells (Xia et al., 1995). This suggests that inhibition of p38 MAPK signaling pathway would promote cell survival by inhibition of apoptosis. Using SB203580, a well-described p38 MAPK inhibitor, induced liver injury by apoptosis has been investigated in several studies. First, Sreekanth et al. demonstrated that SB203580 downregulates p38 MAPK activity and consequently reduced liver injury upon Dengue viral infection (Sreekanth et al., 2016). Another report showed beneficial effect of pterostilbene (i.e. a natural antioxidant found in blueberries) treatment on hepatocytes in the context of sespis-induced liver injury. Pterostilbene treatment significantly decreased B-cell lymphoma 2-like protein 4 (Bax) levels and increased B-cell lymphoma 2 (Bcl2) levels, which indicates a reduction of hepatic apoptosis via shutdown of p38 MAPK activity (Liu et al., 2017). Taken together, these studies provide evidence that doramapimod promotes hepatocyte survival in our system through inhibition of p38 MAPK activity.

The last compound of our hepatocyte maintenance cocktail is a rapidly accelerated fibrosarcoma (Raf) kinase inhibitor. Raf belongs to the Ras/Raf/MEK/ERK signal transduction cascade which modulates numerous cellular processes such as growth, proliferation, and survival (Peyssonnaux and Eychene, 2001). Raf kinases phosphorylate MAPK kinases called MEKs which subsequently phosphorylate and activate MAPKs. Due to their direct interaction with the guanosine-5'-triphosphate (GTP)-bound oncoprotein Ras (Moodie et al., 1993, Van Aelst et al., 1993), their high mutation frequency in tumors and their effect on cancer cell growth and survival, Raf kinases have been largely described as attractive targets for cancer therapy (Holderfield et al., 2014). However, we could not find direct evidences in the literature for the positive effect of Raf kinase inhibitors on cynHLC maintenance. Assuming that the Raf kinase inhibitor identified in the survival screen prevents phosphorylation of MEK by Raf, subsequent inhibition of MAPK activity will ultimately lead to cell survival.

Although this three compounds-cocktail allowed maintenance of the cynHLCs for 17 days, it is not sufficient to assess the activity of compounds in a radical cure assay and ultimately

observe potential hypnozoite reactivation. Therefore, further investigations are needed to further improve cynHLC maintenance. The combination of five chemicals (forskolin, a transforming growth factor beta (TGF-β) inhibitor, a Notch inhibitor, a Wnt inhibitor, and a bone morphogenetic protein (BMP) inhibitor) recently reported for primary human hepatocyte maintenance (Xiang et al., 2019) is one approach we would like to test in cynHLCs.

3. Influence of cynHLCs on liver stage parasites

The maturation and maintenance of cynHLCs may have a direct impact on parasite behavior. Upon hepatocyte invasion, a subset of exoerythrocytic forms (EEFs) remained small and uninucleated, confirming that our system supports hypnozoite formation and persistence until 12 dpi. The second subset of the parasite population underwent schizogony after settling itself in the host cell. Expression of upregulated in infective sporozoites gene 4 (UIS4) in both small and large forms confirmed the formation of the parasitophorous vacuole membrane (PVM) upon host cell invasion. In cynHLCs, the schizonts increased in size overtime, but their growth was different from those found in simian primary hepatocytes. The schizonts in both cell types were indistinguishable until 4 dpi; however, at 6 dpi differences in growth and morphology were noticed. In primary cells, the schizonts developed asynchronously. The subset of rapidly growing parasites progressed into bean-shaped forms displaying unstained cytosolic vacuoles visualized by Hsp70 staining. In cynHLCs, the schizonts were significantly smaller from 6 dpi onwards and stayed almost exclusively round. In addition, schizont rupture was not observed in cynHLCs. As we observed low numbers of EEFs, it is possible that the probability of observing the final stage of the liver development is very small. Nevertheless, we cannot exclude that the parasites were unable to complete their development in cynHLCs. This could be for several reasons: (a) schizonts in the current system do not complete the maturation process due to the fetal phenotype of cynHLCs; (b) schizogony is delayed in cynHLCs; (c) schizonts complete their maturation process but cannot release merozoites; (d) cynHLCs detach before schizonts complete their maturation; (e) treatment with the compound cocktail hampers the ultimate stage of parasite development. To test these hypotheses, we first assessed the influence of cultivation medium on parasite growth and development. As the cynHLC maintenance medium is less rich than the primary hepatocyte medium that contains human serum, we first assumed that the composition of the medium might affect parasite development. To test this hypothesis, cynHLCs were maintained in cynHLC medium or primary hepatocyte medium and infected with a fresh batch of transgenic sporozoites (Chapter III). Although the

number of EEFs observed and the hypnozoite:schizont ratios were different for both tested media, the schizonts were smaller than those observed in simian primary hepatocytes for both tested media. This result suggests that the cultivation medium and the quality of the sporozoites are not responsible for the smaller size of liver schizonts observed in cynHLCs compared to primary cells. To address the other stated hypotheses we would need antibodies specific to mature *P. cynomolgi* liver schizonts. For instance, merozoite surface protein 1 (MSP-1) antibodies would allow us to visualize the formation of merosomes or merozoites in schizonts. However, MSP-1 antibodies for *P. cynomolgi* were not available yet and since *P. vivax* antibodies are usually not cross-reacting with *P. cynomolgi* parasites (Devendra Gupta, personal communication), we would need to produce the *P. cynomolgi* specific antibodies. Ideally, we should further improve cynHLC longevity to define the maturation profile of liver schizonts in this cell line and ultimately observe hypnozoite reactivation.

4. Differentiation efficiency and incomplete reprogramming

Other parameters may influence parasite behavior and infection efficiency in iPS-derived cells. The differentiation of iPS cells into hepatocytes is not a synchronous process. Each cell has its own kinetics of development, which gives rise to a population of hepatocytes with different degrees of maturation. For malaria infection, the degree of hepatocyte maturation may correlate with permissiveness to *Plasmodium* (Ng et al., 2015). Furthermore, for both the stepwise and inducible approaches, the differentiation process is not 100% efficient, with the consequence that not all iPS cells will be converted into hepatic cells upon doxycycline induction. With our protocol, 54% of the cells were positive for ALB and 72% expressed HNF4A after 6 days of differentiation by immunofluorescence analysis (n=3 independent experiments). In comparison, authors reported conversion rates ranging from 20% to 80% ALB positive cells for human HLC generation using the inducible approach (Huang et al., 2014, Du et al., 2014). Consequently, we conducted the infection assays with *P. cynomolgi* sporozoites on a heterogeneous population mostly composed of hepatocytes but also of other types of cells that are not permissive to *Plasmodium*. In addition, we cannot exclude that iPS-derived hepatocytes are less permissive to *Plasmodium* than primary hepatocytes. As cynIPS cells have been generated from skin fibroblasts, they may carry different epigenetic signatures compared to cynIPS cells derived from other types of somatic cells. Polo et al. reported that cellular origin might alter the differentiation capacity of mouse iPS cells by retention of epigenetic memory (Polo et al., 2010). More generally, others have described that upon reprogramming, somatic

cells can be trapped in partially reprogrammed states due to incomplete repression of transcription factors and inefficient DNA demethylation (Mikkelsen et al., 2008). This may lead to incomplete differentiation of iPS cells, preventing them from acquiring permissiveness to *Plasmodium*.

5. Inoculation time point

The time point of sporozoite inoculation may also significantly affect the outcome of the infection. Indeed, human HLCs acquire permissiveness for *P. vivax* during differentiation once they reach the hepatic stage (Ng et al., 2015). Based on our findings, we suggest that this phenomenon also occurs in cynHLCs. Indeed, the generated cynIPS cells could not be infected at day 0 with *P. cynomolgi* sporozoites and the increasing SRB1 levels during the differentiation process suggested the progressive acquisition of functions that are essential for *Plasmodium* invasion. All the data presented in this thesis were generated from cynHLCs infected after 4 days of differentiation. We selected this time point based on the time required for induction with Dox to generate the hepatocytes (i.e. 4 days) and the limited maintenance of cynHLCs we faced before identifying the cocktail of compounds for survival. However, recent Western blot analysis showed an increase in SRB1 protein-level between 4-days and 7-days differentiated hepatocytes (Fig. 4). Although SRB1 may not be the only receptor used by *Plasmodium* sporozoites to invade the host cell, this result suggests that the infection rate in our iPS-based system may be further improved by infecting cynHLCs 2 or 3 days later than at day 4 of differentiation. In this regard, our collaborators at the NITD and the BPRC are currently infecting cynHLCs with *P. cynomolgi* sporozoites at different time points, ranging from 2-days to 8-days differentiated cynHLCs, to investigate the optimal time point for infection.

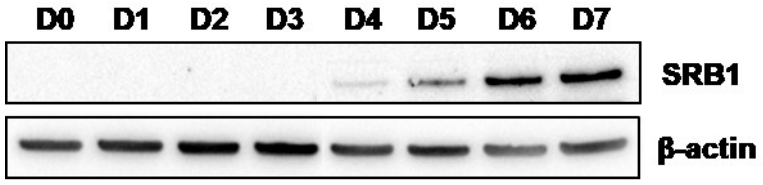

Fig. 4. Representative Western blot analysis of SRB1 and β-actin protein expression over the course of differentiation from cynIPS cells (D0) to cynHLCs (D4-D7).

6. Non-human primate origin

Another factor that can modulate infection and parasite development is the origin of the cynomolgus monkeys used to generate the iPS cells. Indeed, genetic diversity of non-human primates may induce differences in the malaria infection profile. Differences in the virulence of *P. knowlesi*, which also infect cynomolgus monkeys, were observed across animals of different geographical origins. For instance, monkeys from the Philippines were more resistant to infection with *P. knowlesi* than those from Malaysia (Schmidt et al., 1977). In addition, cynomolgus monkeys from Southeast Asia have hybridized with rhesus macaques (Bunlungsup et al., 2017). As rhesus macaques are more susceptible to *P. cynomolgi* than cynomolgus monkeys, a hybridized monkey is expected to be more susceptible to *P. cynomolgi* than e.g. an insular cynomolgus monkey living in Mauritius (Zhang et al., 2017). The non-human primate origin and its degree of hybridization are non-negligible parameters to take into account to interpret the data generated from infection assays. In this thesis, we generated iPS cells from a Chinese cynomolgus monkey. If the tractability of this monkey is correct, we used a hybridized monkey, which is more susceptible than a non-hybridized animal from Mauritius. IPS technology allows investigations on this parameter as iPS cells can be derived from any donor. Consequently, infecting cynHLCs from several *Macaca fascicularis* of various origins would give us some insights on how genetic diversity can influence infection rate, hypnozoite:schizont ratio, and infection profile with *P. cynomolgi*. We started investigating this aspect in this project by generating iPS cells from three different cynomolgus monkeys (one from China and two from the Philippines). However, due to the time constraints, iPS cells were generated from all monkeys but cynHLC generation and infection with *P. cynomolgi* sporozoites were only conducted with cells generated from the Chinese monkey based on iPS cell quality. Infection assays with hepatocytes generated from the two Filipino monkeys may provide some hints on the influence of the non-human primate origin on malaria infection outcomes.

7. Parasite sourcing, transport and storage

Besides the influence of the host cells in an in vitro model, the sporozoites themselves are also important entities that dramatically influence the outcome of an infection. The number of sporozoites transmitted to the human host during a mosquito blood meal is estimated to be from 10 to 100 (Medica and Sinnis, 2005). Even low, this number of sporozoites is enough to cause the disease in patients. For research purposes, we need to inoculate a higher number of

sporozoites to obtain a reasonable number of infected cells and study the mechanisms underlying the disease. The limited sporozoite availability caused by the lack of long-term in vitro culture for *P. cynomolgi* and the costly and ethically debatable monkey facilities severely hampers the development of new vaccines and drugs targeting *Plasmodium* parasites. To solve this poor sourcing, facilities have developed protocols to cryopreserve sporozoites. These are currently used in clinical trials for vaccine development (Epstein et al., 2011, Hoffman et al., 2010). Despite an increase in sporozoite availability, cryopreservation diminishes the quality of sporozoites. Cryopreservation caused an estimated ~6,4-fold loss of infectivity for *P. falciparum* sporozoites (Ruben et al., 2013), a ~10-fold loss of infectivity for *P. vivax* sporozoites in primary hepatocytes co-cultured with supportive fibroblasts (March et al., 2013), and >16 fold-loss of infectivity in HC-04 cells (Patrapuvich et al., 2016). Cryopreservation of *P. cynomolgi* sporozoites has never been reported but data from the Novartis Institute for Tropical Diseases (NITD) described a ~30-fold loss of infectivity after cryopreservation. Others reported instead that *P. vivax* sporozoites retained their capacity to invade HepG2 cells after cryopreservation (1.88% infected cells with fresh *P. vivax* sporozoites and 1.95% with cryopreserved *P. vivax* sporozoites from the same lot) (Chattopadhyay et al., 2010). For the development of our in vitro model, we avoided any potential loss of infectivity due to cryopreservation by using exclusively *P. cynomolgi* sporozoites freshly isolated from salivary glands of *Anopheles stephensi* mosquitoes. However, the lack of insectaries and monkey facilities in Basel obliged us to get access to *P. cynomolgi* sporozoites from the BPRC located in the Netherlands. Sporozoites were extracted from salivary glands of infected *Anopheles stephensi* mosquitoes and shipped to Basel at 4 °C to conduct an infection assay the following day. Assuming that the transportation of sporozoites under cold conditions would reduce their infectivity, two different infections were routinely performed on site at the BPRC. The first infection was immediately conducted shortly after sporozoite isolation and the second one was performed 24 hours later with some sporozoites from the same batch kept at 4 °C. The number of EEFs in primary rhesus monkey hepatocytes from both infections were similar (Anne-Marie Zeeman, personal communication). Although we can confirm that maintaining the sporozoites at 4 °C for 24 hours does not alter their infectivity, we cannot exclude that transportation may have affected this parameter. To assess this, we conducted an infection assay at the BPRC after transferring cynIPS cells to their laboratory. There, cynIPS cells were amplified, differentiated into hepatocytes and infected with freshly isolated sporozoites. Interestingly, the number of EEFs observed was comparable to cynHLCs infected with transported sporozoites (less than 10 EEFs per well of a 96-well plate compared to hundreds in primary rhesus monkey

hepatocytes). Even though this experiment was only performed once, this indicates that the low infection rate observed in our model was most likely not due to the storage and transport of the sporozoites.

Although the parasite strain is a determinant of relapse periodicity in *P. vivax* and potentially in *P. cynomolgi* (White, 2011), it is currently not clear if it also affects the infection rate. Three different strains of *P. cynomolgi* are commonly used: the Berok strain initially isolated in 1964 (Bennett et al., 1966), the B strain (*P. cynomolgi bastianelli*) initially isolated by Garnham in 1959 (Garnham, 1959), and the M strain (*P. cynomolgi* Mulligan strain) first isolated in 1935 (Coatney et al., 1961, Mulligan, 1935). With the exception of one recent study, which described a higher parasitaemia with the Berok strain in erythrocytic cultures (Chua et al., 2019b), there is no report that compares the potential differences between these strains. If high parasitaemia correlates with liver infection efficiency, we would assume that the Berok strain would induce higher numbers of EEFs upon sporozoite inoculation – but this remains to be further investigated. Here we performed all infections with the M strain provided by the BPRC. The NITD recently infected cynHLCs with the B strain. Although other parameters can vary between two sites (i.e. environment, iPS and hepatocyte quality, operator...), we did not observe significant differences between these two strains.

Finally, other parameters like batch-to-batch variability, sporozoite purity, mosquito healthiness, and parasite-mosquito interactions may have an impact on infection rate (Fig. 1). However, it is difficult to assess the impact of each of these factors in our system. It is clear that the quality of the isolation of fresh sporozoites from mosquitoes has a direct impact on the success rate of the infection. Lack of purification and/or temperature control may result in a failed infection, in which none of the hepatocytes are infected, or may introduce mosquito remnants that can induce contamination and ultimately experiment abortion. Taken together, this indicates that the factors related to *P. cynomolgi* sporozoites are not the key parameters affecting the efficiency of the established iPS-based model. Instead, we suggest that the host cell has a bigger impact on the infection rate and parasite development.

In summary, the development of this iPS-based in vitro model for infection with *P. cynomolgi* offers a promising alternative to the current systems using primary hepatocytes or hepatoma cell lines with *P. vivax*. Although the low infection rate and the low metabolic activity of cynHLCs hampers antimalarial drug profiling at the moment, the following new technologies and recent findings in the field may provide measures of improvement.

8. Genetic manipulation of iPS cells

First, genome editing in iPS cells offers the possibility to investigate host-parasite interactions and more specifically the mechanisms underlying hepatocyte invasion, hypnozoite formation and subsequent reactivation. Compared to primary cells, which are sensitive after isolation from tissue and have a finite number of division cycles, iPS cells are robust and have the capacity to self-renew unlimitedly. Moreover, iPS cells can be easily electroporated and subcloned when the selective inhibitor of Rho-associated kinase Y-27632 is used after cell dissociation (Watanabe et al., 2007). These features have enable the genetic manipulation of iPS cells using different approaches reviewed in (Hotta and Yamanaka, 2015). Among these techniques, the clustered regularly interspaced short palindromic repeat (CRISPR) bacterial system has been already widely used in both iPS cells and several parasites species (Bryant et al., 2019). This system originally used as a RNA-mediated adaptive defense mechanism by bacteria and archaea (Wiedenheft et al., 2012) consists in a CRISPR-associated 9 (Cas9) protein, a CRISPR RNA (crRNA) and a *trans* crRNA (tracrRNA) that generate a double stranded DNA break at a specific site (Jinek et al., 2012). Adapted to mammalian cells (Jinek et al., 2013) and other organisms like *Plasmodium (Ghorbal et al., 2014)*, this technology provides a reliable and efficient method to delete a gene of interest in the host cell or in the parasite and study the effect of this genetic modification. To improve the infection rate, for instance, host receptors for entry of *Plasmodium* such as SRB1, CD81, and ephrin type-A receptor 2 (EphA2) could be overexpressed to facilitate hepatocyte invasion. In addition, the parasites can be genetically manipulated. Voorberg et al. established a transgenic parasite line that enabled parasite live imaging and more recently, distinction between activated schizonts and hypnozoites. More importantly, we have shown that this transgenic line is also efficient in cynHLCs (Chapter III). Combining the iPS technology with this transgenic parasite line may help understanding malaria liver stage and may facilitate drug screening using a high content imaging platform.

9. IPS technology enables investigations of CYP2D6 polymorphism

IPS-derived hepatocytes also offer the possibility to study CYP2D6 polymorphism. The latter results in poor, intermediate, or efficient CYP2D6 metabolizers. These different variants can be modelled in vitro using the iPS technology. Generating iPS cells from the respective donors would expand the genetic pool of cells available for basic research and drug development, which is currently limited to a few lots of primary cells and cancer cell lines. For malaria drug

discovery, screening drugs against cells from poor and intermediate CYP2D6 metabolizers may lead to the identification of drugs that could replace primaquine, thus preventing primaquine failures observed with poor and intermediate CYP2D6 genotype (Bennett et al., 2013). Moreover, this approach would not only have an impact on antimalarials but also on many other drugs as the CYP2D6 enzyme affects the metabolism of roughly 50% of the marketed drugs (De Gregori et al., 2010).

10. Towards a model mimicking the in vivo micro-environment of the liver

Finally, increasing the metabolic activity and other functions of mature hepatocytes is a prerequisite for a relevant model to study the mechanisms underlying malaria or any other liver-related disease. Until recently, all the in vitro models for malaria research were in 2D, mostly unicellular, and lacked the complexity of the liver. To bridge that gap, research groups developed new systems like the sandwich culture or the micro-patterned culture of hepatocytes with supportive fibroblasts (Dembele et al., 2014, Gural et al., 2018). The sandwich culture allows cell polarity maintenance and improves hepatocyte longevity (Dembele et al., 2014). The micro-patterned culture of hepatocytes supported with fibroblasts mimics the interaction of hepatocytes with hepatic stellate cells in vivo (Gural et al., 2018). These two alternatives significantly improve hepatic functions as well as malaria infection efficiency. Still these two systems do not fully recapitulate the architecture and the multicellular composition of the liver. Recently, Chua et al. established the first 3D model for malaria infection assays (Chua et al., 2019a). Grown in a cellulose sponge, primary hepatocytes spontaneously formed spheres that sit in the cavities of the sponge. These 3D structures were permissive to both *P. vivax* and *P. cynomolgi*, and drug profiling with common antimalarials was feasible. Most importantly, this 3D approach significantly increased infection rate and primary hepatocyte maintenance. However, this 3D system is exclusively composed of primary hepatocytes, thus lacking key cell types of the liver for the host cell invasion process. Indeed, there are some lines of evidence for a key role of Kupffer cells in the hepatocyte invasion process (Baer et al., 2007, Cha et al., 2015, Frevert et al., 2005, Frevert et al., 2006, Meis et al., 1983). Kupffer cells, which are the macrophages of the liver, would act at the gateway for sporozoites to invade the underlying hepatocytes. Thus, developing a model with hepatocytes, stellate cells and Kupffer cells may facilitate the elucidation of specific invasion mechanisms and improve the infection rate. Establishing such a model from iPS cells is now possible either by combining the single cell types together in a sphere or by the generation of hepatic organoids. Ouchi et al. have developed

a protocol in which human iPS cells can be differentiated into liver organoids composed of hepatocyte, Kupffer and hepatic stellate like cells within 20 days (Ouchi et al., 2019). These multicellular 3D structures recapitulate mature liver functions and better resemble the liver microenvironment. Applying this technology to cynomolgus monkey cells would provide a powerful platform to study hypnozoite biology and accelerate malaria drug discovery.

In conclusion, hepatocyte infection models for malaria research are a rapidly progressing field. Many exciting developments have occurred over the last couple of years. By providing a new cultivation system for *P. cynomolgi* liver stages in iPS-derived hepatocyte-like cells of the cynomolgus monkey, this Ph.D. thesis may contribute to a better understanding of the malaria liver stages and hopefully to new antimalarials that are effective against hypnozoites.

References

BAER, K., ROOSEVELT, M., CLARKSON, A. B., JR., VAN ROOIJEN, N., SCHNIEDER, T. & FREVERT, U. 2007. Kupffer cells are obligatory for Plasmodium yoelii sporozoite infection of the liver. *Cell Microbiol,* 9**,** 397-412.

BALDWIN, J., FARAJALLAH, A. M., MALMQUIST, N. A., RATHOD, P. K. & PHILLIPS, M. A. 2002. Malarial Dihydroorotate Dehydrogenase: SUBSTRATE AND INHIBITOR SPECIFICITY. *Journal of Biological Chemistry,* 277**,** 41827-41834.

BAXTER, M., WITHEY, S., HARRISON, S., SEGERITZ, C. P., ZHANG, F., ATKINSON-DELL, R., ROWE, C., GERRARD, D. T., SISON-YOUNG, R., JENKINS, R., HENRY, J., BERRY, A. A., MOHAMET, L., BEST, M., FENWICK, S. W., MALIK, H., KITTERINGHAM, N. R., GOLDRING, C. E., PIPER HANLEY, K., VALLIER, L. & HANLEY, N. A. 2015. Phenotypic and functional analyses show stem cell-derived hepatocyte-like cells better mimic fetal rather than adult hepatocytes. *J Hepatol,* 62**,** 581-9.

BENNETT, G. F., WARREN, M. & CHEONG, W. 1966. Biology of the simian malarias of Southeast Asia. II. The susceptibility of some Malaysian mosquitoes to infection with five strains of Plasmodium cynomolgi. *The Journal of parasitology***,** 625-631.

BENNETT, J. W., PYBUS, B. S., YADAVA, A., TOSH, D., SOUSA, J. C., MCCARTHY, W. F., DEYE, G., MELENDEZ, V. & OCKENHOUSE, C. F. 2013. Primaquine Failure and Cytochrome P-450 2D6 in Plasmodium vivax Malaria. *New England Journal of Medicine,* 369**,** 1381-1382.

BRYANT, J. M., BAUMGARTEN, S., GLOVER, L., HUTCHINSON, S. & RACHIDI, N. 2019. CRISPR in Parasitology: Not Exactly Cut and Dried! *Trends Parasitol,* 35**,** 409-422.

BUNLUNGSUP, S., KANTHASWAMY, S., OLDT, R. F., SMITH, D. G., HOUGHTON, P., HAMADA, Y. & MALAIVIJITNOND, S. 2017. Genetic analysis of samples from wild populations opens new perspectives on hybridization between long-tailed (Macaca fascicularis) and rhesus macaques (Macaca mulatta). *Am J Primatol,* 79.

CAI, J., ZHAO, Y., LIU, Y., YE, F., SONG, Z., QIN, H., MENG, S., CHEN, Y., ZHOU, R., SONG, X., GUO, Y., DING, M. & DENG, H. 2007. Directed differentiation of human embryonic stem cells into functional hepatic cells. *Hepatology,* 45**,** 1229-39.

CHA, S.-J., PARK, K., SRINIVASAN, P., SCHINDLER, C. W., VAN ROOIJEN, N., STINS, M. & JACOBS-LORENA, M. 2015. CD68 acts as a major gateway for malaria sporozoite liver infection. *The Journal of Experimental Medicine,* 212**,** 1391.

CHATTOPADHYAY, R., VELMURUGAN, S., CHAKIATH, C., ANDREWS DONKOR, L., MILHOUS, W., BARNWELL, J. W., COLLINS, W. E. & HOFFMAN, S. L. 2010. Establishment of an in vitro assay for assessing the effects of drugs on the liver stages of Plasmodium vivax malaria. *PLoS One,* 5**,** e14275.

CHEN, Y. F., TSENG, C. Y., WANG, H. W., KUO, H. C., YANG, V. W. & LEE, O. K. 2012. Rapid generation of mature hepatocyte-like cells from human induced pluripotent stem cells by an efficient three-step protocol. *Hepatology,* 55**,** 1193-203.

CHUA, A. C. Y., ANANTHANARAYANAN, A., ONG, J. J. Y., WONG, J. Y., YIP, A., SINGH, N. H., QU, Y., DEMBELE, L., MCMILLIAN, M., UBALEE, R., DAVIDSON, S., TUNGTAENG, A., IMERBSIN, R., GUPTA, K., ANDOLINA, C., LEE, F., K, S. W. T., NOSTEN, F., RUSSELL, B., LANGE, A., DIAGANA, T. T., RENIA, L., YEUNG, B. K. S., YU, H. & BIFANI, P. 2019a. Hepatic spheroids used as an in vitro model to study malaria relapse. *Biomaterials,* 216**,** 119221.

CHUA, A. C. Y., ONG, J. J. Y., MALLERET, B., SUWANARUSK, R., KOSAISAVEE, V., ZEEMAN, A.-M., COOPER, C. A., TAN, K. S. W., ZHANG, R., TAN, B. H., ABAS,

S. N., YIP, A., ELLIOT, A., JOYNER, C. J., CHO, J. S., BREYER, K., BARAN, S., LANGE, A., MAHER, S. P., NOSTEN, F., BODENREIDER, C., YEUNG, B. K. S., MAZIER, D., GALINSKI, M. R., DEREUDDRE-BOSQUET, N., LE GRAND, R., KOCKEN, C. H. M., RÉNIA, L., KYLE, D. E., DIAGANA, T. T., SNOUNOU, G., RUSSELL, B. & BIFANI, P. 2019b. Robust continuous in vitro culture of the Plasmodium cynomolgi erythrocytic stages. *Nature Communications,* 10**,** 3635.

COATNEY, G., COLLINS, W., WARREN, M. & CONTACOS, P. 1971. The primate malarias US Government Printing Office. *Washington, DC: Government Printing Office*.

COATNEY, G. R., ELDER, H. A., CONTACOS, P. G., GETZ, M. E., GREENLAND, R., ROSSAN, R. N. & SCHMIDT, L. H. 1961. Transmission of the M strain of Plasmodium cynomolgi to man. *Am J Trop Med Hyg,* 10**,** 673-8.

COTERON, J. M., MARCO, M., ESQUIVIAS, J., DENG, X., WHITE, K. L., WHITE, J., KOLTUN, M., EL MAZOUNI, F., KOKKONDA, S., KATNENI, K., BHAMIDIPATI, R., SHACKLEFORD, D. M., ANGULO-BARTUREN, I., FERRER, S. B., JIMENEZ-DIAZ, M. B., GAMO, F. J., GOLDSMITH, E. J., CHARMAN, W. N., BATHURST, I., FLOYD, D., MATTHEWS, D., BURROWS, J. N., RATHOD, P. K., CHARMAN, S. A. & PHILLIPS, M. A. 2011. Structure-guided lead optimization of triazolopyrimidine-ring substituents identifies potent Plasmodium falciparum dihydroorotate dehydrogenase inhibitors with clinical candidate potential. *J Med Chem,* 54**,** 5540-61.

CRAMER, D. V., CHAPMAN, F. A., JAFFEE, B. D., ZAJAC, I., HREHA-EIRAS, G., YASUNAGA, C., WU, G.-D. & MAKOWKA, L. 1992. The prolongation of concordant hamster-to-rat cardiac xenografts by brequinar sodium. *Transplantation,* 54**,** 403-408.

DE GREGORI, M., ALLEGRI, M., DE GREGORI, S., GARBIN, G., TINELLI, C., REGAZZI, M., GOVONI, S. & RANZANI, G. N. 2010. How and why to screen for CYP2D6 interindividual variability in patients under pharmacological treatments. *Curr Drug Metab,* 11**,** 276-82.

DEMBELE, L., FRANETICH, J. F., LORTHIOIS, A., GEGO, A., ZEEMAN, A. M., KOCKEN, C. H., LE GRAND, R., DEREUDDRE-BOSQUET, N., VAN GEMERT, G. J., SAUERWEIN, R., VAILLANT, J. C., HANNOUN, L., FUCHTER, M. J., DIAGANA, T. T., MALMQUIST, N. A., SCHERF, A., SNOUNOU, G. & MAZIER, D. 2014. Persistence and activation of malaria hypnozoites in long-term primary hepatocyte cultures. *Nat Med,* 20**,** 307-12.

DU, Y., WANG, J., JIA, J., SONG, N., XIANG, C., XU, J., HOU, Z., SU, X., LIU, B. & JIANG, T. 2014. Human hepatocytes with drug metabolic function induced from fibroblasts by lineage reprogramming. *Cell stem cell,* 14**,** 394-403.

EPSTEIN, J. E., TEWARI, K., LYKE, K. E., SIM, B. K. L., BILLINGSLEY, P. F., LAURENS, M. B., GUNASEKERA, A., CHAKRAVARTY, S., JAMES, E. R., SEDEGAH, M., RICHMAN, A., VELMURUGAN, S., REYES, S., LI, M., TUCKER, K., AHUMADA, A., RUBEN, A. J., LI, T., STAFFORD, R., EAPPEN, A. G., TAMMINGA, C., BENNETT, J. W., OCKENHOUSE, C. F., MURPHY, J. R., KOMISAR, J., THOMAS, N., LOYEVSKY, M., BIRKETT, A., PLOWE, C. V., LOUCQ, C., EDELMAN, R., RICHIE, T. L., SEDER, R. A. & HOFFMAN, S. L. 2011. Live Attenuated Malaria Vaccine Designed to Protect Through Hepatic CD8+ T Cell Immunity. *Science,* 334**,** 475.

FREVERT, U., ENGELMANN, S., ZOUGBEDE, S., STANGE, J., NG, B., MATUSCHEWSKI, K., LIEBES, L. & YEE, H. 2005. Intravital observation of Plasmodium berghei sporozoite infection of the liver. *PLoS Biol,* 3**,** e192.

FREVERT, U., USYNIN, I., BAER, K. & KLOTZ, C. 2006. Nomadic or sessile: can Kupffer cells function as portals for malaria sporozoites to the liver? *Cell Microbiol,* 8**,** 1537-46.

GAO, Y., ZHANG, X., ZHANG, L., CEN, J., NI, X., LIAO, X., YANG, C., LI, Y., CHEN, X., ZHANG, Z., SHU, Y., CHENG, X., HAY, D. C., LAI, D., PAN, G., WEI, G. & HUI, L. 2017. Distinct Gene Expression and Epigenetic Signatures in Hepatocyte-like Cells Produced by Different Strategies from the Same Donor. *Stem Cell Reports,* 9**,** 1813-1824.

GARNHAM, P. C. C. 1959. A New Sub-Species of Plasmodium cynomolgi. *Rivista di Parassitologia,* 20**,** 273-8.

GHORBAL, M., GORMAN, M., MACPHERSON, C. R., MARTINS, R. M., SCHERF, A. & LOPEZ-RUBIO, J. J. 2014. Genome editing in the human malaria parasite Plasmodium falciparum using the CRISPR-Cas9 system. *Nat Biotechnol,* 32**,** 819-21.

GURAL, N., MANCIO-SILVA, L., MILLER, A. B., GALSTIAN, A., BUTTY, V. L., LEVINE, S. S., PATRAPUVICH, R., DESAI, S. P., MIKOLAJCZAK, S. A., KAPPE, S. H. I., FLEMING, H. E., MARCH, S., SATTABONGKOT, J. & BHATIA, S. N. 2018. In Vitro Culture, Drug Sensitivity, and Transcriptome of Plasmodium Vivax Hypnozoites. *Cell Host Microbe,* 23**,** 395-406 e4.

HAN, S., BOURDON, A., HAMOU, W., DZIEDZIC, N., GOLDMAN, O. & GOUON-EVANS, V. 2012. Generation of functional hepatic cells from pluripotent stem cells. *J Stem Cell Res Ther,* Suppl 10**,** 1-7.

HOEPFNER, D., MCNAMARA, C. W., LIM, C. S., STUDER, C., RIEDL, R., AUST, T., MCCORMACK, S. L., PLOUFFE, D. M., MEISTER, S., SCHUIERER, S., PLIKAT, U., HARTMANN, N., STAEDTLER, F., COTESTA, S., SCHMITT, E. K., PETERSEN, F., SUPEK, F., GLYNNE, R. J., TALLARICO, J. A., PORTER, J. A., FISHMAN, M. C., BODENREIDER, C., DIAGANA, T. T., MOVVA, N. R. & WINZELER, E. A. 2012. Selective and specific inhibition of the plasmodium falciparum lysyl-tRNA synthetase by the fungal secondary metabolite cladosporin. *Cell Host Microbe,* 11**,** 654-63.

HOFFMAN, S. L., BILLINGSLEY, P. F., JAMES, E., RICHMAN, A., LOYEVSKY, M., LI, T., CHAKRAVARTY, S., GUNASEKERA, A., CHATTOPADHYAY, R., LI, M., STAFFORD, R., AHUMADA, A., EPSTEIN, J. E., SEDEGAH, M., REYES, S., RICHIE, T. L., LYKE, K. E., EDELMAN, R., LAURENS, M., PLOWE, C. V. & SIM, B. K. L. 2010. Development of a metabolically active, non-replicating sporozoite vaccine to prevent Plasmodium falciparum malaria. *Human Vaccines,* 6**,** 97-106.

HOLDERFIELD, M., DEUKER, M. M., MCCORMICK, F. & MCMAHON, M. 2014. Targeting RAF kinases for cancer therapy: BRAF-mutated melanoma and beyond. *Nature Reviews Cancer,* 14**,** 455.

HOTTA, A. & YAMANAKA, S. 2015. From Genomics to Gene Therapy: Induced Pluripotent Stem Cells Meet Genome Editing. *Annu Rev Genet,* 49**,** 47-70.

HU, C. & LI, L. 2015. Two Effective Routes for Removing Lineage Restriction Roadblocks: From Somatic Cells to Hepatocytes. *Int J Mol Sci,* 16**,** 20873-95.

HUANG, P., HE, Z., JI, S., SUN, H., XIANG, D., LIU, C., HU, Y., WANG, X. & HUI, L. 2011. Induction of functional hepatocyte-like cells from mouse fibroblasts by defined factors. *nature,* 475**,** 386.

HUANG, P., ZHANG, L., GAO, Y., HE, Z., YAO, D., WU, Z., CEN, J., CHEN, X., LIU, C., HU, Y., LAI, D., HU, Z., CHEN, L., ZHANG, Y., CHENG, X., MA, X., PAN, G., WANG, X. & HUI, L. 2014. Direct reprogramming of human fibroblasts to functional and expandable hepatocytes. *Cell Stem Cell,* 14**,** 370-84.

IMOSE, M., NAGAKI, M., KIMURA, K., TAKAI, S., IMAO, M., NAIKI, T., OSAWA, Y., ASANO, T., HAYASHI, H. & MORIWAKI, H. 2004. Leflunomide protects from T-cell–mediated liver injury in mice through inhibition of nuclear factor κB. *Hepatology,* 40**,** 1160-1169.

JINEK, M., CHYLINSKI, K., FONFARA, I., HAUER, M., DOUDNA, J. A. & CHARPENTIER, E. 2012. A programmable dual-RNA–guided DNA endonuclease in adaptive bacterial immunity. *Science,* 337**,** 816-821.

JINEK, M., EAST, A., CHENG, A., LIN, S., MA, E. & DOUDNA, J. 2013. RNA-programmed genome editing in human cells. *Elife,* 2**,** e00471.

JOZEFCZUK, J., PRIGIONE, A., CHAVEZ, L. & ADJAYE, J. 2011. Comparative Analysis of Human Embryonic Stem Cell and Induced Pluripotent Stem Cell-Derived Hepatocyte-Like Cells Reveals Current Drawbacks and Possible Strategies for Improved Differentiation. *Stem Cells and Development,* 20**,** 1259-1275.

KIA, R., SISON, R. L. C., HESLOP, J., KITTERINGHAM, N. R., HANLEY, N., MILLS, J. S., PARK, B. K. & GOLDRING, C. E. P. 2013. Stem cell-derived hepatocytes as a predictive model for drug-induced liver injury: are we there yet? *British Journal of Clinical Pharmacology,* 75**,** 885-896.

KOKKONDA, S., DENG, X., WHITE, K. L., COTERON, J. M., MARCO, M., DE LAS HERAS, L., WHITE, J., EL MAZOUNI, F., TOMCHICK, D. R., MANJALANAGARA, K., RUDRA, K. R., CHEN, G., MORIZZI, J., RYAN, E., KAMINSKY, W., LEROY, D., MARTÍNEZ-MARTÍNEZ, M. S., JIMENEZ-DIAZ, M. B., BAZAGA, S. F., ANGULO-BARTUREN, I., WATERSON, D., BURROWS, J. N., MATTHEWS, D., CHARMAN, S. A., PHILLIPS, M. A. & RATHOD, P. K. 2016. Tetrahydro-2-naphthyl and 2-Indanyl Triazolopyrimidines Targeting Plasmodium falciparum Dihydroorotate Dehydrogenase Display Potent and Selective Antimalarial Activity. *Journal of Medicinal Chemistry,* 59**,** 5416-5431.

LATCHOUMYCANDANE, C., SEAH, Q. M., TAN, R. C., SATTABONGKOT, J., BEERHEIDE, W. & BOELSTERLI, U. A. 2006. Leflunomide or A77 1726 protect from acetaminophen-induced cell injury through inhibition of JNK-mediated mitochondrial permeability transition in immortalized human hepatocytes. *Toxicology and applied pharmacology,* 217**,** 125-133.

LIU, X., YANG, X., HAN, L., YE, F., LIU, M., FAN, W., ZHANG, K., KONG, Y., ZHANG, J., SHI, L., CHEN, Y., ZHANG, X. & LIN, S. 2017. Pterostilbene alleviates polymicrobial sepsis-induced liver injury: Possible role of SIRT1 signaling. *Int Immunopharmacol,* 49**,** 50-59.

LÖFFLER, M., FAIRBANKS, L. D., ZAMEITAT, E., MARINAKI, A. M. & SIMMONDS, H. A. 2005. Pyrimidine pathways in health and disease. *Trends in molecular medicine,* 11**,** 430-437.

MALLANNA, S. K. & DUNCAN, S. A. 2013. Differentiation of hepatocytes from pluripotent stem cells. *Curr Protoc Stem Cell Biol,* 26**,** Unit 1G 4.

MARCH, S., NG, S., VELMURUGAN, S., GALSTIAN, A., SHAN, J., LOGAN, D. J., CARPENTER, A. E., THOMAS, D., SIM, B. K., MOTA, M. M., HOFFMAN, S. L. & BHATIA, S. N. 2013. A microscale human liver platform that supports the hepatic stages of Plasmodium falciparum and vivax. *Cell Host Microbe,* 14**,** 104-15.

MEDICA, D. L. & SINNIS, P. 2005. Quantitative Dynamics of Plasmodium yoelii Sporozoite Transmission by Infected Anopheline Mosquitoes. *Infection and Immunity,* 73**,** 4363.

MEIS, J. F., VERHAVE, J. P., JAP, P. H. & MEUWISSEN, J. H. 1983. An ultrastructural study on the role of Kupffer cells in the process of infection by Plasmodium berghei sporozoites in rats. *Parasitology,* 86 (Pt 2)**,** 231-42.

MIGITA, K., MIYASHITA, T., MAEDA, Y., NAKAMURA, M., YATSUHASHI, H., ISHIBASHI, H. & EGUCHI, K. 2005. An active metabolite of leflunomide, A77 1726, inhibits the production of serum amyloid A protein in human hepatocytes. *Rheumatology,* 44**,** 443-448.

MIKKELSEN, T. S., HANNA, J., ZHANG, X., KU, M., WERNIG, M., SCHORDERET, P., BERNSTEIN, B. E., JAENISCH, R., LANDER, E. S. & MEISSNER, A. 2008. Dissecting direct reprogramming through integrative genomic analysis. *Nature,* 454**,** 49-55.

MOODIE, S. A., WILLUMSEN, B. M., WEBER, M. J. & WOLFMAN, A. 1993. Complexes of Ras. GTP with Raf-1 and mitogen-activated protein kinase kinase. *Science,* 260**,** 1658-1661.

MULLIGAN, H. 1935. Descriptions of Two Species of Monkey Pías-medium isolated from Silenus irus. *Arch. Protistenkunde,* 84.

NAKAMORI, D., TAKAYAMA, K., NAGAMOTO, Y., MITANI, S., SAKURAI, F., TACHIBANA, M. & MIZUGUCHI, H. 2016. Hepatic maturation of human iPS cell-derived hepatocyte-like cells by ATF5, c/EBPalpha, and PROX1 transduction. *Biochem Biophys Res Commun,* 469**,** 424-9.

NEBREDA, A. R. & PORRAS, A. 2000. p38 MAP kinases: beyond the stress response. *Trends in Biochemical Sciences,* 25**,** 257-260.

NG, S., SCHWARTZ, R. E., MARCH, S., GALSTIAN, A., GURAL, N., SHAN, J., PRABHU, M., MOTA, M. M. & BHATIA, S. N. 2015. Human iPSC-derived hepatocyte-like cells support Plasmodium liver-stage infection in vitro. *Stem Cell Reports,* 4**,** 348-59.

OGAWA, S., SURAPISITCHAT, J., VIRTANEN, C., OGAWA, M., NIAPOUR, M., SUGAMORI, K. S., WANG, S., TAMBLYN, L., GUILLEMETTE, C., HOFFMANN, E., ZHAO, B., STROM, S., LAPOSA, R. R., TYNDALE, R. F., GRANT, D. M. & KELLER, G. 2013. Three-dimensional culture and cAMP signaling promote the maturation of human pluripotent stem cell-derived hepatocytes. *Development,* 140**,** 3285.

OUCHI, R., TOGO, S., KIMURA, M., SHINOZAWA, T., KOIDO, M., KOIKE, H., THOMPSON, W., KARNS, R. A., MAYHEW, C. N., MCGRATH, P. S., MCCAULEY, H. A., ZHANG, R.-R., LEWIS, K., HAKOZAKI, S., FERGUSON, A., SAIKI, N., YONEYAMA, Y., TAKEUCHI, I., MABUCHI, Y., AKAZAWA, C., YOSHIKAWA, H. Y., WELLS, J. M. & TAKEBE, T. 2019. Modeling Steatohepatitis in Humans with Pluripotent Stem Cell-Derived Organoids. *Cell Metabolism,* 30**,** 374-384.e6.

PATRAPUVICH, R., LERDPANYANGAM, K., JENWITHISUK, R., RUNGIN, S., BOONHOK, R., DUANGMANEE, A., YIMAMNUAYCHOK, N. & SATTABONGKOT, J. 2016. Viability and infectivity of cryopreserved Plasmodium vivax sporozoites. *Southeast Asian Journal of Tropical Medicine and Public Health,* 47**,** 171.

PETERS, G., NADAL, J., LAURENSSE, E., DE KANT, E. & PINEDO, H. 1990. Retention of in vivo antipyrimidine effects of Brequinar sodium (DUP-785; NSC 368390) in murine liver, bone marrow and colon cancer. *Biochemical pharmacology,* 39**,** 135-144.

PEYSSONNAUX, C. & EYCHENE, A. 2001. The Raf/MEK/ERK pathway: new concepts of activation. *Biol Cell,* 93**,** 53-62.

PHILLIPS, M. A., LOTHARIUS, J., MARSH, K., WHITE, J., DAYAN, A., WHITE, K. L., NJOROGE, J. W., EL MAZOUNI, F., LAO, Y., KOKKONDA, S., TOMCHICK, D. R., DENG, X., LAIRD, T., BHATIA, S. N., MARCH, S., NG, C. L., FIDOCK, D. A., WITTLIN, S., LAFUENTE-MONASTERIO, M., BENITO, F. J. G., ALONSO, L. M. S., MARTINEZ, M. S., JIMENEZ-DIAZ, M. B., BAZAGA, S. F., ANGULO-

BARTUREN, I., HASELDEN, J. N., LOUTTIT, J., CUI, Y., SRIDHAR, A., ZEEMAN, A.-M., KOCKEN, C., SAUERWEIN, R., DECHERING, K., AVERY, V. M., DUFFY, S., DELVES, M., SINDEN, R., RUECKER, A., WICKHAM, K. S., ROCHFORD, R., GAHAGEN, J., IYER, L., RICCIO, E., MIRSALIS, J., BATHHURST, I., RUECKLE, T., DING, X., CAMPO, B., LEROY, D., ROGERS, M. J., RATHOD, P. K., BURROWS, J. N. & CHARMAN, S. A. 2015. A long-duration dihydroorotate dehydrogenase inhibitor (DSM265) for prevention and treatment of malaria. *Science Translational Medicine,* 7**,** 296ra111.

PHILLIPS, M. A. & RATHOD, P. K. 2010. Plasmodium dihydroorotate dehydrogenase: a promising target for novel anti-malarial chemotherapy. *Infect Disord Drug Targets,* 10**,** 226-39.

POLO, J. M., LIU, S., FIGUEROA, M. E., KULALERT, W., EMINLI, S., TAN, K. Y., APOSTOLOU, E., STADTFELD, M., LI, Y., SHIODA, T., NATESAN, S., WAGERS, A. J., MELNICK, A., EVANS, T. & HOCHEDLINGER, K. 2010. Cell type of origin influences the molecular and functional properties of mouse induced pluripotent stem cells. *Nature Biotechnology,* 28**,** 848.

PYBUS, B. S., MARCSISIN, S. R., JIN, X., DEYE, G., SOUSA, J. C., LI, Q., CARIDHA, D., ZENG, Q., REICHARD, G. A., OCKENHOUSE, C., BENNETT, J., WALKER, L. A., OHRT, C. & MELENDEZ, V. 2013. The metabolism of primaquine to its active metabolite is dependent on CYP 2D6. *Malaria Journal,* 12**,** 212.

RUBEN, A., AWE, A., HOFFMAN, S. L., LEE SIM, B. K., BILLINGSLEY, P. F., MANOJ, A., CHAKRAVARTY, S., GUNASEKERA, A., LI, T., STAFFORD, R., LI, M. L. & JAMES, E. R. 2013. 157 Cryopreservation of Plasmodium falciparum Sporozoites and Sanaria® PfSPZ Vaccine. *Cryobiology,* 67**,** 442.

SCHMIDT, L. H., FRADKIN, R., HARRISON, J. & ROSSAN, R. N. 1977. Differences in the virulence of Plasmodium knowlesi for Macaca irus (fascicularis) of Philippine and Malayan origins. *Am J Trop Med Hyg,* 26**,** 612-22.

SCHWARTZ, R. E., FLEMING, H. E., KHETANI, S. R. & BHATIA, S. N. 2014. Pluripotent stem cell-derived hepatocyte-like cells. *Biotechnol Adv,* 32**,** 504-13.

SEKIYA, S. & SUZUKI, A. 2011. Direct conversion of mouse fibroblasts to hepatocyte-like cells by defined factors. *Nature,* 475**,** 390.

SHAN, J., SCHWARTZ, R. E., ROSS, N. T., LOGAN, D. J., THOMAS, D., DUNCAN, S. A., NORTH, T. E., GOESSLING, W., CARPENTER, A. E. & BHATIA, S. N. 2013. Identification of small molecules for human hepatocyte expansion and iPS differentiation. *Nat Chem Biol,* 9**,** 514-20.

SI-TAYEB, K., NOTO, F. K., NAGAOKA, M., LI, J., BATTLE, M. A., DURIS, C., NORTH, P. E., DALTON, S. & DUNCAN, S. A. 2010. Highly efficient generation of human hepatocyte-like cells from induced pluripotent stem cells. *Hepatology,* 51**,** 297-305.

SONG, W., LU, Y. C., FRANKEL, A. S., AN, D., SCHWARTZ, R. E. & MA, M. 2015. Engraftment of human induced pluripotent stem cell-derived hepatocytes in immunocompetent mice via 3D co-aggregation and encapsulation. *Sci Rep,* 5**,** 16884.

SREEKANTH, G. P., CHUNCHARUNEE, A., SIRIMONTAPORN, A., PANAAMPON, J., NOISAKRAN, S., YENCHITSOMANUS, P. T. & LIMJINDAPORN, T. 2016. SB203580 Modulates p38 MAPK Signaling and Dengue Virus-Induced Liver Injury by Reducing MAPKAPK2, HSP27, and ATF2 Phosphorylation. *PLoS One,* 11**,** e0149486.

TAKEBE, T., SEKINE, K., ENOMURA, M., KOIKE, H., KIMURA, M., OGAERI, T., ZHANG, R. R., UENO, Y., ZHENG, Y. W., KOIKE, N., AOYAMA, S., ADACHI, Y. & TANIGUCHI, H. 2013. Vascularized and functional human liver from an iPSC-derived organ bud transplant. *Nature,* 499**,** 481-4.

TOUBOUL, T., HANNAN, N. R. F., CORBINEAU, S., MARTINEZ, A., MARTINET, C., BRANCHEREAU, S., MAINOT, S., STRICK-MARCHAND, H., PEDERSEN, R., DI SANTO, J., WEBER, A. & VALLIER, L. 2010. Generation of functional hepatocytes from human embryonic stem cells under chemically defined conditions that recapitulate liver development. *Hepatology,* 51**,** 1754-1765.

VAN AELST, L., BARR, M., MARCUS, S., POLVERINO, A. & WIGLER, M. 1993. Complex formation between RAS and RAF and other protein kinases. *Proceedings of the National Academy of Sciences,* 90**,** 6213-6217.

WATANABE, K., UENO, M., KAMIYA, D., NISHIYAMA, A., MATSUMURA, M., WATAYA, T., TAKAHASHI, J. B., NISHIKAWA, S., NISHIKAWA, S., MUGURUMA, K. & SASAI, Y. 2007. A ROCK inhibitor permits survival of dissociated human embryonic stem cells. *Nat Biotechnol,* 25**,** 681-6.

WHITE, N. J. 2011. Determinants of relapse periodicity in Plasmodium vivax malaria. *Malaria Journal,* 10**,** 297.

WIEDENHEFT, B., STERNBERG, S. H. & DOUDNA, J. A. 2012. RNA-guided genetic silencing systems in bacteria and archaea. *Nature,* 482**,** 331.

XIA, Z., DICKENS, M., RAINGEAUD, J., DAVIS, R. J. & GREENBERG, M. E. 1995. Opposing effects of ERK and JNK-p38 MAP kinases on apoptosis. *Science,* 270**,** 1326-31.

XIANG, C., DU, Y., MENG, G., SOON YI, L., SUN, S., SONG, N., ZHANG, X., XIAO, Y., WANG, J., YI, Z., LIU, Y., XIE, B., WU, M., SHU, J., SUN, D., JIA, J., LIANG, Z., SUN, D., HUANG, Y., SHI, Y., XU, J., LU, F., LI, C., XIANG, K., YUAN, Z., LU, S. & DENG, H. 2019. Long-term functional maintenance of primary human hepatocytes in vitro. *Science,* 364**,** 399-402.

ZHANG, X., MENG, Y., HOUGHTON, P., LIU, M., KANTHASWAMY, S., OLDT, R., NG, J., TRASK, J. S., HUANG, R., SINGH, B., DU, H. & SMITH, D. G. 2017. Ancestry, Plasmodium cynomolgi prevalence and rhesus macaque admixture in cynomolgus macaques (Macaca fascicularis) bred for export in Chinese breeding farms. *J Med Primatol,* 46**,** 31-41.

Conclusions and outlook

The development of an iPS-based infection model to produce hypnozoites will contribute to a better understanding of the mechanisms underlying dormancy in malaria relapsing species such as *P. cynomolgi* and *P. vivax*. Based on protocols established for human cells, we developed an efficient method to generate iPS cells and hepatocyte-like cells from *Macaca fascicularis.* The produced hepatic cells were successfully infected by *P. cynomolgi* sporozoites, and the subsequently formed liver-stage parasites were characterized with *P. cynomolgi* specific antibodies. Similar to primary hepatocytes, iPS-derived hepatocyte-like cells supported hypnozoite persistence as well as liver schizont development.

Using iPS technology for malaria drug discovery offers several advantages over primary cells. First, iPS cells have the capacity to self-renew, which enables large-scale production from a unique donor, overcoming the donor-to-donor variability observed with primary hepatocytes. Second, iPS cells can be derived from any donor. For malaria research, this would expand the limited genetic pool currently offered by primary hepatocytes. In particular, it would allow the screening of drugs suitable for low, moderate, and high CYP2D6 metabolizers, and to accelerate the search for drugs that can be administered to G6PD deficient patients. Finally, host cell-parasite interactions can be investigated through the genetic manipulation of iPS cells.

A crucial milestone for this work was the finding that doramapimod, a DHODH inhibitor and a Raf inhibitor prolonged the lifetime of the iPS-derived hepatocytes, and that a combination of these three small molecules allowed to maintain the hepatocytes in culture long enough for *P. cynomolgi* infection experiments to study the development of liver stages over time.

We also showed that a recently developed transgenic parasite line can be successfully used in combination with our iPS-based model. This molecular tool enabled detection and distinction between hypnozoites (GFP positive) and activated liver schizonts (GFP/mCherry double-positive). Therefore, using these parasites in combination with iPS cells offers an efficient system to study malaria liver stage dormancy and subsequent reactivation. In addition, GFP and mCherry signals can be used as readouts in drug screening assays to identify compounds with anti-hypnozoite and/or anti-schizont activity - accompanied by monitoring of potential hypnozoite reactivation over time.

The work presented in this thesis demonstrates that stem cell-derived hepatocytes and *P. cynomolgi* are prospective alternatives to primary hepatocytes and *P. vivax*. Although the data generated with the iPS-based model are still developable in terms of infection rate and

antimalarial drug profiling, we are convinced that this new in vitro system will be valuable and promising for the field. The iPS-based system was successfully transferred to our collaborators, the BPRC and the NITD in order to validate the iPS-based system and make it useful for the field. Infection of iPS-derived hepatocytes with *P. cynomolgi* sporozoites was successfully reproduced on two different sites, confirming the robustness of the established protocol. Moreover, the NITD scaled down the assay from 96-well to 384-well plate format, which will provide more flexibility and a higher screening capacity in the future. This active collaboration with both partners will allow us to combine our efforts in improving the current system and ultimately bridge the gap between the proof of concept and the establishment of a standard procedure to study and tackle the hypnozoite reservoir.